12-2010

Understanding GAFP, A Plant Lectin with Broad Spectrum Inhibitory Activity

Alexis Nagel
Clemson University, agilbo@clemson.edu

UNDERSTANDING GAFP, A PLANT LECTIN WITH BROAD SPECTRUM INHIBITORY ACTIVITY

A Thesis
Presented to
the Graduate School of
Clemson University

In Partial Fulfillment
of the Requirements for the Degree
Doctor of Philosophy
Biochemistry and Molecular Biology

---

by
Alexis Katherine Nagel
December 2010

Accepted by:
Dr. Guido Schnabel, Principal Investigator
Dr. William Marcotte, Committee Chair
Dr. Kerry Smith
Dr. Brandon Moore
Dr. Brian Dominy

ABSTRACT

South Carolina and Georgia are the largest peach producing regions in the Southeastern United States, generating about $60 million worth (~90,000 tons) of fruit per year on average. Peaches and other stone-fruits (*Prunus sp.*) can be afflicted by a variety of root-associated diseases which negatively impact annual yield and long-term tree mortality. An engineered *Prunus* rootstock with enhanced resistance to soil-borne pathogens would therefore be of great benefit to the Southeastern peach industry. The *Gastrodia* anti-fungal protein (GAFP) is a monocot mannose-binding lectin which is able to inhibit the growth of multiple species of plant pathogenic fungi. Previous findings from our lab demonstrated that GAFP-1 expression in tobacco resulted in increased tolerance to infection by the stramenopile, root-knot nematode (RKN), and fungal pathogens *Phytophthora nicotianae*, *Meloidogyne incognita*, and *Rhizoctonia solani*, respectively. Further work in transgenic plum suggested that expression of GAFP-1 was also able to impart protective effects against the stramenopile, *P. cinnamomi*, and the RKN *M. incognita*, in a *Prunus* species. GAFP-1 purified from tobacco directly inhibited the mycelium of *P. cinnamomi* and *P. nicotianae* in a concentration dependent manner *in vitro*. Contact with the lectin, however, did not impair J2 mobility or egg hatch in *M. incognita* over 96 h. GAFP-1 strongly associated with the cell wall pellets prepared from *P. cinnamomi* and the fungus *Trichoderma viride*, providing evidence that GAFP-1 can bind cell wall components of a stramenopile pathogen as it has been hypothesized to do in fungi. Neither *gafp-1* transcripts nor the GAFP-1 lectin were detected within non-transformed plum tissues grafted to transgenic plum rootstocks after two years, suggesting that tissue expressing the lectin may be able to retain the foreign gene products so that they will not enter the fruit where they could potentially be consumed. Future plans include multi-year disease trials with transgenic plum lines against fungal

and non-fungal pathogens, monitoring of chimeric-grafted plants for the possible accumulation of GAFP-1 in non-transformed tissues after seasonal changes in the field, and further investigation into the mechanism of a lectin which has great potential for agricultural application.

DEDICATION

This manuscript is dedicated to all the people who helped me, whether directly or indirectly, to accomplish this work. I would particularly like to thank my husband, whose sacrifices made all of this possible.

ACKNOWLEDGEMENTS

I would like to acknowledge Dr. Ralph Scorza and Dr. Cesar Petri who are affiliated with the USDA-ARS Appalachian Fruit Research Station from Kearneysville, WV. They contributed to the work presented in Chapter 2 and co-authored the resulting publication (Nagel et al., 2008). Likewise, Hetal Kalariya, a fellow graduate student from the Department of Entomology, Soils, and Plant Sciences at Clemson University, SC assisted with the experiments presented in Chapter 3 and co-authored on that research which was eventually published (Nagel et al., 2010). I am thankful to Dr. Andy Nyczepir of the USDA-ARS Southeastern Fruit and Tree Nut Research Laboratory in Byron, GA and Dr. Paula Agudelo and David Harshman from the Department of Entomology, Soils, and Plant Sciences at Clemson University, SC for donating of isolates of *M. incognita*. Dr. Steve Jeffers and his technician Lynn Luszcz from the Department of Entomology, Soils, and Plant Sciences donated not only *Phytophthora sp.* isolates but also their equipment. Dr. William Bridges from the Department of Mathematics at Clemson was very helpful with statistical analysis. I would also like to extend my thanks to Dr. Michael Sehorn from the Clemson Department of Genetics and Biochemistry who tutored me in chromatographic techniques, as well as Dr. Matt Turnbull from the Department of Biological Sciences who instructed me in fluorescence microscopy and allowed me use of his microscope. I would like to thank Dr. Simon Scott of the Department of Entomology, Soils, and Plant Sciences, and lab members Karen Bryson, Courtney McClive, Wendy Chai, and Dr. Fuxing Zhu, for technical assistance. Lastly, I am very grateful to my principle investigator, Dr. Guido Schnabel, and my committee members, Dr.'s William Marcotte, Kerry Smith, Brandon Moore, and Brian Dominy, without whose help and input this project could not have been accomplished. The research

presented in this manuscript was funded by the United States Department of Agriculture, South Carolina Peach Council, and Robert Coker South Carolina Farm Bureau Fellowship.

TABLE OF CONTENTS

Page

TABLE OF CONTENTS (CONTINUED)

Page

TABLE OF CONTENTS (CONTINUED)

Page

LIST OF TABLES

LIST OF TABLES (CONTINUED)

Table Page

LIST OF FIGURES

LIST OF FIGURES (CONTINUED)

LIST OF FIGURES (CONTINUED)

Figure Page

LIST OF FIGURES (CONTINUED)

Figure Page

CHAPTER ONE

INTRODUCTION

South Carolina and Georgia are the second and third largest peach producing regions in the United States, respectively. Together these states generate approximately $60 million worth (~90,000 tons) of fruit per year on average (IPM, 2004; NASS, 2006; NASS, 2009). Peaches and other stone-fruit species (*Prunus sp*.) from these areas face heavy pest pressure due to the warm and wet conditions which predominate in the Southeastern U.S. Common diseases of *Prunus* are caused by pathogens which can infect the fruit [e.g. brown rot (*Monilinia fructicola, M. laxa, M. fructigena*), peach scab (*Cladosporium carpophilum*), bacterial spot (*Xanthomonas arboricola pv. pruni*), etc.] or the tree itself [e.g. Armillaria root and crown rot (*Armillaria tabescens, A. mellea*), Phytophthora root and crown rot (*Phytophthora sp.*), plant parasitic ring (*Mesocriconema xenoplax*) and root-knot nematodes (*Meloidogyne sp.*), and bacterial canker (*Pseudomonas syringae*)] (IPM, 2004; Ogawa *et al*., 1995). Infection by such pathogens challenges the sustainability of the industry. Pathogens of the fruit can severely affect the quality of the produce and annual yield, but vegetative diseases will negatively impact tree vigor and mortality over a longer period of time. Many stone-fruit species require preventative applications of chemical pesticides for successful pathogen control (IPM, 2004). The sustainability of chemical control strategies is questionable, however, since pesticides can have potentially harmful short- and long-term effects on the environment and human health (Arbuckle *et al*., 2001; EPA, 2009; Eskenazi *et al.*, 1999; Garry, 2004). Additionally, pathogens can develop resistance to existing compounds after prolonged exposure, which decreases the efficacy of current disease control methods. For example, decreased sensitivities to fungicides in brown-rot causing *Monilinia* species have been

reported in many peach producing areas (Elmer and Gaunt., 1994; Ma *et al*., 2003; Ma *et al*., 2005; Michailides *et al*., 1987). Of large concern to Southeastern growers is the identification of *M. fructicola* field isolates with increased resistance to fungicides from three approved chemical classes, the benzimidizoles (BZIs) (Zehr *et al*., 1991), de-methylation inhibitors (DMIs) (Zehr *et al*., 1999; Schnabel *et al*., 2004; Schnabel and Dai, 2004), and quinone outside inhibitors (QoIs) (Amiri *et al*., 2010). It is now essential that different mode-of-action pesticides be rotated so that unnecessary selection pressure on target organisms can be avoided (IPM, 2004). Peach production generates a significant amount of agricultural revenue for the Southeast, and for this reason it is necessary that existing pest management methods be continually evaluated, and novel tactics for pathogen control developed, so that growers will continue to have new options for combating diseases.

As opposed to traditional breeding, disease resistance is now being improved in agricultural crops through genetic modification of defense-related traits. The United States was one of the first countries to cultivate genetically modified (GM) crops, beginning with the deregulation of the ripening-delayed FLAVR SAVR™ tomato in 1992 (James, 2008; Medley, 1992). Today, the U.S. has over 150 million acres devoted to GM crops such as maize, sugarcane, wheat, soybean, sugar beet, cotton, canola, and alfalfa (James, 2008). The most common GM crops to be cultivated in the U.S., as well as globally, are those engineered for increased tolerance to herbicides and insects (James, 2003; Schahczenski and Adam, 2006). Gene-stacked GM crops which contain both types of resistance are also now in production (James *et al*., 2008). Transgenic strategies for herbicide resistance in crops include expression of phosphinothricin acetyltransferase (PAT) proteins from *Streptomyces* or over-expression of 5-enolpyruvylshikimate- 3-phosphate (EPSP) synthase (Schahczenski and Adam, 2006). These enzymes confer increased resistance to broad-spectrum glufosinate-ammonium- and

glyphosphate-containing herbicides, respectively (Hérouet *et al*., 2005; Shah *et al*., 1986). Many commercialized insect-resistant transgenic crops express *Bt* toxins, or CRYSTAL (cry) proteins, which are a diverse group of alpha-endotoxins found in spores of the gram-positive bacterium *Bacillus thuringiensis* (Fontes *et al.*, 2002). The proteins become activated by proteolysis in the insect gut when plant material possessing the endotoxin is consumed. The toxins create pores in epithelial cell membranes (Hofte and Whiteley, 1989), resulting in disruption of transmembrane gradients and the eventual death of the insect. Other anti-metabolic proteins such as serine protease and α-amylase inhibitors, which respectively prevent the breakdown of proteins and complex starches, are also effective insecticidal agents when expressed in a heterologous system (Duan *et al*., 1996; Gatehouse *et al.*, 1997; Shade *et al.*, 1994; Shroeder *et al.*, 1995; Xu *et al*., 1996). Exposure to such plant-derived molecules is not expected to have negative impacts on human health due to existing dietary adaptations and inactivation of these compounds through cooking (Duan *et al.*, 1996; Hérouet *et al*., 2005), however some still question the safety of GM produce (Boccaletti and Moro, 2000; Bukenya and Wright, 2007; Burton *et al.*, 2001; Fontes *et al*., 2002). Despite concerns over biosafety, the total geographic area devoted to GM crops has ballooned to more than 300 million acres in 25 countries since 1996 (James, 2008). Engineering of agricultural crops for increased resistance to diseases has now become a viable alternative to traditional pest management methods.

Perennial woody species such as fruit-bearing trees and vines are also being engineered for decreased disease susceptibility (Petri and Burgos, 2005; Lavi *et al*., 2006). The transgenic papaya expressing the coat protein (*cp*) gene of the *Papaya ringspot virus* (PRSV) (Fitch *et al*., 1992, Lius *et al*., 1997) is probably one of the most well-known examples of a successful GM woody crop. The Hawaiian papaya industry was close to being decimated by PRSV infection before the highly resistant transgenic papaya “55-1” line was commercialized in 1998 (Gonsalves

et al., 1998). It is thought that viral coat protein expression *in vivo* prevents decapsidation of the virus particle and subsequent expression of viral genes in the plant cell. Coat protein expression is being explored in GM citrus crops such as lime (Dominguez *et al*., 2002), orange (Ghorbel *et al*., 2000) and grapefruit (Yang *et al*., 2000) to protect against *Citrus tristeza virus*. In GM plum *cp* expression has been shown to deter infection by the *Plum pox virus* (Malinowski *et al*. 2006). Increased mortality of Lepidopteran insects was observed on *Bt* toxin-producing walnut (Dandekar *et al*., 1998) and Japanese persimmon (Tao *et al*., 1997). Transformation of grape vine with the chitinase-encoding *RCC2* gene from rice resulted in enhanced resistance to the fungi *Uncinula necator* and *Elisinoe ampelina*, the causal agents of powdery mildew and anthracnose, respectively (Yamamoto *et al*., 2000). Likewise the introduction of endo- and exochitinase genes *ech42* and *nag70*, respectively, from the fungus *Trichoderma atroviride* into apple lessened the effects of fungal scab caused by *Venturia inaequalis* (Faize *et al*., 2003).

Many soil-borne diseases can negatively impact fruit production, however there not many examples of GM fruit trees which have been developed for resistance to root-associated pathogens. One of the few studies to demonstrate such a concept is that of Fagoaga *et al.* (2001), in which citrus lines expressing a pathogenesis-related gene (PR-5) from tomato were shown to be tolerant to infection by the stramenopile *Phytophthora citrophthora*. The economic consequences of some rootstock diseases can be quite severe, as demonstrated by the effects of Peach Tree Short life (PTSL) and Armillaria root rot (ARR) on *Prunus* in the Southeast. PTSL, a disease complex involving the ring nematode *Mesocriconema xenoplax* and the gram-negative bacterium *Pseudomonas syringae*, and ARR, which is caused primarily by the basidiomycete *Armillaria tabescens*, are the two leading causes of peach tree mortality in South Carolina and Georgia (Beckman, 1997; Beckman, 1998; Schnabel *et al*., 2005). Both are facilitated by cold injury and are estimated to result in lifetime losses of around $5-10 million. Because physical

access to the root system is restricted, the efficacy of traditional and chemical control methods on soil-borne diseases can also be limited. The development of GM woody rootstocks with enhanced tolerance to various root diseases could become an important part of future integrated pest management (IPM) practices.

Plant lectins are a promising class of molecules for engineering resistance to root-associated pathogens. Lectins are proteins which can accommodate specific mono- or polysaccharide ligands within their carbohydrate recognition domain(s) (CRDs). Lectins are distinct from other carbohydrate-binding enzymes, however, in that ligand modification does not occur within the CRD itself (Peumans and Van Damme, 1995). A lectin, which possesses at least one CRD, can be associated with unrelated peptide domains which are capable of catalytic activity. Seven families of plant lectins have been classified based upon sequence information and structural analysis: the *Cucurbitaceae* phloem lectins, amaranthins, jacalin-related lectins, chitin-binding lectins, legume lectins, type 2 ribosome-inactivating proteins (RIPs), and monocot mannose-binding lectins (MMBLs), (Van Damme *et al*., 1998). Many plant lectins act to defend their hosts against bacterial, fungal, and insect invaders (Peumans and Van Damme, 1995; Van Damme *et al*., 1998), and lectins from multiple plant and protein families have demonstrated activity against harmful pests and diseases when heterologously expressed (Gatehouse *et al*., 1997; Koo *et al*., 2002; Lee *et al*., 2003; Schroeder *et al*., 1995; Shade *et al*., 1994; Ripoll *et al*., 2003).

One MMBL, the *Gastrodia* anti-fungal protein (GAFP), is active against a range of phytopathogens. GAFP comes from the achlorophyllic orchid *Gastrodia elata*, which obtains the nutrients necessary for its growth and reproduction from a symbiotically associated fungus, the basidiomycete *Armillaria mellea* (Wang *et al*., 2001; Hu *et al*., 1988). Hyphae from the saprophytic fungus are able to superficially infect the root system of the orchid, but fungal growth

is eventually halted at the outer cortical layer (Hu and Huang, 1994). The native GAFP promoter is responsive to plant defense hormones jasmonic and salicylic acid (Sa *et al*., 2003), and invasion of *G. elata* primary corms by *A. mellea* triggers a high degree of root-specific expression (it is estimated that 51% of the total cellular protein content in infected primary corms is GAFP, versus only 1.7% in non-infected corms) (Hu and Huang, 1994; Wang *et al*., 2001; Xu *et al*., 1998; Yang and Hu, 1990). Chitinase and β-1,3 glucanase enzymes, which are produced at 5 to 10 times lower levels than the MMBL within infected roots, exhibited about 34 and 56 times less inhibitory activity than purified GAFP on the basidiomycete *T. viride*, respectively (Yang and Hu, 1990). This provided evidence that the GAFP lectin is the primary protein responsible for inhibiting the growth of the fungal hyphae within *G. elata*. The fungal hyphae are then presumably digested by the action of cell wall degrading enzymes and the released nutrients are transported to other areas of the developing plant.

When purified from induced corms, GAFP demonstrated strong inhibitory activity *in vitro* against many species of plant parasitic fungi, including *Armillaria mellea, Trichoderma viride, Rhizoctonia solani, Valsa ambiens, Gibberella zeae, Ganoderma lucidum,* and *Botrytis cinerea* (Hu and Huang, 1994; Xu *et al*., 1998). Moreover, expression of GAFP in transgenic cotton increased resistance to the ascomycete *Verticillium dahliae* (Wang *et al*., 2004), and in transgenic tobacco expression of the lectin resulted in enhanced tolerance to the stramenopile pathogen *Phytophthora nicotianae*, the root-knot nematode *Meloidogyne incognita*, and the basidiomycete fungus *R. solani* (Cox *et al*., 2006). The fact that this lectin has demonstrated activity against harmful organisms in multiple GM systems enhances its potential for use as a biostatic agent. In addition, the latter study was the first to provide evidence that GAFP might be able to target pathogens of non-fungal origin. The GAFP lectin would therefore be ideal for the engineering of a disease-resistant rootstock for stone-fruits due to its broad-spectrum activity

against plant pathogens. In the following chapters I describe my efforts to characterize the action of GAFP-1 against fungal and non-fungal pathogens both *in vivo* and *in vitro*.

LITERATURE CITED

Amiri, A., P.M. Brannen,, and G. Schnabel. 2010. Reduced sensitivity in *Monilinia fructicola* field isolates from South Carolina and Georgia to respiration inhibitor fungicides. Plant Dis. 94:737-743.

Arbuckle, T.E., Z. Lin, and L.S. Mery. 2001. An exploratory analysis of the effect of pesticide exposure on the risk of spontaneous abortion in an Ontario farm population. Env. Health Perspectives 109:851-857.

Beckman, T.G., W.R. Okie, A.P. Nyczepir, G. L. Reighard, E.I. Zehr, and W.C. Newall. 1997. History, current status and future potential of the Guardian™ (BY520-9) peach rootstock. Acta Hort. (ISHS) 451:251-258. <http://www.actahort.org/books/451/451_27.htm/>.

Beckman, T.G. 1998. Developing Armillaria resistant rootstocks for peach. Acta Hort. (ISHS) 465:219-224. <http://www.actahort.org/books/465/465_26.htm/>.

Boccaletti, S. and D. Moro. 2000. Consumer willingness-to-pay for GM food products in Italy. AgBioForum. 3:259-267. 1 July 2009. <http://www.agbioforum.org/>.

Bukenya, J.O. and N.R. Wright. 2007. Determinants of Consumer Attitudes and Purchase Intentions with Regard to Genetically Modified Tomatoes. Agribusiness 23:117-130.

Burton, M., D. Rigby, T. Young, and S. James. 2001. Consumer attitudes to genetically modified organisms in food in the UK. European Rev. Agr. Econ. 28:479-498.

Cox, K., D. Layne, R. Scorza, and G. Schnabel. 2006. Gastrodia anti-fungal protein from the orchid *Gastrodia elata* confers disease resistance to root pathogens in transgenic tobacco. Planta 224:1373-1383.

Dandekar, A.M., G.H. McGranahan, P.V. Vail, S.L. Uratsu, C. Leslie, and J.S. Tebbets. 1998. High levels of expression of full length cryIA(c) gene from *Bacillus thuringiensis* in transgenic somatic walnut embryos. Plant Sci. 131:181-193.

Dominguez, A., A. Hermoso de Mendoza, J. Guerri, M. Cambra, L. Navarro, P. Moreno, and L. Peña. 2002. Pathogen-derived resistance to *Citrus tristeza virus* (CTV) in trangenic mexican lime (*Citrus aurantifolia* (Christ.) Swing.) plants expressing its *p25* coat protein gene. Mol. Breeding. 10:1-10.

Duan, X., X. Li, Q. Xue, M. Abo-El-Saad, D. Xu, and R. Wu. 1996. Transgenic rice plants harboring an introduced potato proteinase inhibitor II gene are insect resistant. Nat. Biotechnol. 14:494-496.

Elmer, P.A.G., and R.E. Gaunt. 1994. The biological characteristics of dicarboximide-resistant isolates of *Monilinia fructicola* from New Zealand stone-fruit orchards. Plant Path. 43:130-137.

EPA: Environmental Protection Agency. 2009. Pesticide spray and dust drift. Pesticides: topical and chemical fact sheets, U.S. Env. Protection Agency. 11 July 2009. < http://www.epa.gov/ opp00001/factsheets/spraydrift.htm/>.

Eskenazi, B., A. Bradman, and R. Castorina. 1999. Exposures of children to organophosphate pesticides and their potential adverse health effects. Env. Health Perspectives 107:409-419.

Fagoaga, C., I. Rodrigo, V. Conejero, C. Hinarejos, J.J. Tuset, J. Arnau, J.A. Pina, L. Navarro, and L. Pena. 2001. Increased tolerance to Phytophthora citrophthora in transgenic orange plants constitutively expressing a tomato pathogenesis related protein PR-5. Mol. Breeding 7:175–185.

Faize, M., M. Malnoy, F. Dupuis, M. Chevalier, L. Parisi, and E. Chevreau. 2003. Chitinases of Trichoderma atroviride induce scab resistance and some metabolic changes in two cultivars of apple. Phytopathology 93:1496–1504.

Fitch, M.M.M., R.M. Manshardt, D. Gonsalves, J.L. Slightom, and J.C. Sanford. 1992. Virus resistance papaya plants derived from tissues bombarded with the coat protein gene of Papaya ringspot virus. Biotechnology 10:1466 (abstr.).

Fontes, E.M.G., Pires, C.S.S., E.R. Suji, and A.R. Panizzi. 2002. The environmental effects of genetically modified crops resistant to insects. Neotropical Entomol. 31:497-513.

Gatehouse, A.M.R., G.M. Davison, C.A. Newell, A. Merryweather, W.D.O. Hamilton, E.P.J. Burgess, R.J.C. Gilbert, and J.A. Gatehouse. 1997. Transgenic potato plants with enhanced resistance to the tomato moth, *Lacanobia oleracea*, growthroom trials. Mol. Breed. 3:49-63.

Garry, V.F. 2004. Pesticides and children. Toxicology and Appl. Pharmacology 198:152-163.

Ghorbel, R., A. Domínguez, L. Navarro, and L. Peña. 2000. High efficiency genetic transformation of sour orange (Citrus aurantium) and production of transgenic trees containing the coat protein gene of citrus tristeza virus. Tree Physiol. 20:1183–1189.

Gonsalves, D., Ferreira, S., Manshardt, R., Fitch, M., and Slightom, J. 1998. Transgenic virus resistant papaya: New hope for control of papaya ringspot virus in Hawaii. APS*net* Feature, American Pythopathological Society. 12 July 2010. < http://www.apsnet.org/education/feature/papaya/>.

Hérouet, C., D.J. Esdaile, B.A. Mallyon, E. Debruyne, A. Schulz, T. Currier, K. Hendrickx, R.-J. van der Klis, and D. Rouan. 2005. Safety evaluation of the phosphinothricin acetyltransferase proteins encoded by the *pat* and *bar* sequences that confer tolerance to glufosinate-ammonium herbicide in transgenic plants. Regulat. Toxicology and Pharmacology 41:134-139.

Hofte, H. and H.R. Whiteley. 1989. Insecticidal crystal proteins of *Bacillus thuringiensis*. Microbiological Rev. 53:242-255.

Hu, Z., Z. Yang, and J. Wang. 1988. Isolation and partial characterization of an antifungal protein from *Gastrodia elata* corm. Acta Botanica Yunnanica 10(4):373 (abstr.).

Hu, Z. and Q.Z. Huang. 1994. Induction and accumulation of the antifungal protein in Gastrodia elata. Acta Botannica Yunnanica 16:169-177.

IPM: Integrated Pest Management. 2004. Crop profiles for peaches in Georgia and South Carolina. Regional IPM Centers, U.S. Dept. Agr. 10 December 2007. <http://www.ipmcenters.org/cropprofiles/docs/GASCpeaches.html/>.

James, C. 2003. Global review of commercialized transgenic crops. Current Sci. 84:303-309.

James, C. 2008. Brief 39: Global status of commercialized biotech/GM crops. Intl. Service for the Acquisition of Agri-biotech Applications. <http://www.isaaa.org/resources/publications/briefs/39/download/isaaa-brief-39-2008.pdf/>.

Koo, J.C., H.J. Chun, H.C. Park, M.C. Kim, Y.D. Koo, S.C. Koo, H.M. Ok, S.J. Park, S.H. Lee, D.J. Yun, C.O. Lim, J.D. Bahk, S.Y. Lee, and M.J. Cho. 2002. Over-expression of a seed specific hevein-like antimicrobial peptide from *Pharbitis nil* enhances resistance to a fungal pathogen in transgenic tobacco plants. Plant Mol. Biol. 50:441–452.

Lavi, U., S. Gurevitz, G.B. Ari, D. Saada, K. Kashkush, T. Paz, T. Twito, Y. Cohen, J. Hillel, and G. Simchen. 2006. Potential applications of modern biological techniques in breeding fruit trees. J. Fruit and Ornamental Plant Res. 14:13-19.

Lee, O.K., B. Lee, N. Park, J.C. Koo, Y.H. Kim, T.P. Da, C. Karigar, H.J. Chun, B.R. Jeonga, D.H. Kim, J. Nam, J.G. Yun, S.S. Kwak, M.J. Cho, D.J. Yun. 2003. Pn-AMPs, the hevein-like proteins from *Pharbitis nil* confers disease resistance against phytopathogenic fungi in tomato, *Lycopersicum esculentum.* Phytochemistry 62:1073-1079.

Lius, S., R.M. Manshardt, M.M.M Fitch., J.L. Slightom, J.C. Sanford, and D. Gonsalves. 1997. Pathogen-derived resistance provides papaya with effective protection against papya ringspot virus. Mol. Breeding 3:161-168.

Ma, Z., M.A. Yoshimura, and T.J. Michailides. 2003. Identification and characterization of benzimidazole resistance in *Monilinia fructicola* from stone fruit orchards in California. App. Env. Microbiol. 69:7145-7152.

Ma, Z., M.A. Yoshimura, B.A. Holtz, and T.J. Michailides. 2005. Characterization and PCR-based detection of benzimidazole-resitant isolates of *Monilinia laxa* in California. Pest Mgt. Sci. 61:449-457.

Malinowski, T., M. Cambra, N. Capote, M.T. Gorris, R. Scorza, M. Ravelonandro. 2006. Field trials of plum clones transformed with the *Plum pox virus* coat protein (PPV-CP) gene. Plant Dis. 90:1012-1018.

Michailides, T.J., J.M. Ogawa, and D.C. Opgenorth. 1987. Shift of *Monilinia* spp and distribution of isolates sensitive and resistant to benomyl in California prune and apricot orchards. Plant Dis. 71:893–896.

Medley, T.L. 1992. Interpretive ruling on Calgene, Inc., petition for determination of regulatory status of FLAVR SAVR™ tomato. Fed. Regis. 57:47608-47616.

NASS: National Agricultural Statistics Service. 2006. Peach production report. U.S. Dept. Agr. 10 July 2010. < http://www.nass.usda.gov/Statistics_by_State/South_Carolina/Publications/ Current_News_Release/Peach_Production/PEACH0706.pdf/>.

NASS: National Agricultural Statistics Service. 2009. Farm facts for South Carolina. Issue No. 2-09. U.S. Dept. Agr. 3 December 2009. <http://www.nass.usda.gov/Statistics_by_State/ South_Carolina/Publications/Farm_Facts/SC_ff021309.pdf/>.

Ogawa, J.M., E.I. Zehr, and A.R. Biggs. 1995. Part I: Infections diseases, diseases caused by fungi, fruit diseases: Brown Rot, p. 7-10. In: J.M. Ogawa, E.I. Zehr, G.W. Bird, D.F. Ritchie, K. Uriu, and J.K. Uyemoto (eds.). Compendium of stone-fruit diseases. Amer. Phytopathol. Soc. Press, St. Paul, MN.

Petri, C. and L. Burgos. 2005. Transformation of fruit trees. Useful breeding tool or continued future prospect. Transgenic Res. 14:15-26.

Peumans, W.J. and E.J.M. Van Damme. 1995. Lectins as plant defense proteins. Plant Physiol. 109:347–352.

Ripoll, C., B. Favery, P. Lecomte, E. Van Damme, W. Peumans, P. Abad, L. Jouanin. 2003. Evaluation of the ability of lectin from snowdrop (*Galanthus nivalis*) to protect plants against root-knot nematodes. Plant Sci. 164:517-523.

Sa, Q., Y. Wang, W. Li, L. Zhang, and Y. Sun. 2003. The promoter of an antifungal protein gene from *Gastrodia elata* confers tissue-specific and fungus-inducible expression patterns and responds to both salicylic acid and jasmonic acid. Plant Cell Rep. 22:79-84.

Shah, D.M., R.B. Horsch, H.J. Klee, G.M. Kishore, J.A. Winter, N.R. Siegel, S.G. Rogers, and R.T. Fraley. 1986. Engineering herbicide tolerance in transgenic plants. Science 233:478-481.

Shroeder, H.E., S. Gollasch, A. Moore, L.M. Tabe, S. Craig, D.C. Hardie, M.J. Chrispeels, D. Spencer, and T.J.V. Higgins. 1995. Bean alpha-amylase inhibitor confers resistance to pea weevil (*Bruchus pisorum*) in transgenic peas (*Pisum sativum* L.). Plant Physiol. 107:1233-1239.

Schnabel, G., P.K. Bryson, W.C. Bridges, and P.M. Brannen. 2004. Reduced sensitivity in *Monilinia fructicola* to propiconazole in Georgia and implications for disease management. Plant Dis. 88. 1000-1004.

Schnabel, G. and Q. Dai. 2004. Heterologous expression of the P450 sterol 14α-demethylase gene from *Monilinia fructicola* reduces sensitivity to some but not all DMI fungicides. Pesticide Biochem. Physiol. 78:31-38.

Schnabel, G., J.S. Ash, and P.K. Bryson. 2005. Identification and characterization of Armillaria tabescens from the southeastern United States. Mycol. Res. 109:1208-1222.

Schahczenski, J. and K. Adam. 2006. Transgenic Crops. ATTRA, National Sustainable Agriculture Information Service, U.S. Dept. Agr. 15 December 2007. <http://www.attra.ncat.org/attra-pub/PDF/geneticeng.pdf/>.

Shade, R.E., H.E. Schroeder, J.J. Pueyo, L.M. Tabe, L.L. Murdock, T.J.V. Higgins & M.J. Chrispeels. 1994. Transgenic pea seeds expressing the alpha-amylase inhibitor of the common bean are resistant to bruchid beetles. Nature Biotechnology 12:793 (abstr.).

Tao, R., A.M. Dandekar, S.L. Uratsu, P.V. Vail, and J.S. Tebbets. 1997. Engineering genetic resistance against insects in Japanese persimmon using the *cry*IA(c) gene of *Bacillus thuringiensis*. J. Am. Soc. Hort. Sci. 122:764-771.

Van Damme, E.J.M., W.J. Peumans, A. Barre, and P. Rouge. 1998. Plant Lectins: a composite of several distinct families of structurally and evolutionary related proteins with diverse biological roles. Critical Rev. Plant Sci. 17:575–692.

Wang, X., G. Bauw, E.J.M. Van Damme, W.J. Peumans, Z.-L. Chen, M. Van Montagu, G. Angenon, and W. Dillen. 2001. Gastrodianin-like mannose-binding proteins: a novel class of plant proteins with antifungal properties. Plant J. 25:651:661.

Wang, Y., D. Chen, D. Wang, Q. Huang, Z. Yao, F. Liu, X. Wei, R. Li, Z. Zhang, and Y. Sun. 2004. Over-expression of *Gastrodia* anti-fungal protein enhances *Verticillium* wilt resistance in coloured cotton. Plant Breeding 123:454-459.

Xu, D.P., Q.Z. Xue, D. McElroy, Y. Malwal, V.A. Hilder, and R. Wu. 1996. Constitutive expression of a cowpea trypsin-inhibitor gene, *CpT1*, in transgenic rice plants confers resistance to 2 major rice insect pests. Mol. Breed. 2(2):167 (abstr.).

Xu, Q., Y. Liu, X. Wang, H. Gu, and Z. Chen. 1998. Purification and characterization of a novel anti-fungal protein from *Gastrodia elata*. Plant Physiol. Biochem. 36:899-905.

Yamamoto T., H. Iketani, H. Ieki, Y. Nishizawa, K. Notsuka, T. Hibi, T. Hayashi, and N. Matsuta. 2000. Transgenic grapevine plants expressing a rice chitinase with enhanced resistance to fungal pathogens. Plant Cell Rep. 19:639–646.

Yang, S.L. and Z. Hu. 1990. A preliminary study on the chitinase and β-1,3-Glucanase in corms of *Gastrodia elata.* Acta Botannica Yunnanica 12(4):421 (abstr.).

Yang, Z.N., I.L. Ingelbrecht, E. Louzada, M. Skaria, and T.E. Mirkov. 2000. Agrobacterium-mediated transformation of the commercially important grapefruit cultivar Rio Red (Citrus paradisi Macf.) Plant Cell Rep. 19:1203–1211.

Zehr, E.I., J.E. Toler, and L.A. Luszcz. 1991. Spread and persistence of benomyl-resistant *Monilinia fructicola* in South Carolina peach orchards. Plant Dis. 75:590-593.

Zehr, E.I., L.A. Luszcz, W.C. Olien, W.C. Newall, and J.E. Toler. 1999. Reduced sensitivity in *Monilinia fructicola* to propiconazole following prolonged exposure in peach orchards. Plant Dis. 83:913-916.

CHAPTER TWO

GENERATION AND CHARACTERIZATION OF TRANSGENIC PLUM LINES EXPRESSING THE *GASTRODIA* ANTI-FUNGAL PROTEIN

This work has been published:

Nagel, A.K., R. Scorza, C. Petri, and G. Schnabel. 2008. Generation and characterization of transgenic plum lines expressing the *Gastrodia*-Anti Fungal Protein. HortSci. 43:1514–1521.

ABSTRACT

It was demonstrated previously that expression of the anti-fungal GAFP-VNF lectin in tobacco (*Nicotianae tabacum*) confers increased tolerance to infection by taxonomically unrelated root pathogens *Rhizoctonia solani* (basidiomycota), *Phytophthora nicotianae* (heterokontophyta or stramenopiles), and *Meloidogyne incognita* (nematoda) (Cox *et al*., 2006). The ability of GAFP-VNF (GAFP-1) expression to reduce symptoms of stramenopile and nematode infection was explored in a stone-fruit species in this study. *Agrobacterium tumefacien*-mediated transformation yielded three *gafp-1* expressing plum (*Prunus domestica* var. 'Stanley') lines, designated 4J, 4I, and 5D. These lines possessed one, two, and four copies of the *gafp-1* gene, respectively. Lines 4J and 4I, which were not morphologically different from the non-transformed control line, exhibited significantly reduced symptoms of *P. cinnamomi* infection and a significantly lower degree of galling and egg mass formation in response to challenge with *M. incognita*. Nematode reproduction was significantly reduced in line 4J but not in line 4I or 5D. Line 5D, which diverged considerably from the non-transformed control line with respect to leaf

morphology and growth habit, did not display significantly reduced symptoms of infection by stramenopile or nematode pathogens. The altered morphology of the 5D line may be indicative of a detrimental insertion event. Any negative effects of the transformation process on plant physiology could have outweighed the potential benefits of GAFP-1 expression in this line. The results of this study suggest that the expression of *gafp-1* in the roots of a stone-fruit species can confer tolerance to Phytophthora root rot and root-knot nematode infestation.

INTRODUCTION

The root-knot nematode (RKN) and Phytophthora root rot (PRR) are two diseases associated with premature tree decline in stone-fruit orchards. RKN belonging to the genus *Meloidogyne* are sedentary endo-parasites that are ubiquitous in soils of the Southeastern United States. For example, *M. incognita* were found in 95% of the peach orchards sampled in South Carolina (Nyczepir *et al*., 1997). *Meloidogyne sp*. parasitize the root systems in a number of herbaceous and woody hosts, and infestation by RKN can cause significant damage to *Prunus* in the form of stunted growth, loss of vigor, and early defoliation of one to two-year-old trees. Pre-plant fumigation (e.g. Telone II), improves tree stand establishment and gives control for 2-5 years. However, the efficacy of the control procedure depends on the quality of the fumigation, the nematode species, and the rootstock resistance (Nyczepir, 1991; Sharpe *et al*, 1993). Current research efforts in the Southeast and in California have shifted toward various forms of non-chemical nematode control due to environmental concerns associated with soil fumigation.

PRR disease affects a wide variety of plant species, including stone-fruits such as peach, plum, apricot, nectarine and cherry (IPM, 1999), and is caused by stramenopile pathogens from the genus *Phytophthora*. *Phytophthora* species generally attack plant tissues at the soil line,

producing an area of necrotic tissue which eventually girdles the trunk. However primary infection can also occur within the rootstock or scion tissues. Disease onset can occur at any age of the tree, and infection is favored when warm temperatures and excessive soil moisture persist (Brown and Mircetich, 1995). Management practices for *Phytophthora sp*. are vital, and although some fungicides [e.g. fosetyl-al (Aliette®) and Ridomil®] are effective in controlling infection, they are generally utilized as post-disease onset rescue treatments. For these reasons it would be prudent to combine chemical control strategies with more sustainable methods such as effective water management practices and breeding of tolerant rootstocks (IPM, 1999).

The *Gastrodia* anti-fungal protein (GAFP), a monocot mannose-binding lectin (MMBL) found in the Asiatic orchid *Gastrodia elata* (Hu *et al*, 1988), is a promising agent for engineering increased tolerance to RKN and PRR in a stone-fruit species. Tobacco (*Nicotianae tabacum*) plants expressing the GAFP-VNF isoform demonstrated reduced symptom severity when challenged with the stramenopile *P. nicotianae*, the RKN *M. incognita*, as well as the basidiomycete fungus *Rhizoctonia solani* (Cox *et al.*, 2006). This study was the first to indicate that GAFP, a lectin with established anti-fungal activity, may be able to target selected non-fungal organisms. The objective of this study was to evaluate GAFP-VNF expressing stone-fruit trees for increased tolerance to PRR and RKN.

MATERIALS AND METHODS

["Transformation of plum" and "DNA blotting" were performed by Dr. Cesar Petri, affiliated with the lab of Dr. Ralph Scorza (USDA-ARS-AFRS, Kearneysville, WV).]

Transformation of plum

Plum was chosen as the model *Prunus* species due to the availability of a reliable transformation protocol. The nucleotide sequence of the *gafp-1-vnf* isoform (from here on referred to as *gafp-1*) was inserted into the multiple cloning site of the binary vector pAVAT1, a derivative of the pTHW136 expression vector, under the control of the 35S promoter and omega leader sequence as described by Wang *et al.*, 2001. The resulting chimeric vector (Plant Genetic Systems N. V., Gent, Belgium) was designated pAVNFbin. *Agrobacterium tumefaciens* strain EHA 101 was transformed with the pAVNFbin vector using the freeze-thaw protocol (Chen *et al.*, 1994). Bacterial colonies were selected on Luria broth agar (10 g/L tryptone, 5 g/L yeast extract, 10 g/L NaCl, 18 g/L agar; pH 7) amended with 50 mg/L kanamycin and 150 mg/L spectinomycin. The presence of *gafp-1* was confirmed in selected colonies by PCR with *gafp-1* specific primers (Wang *et al*. 2001). Plum (*Prunus domestica* var. 'Stanley') hypocotyls from seeds of open-pollinated 'Stanley' were transformed following the protocols of Padilla *et al.* (2003). After transformation, genomic DNA was isolated from root and leaf tissue of transformed plums using the DNeasy Plant Mini Kit (Qiagen, Valencia, CA) and amplified by PCR as described above to initially verify the presence of *gafp-1*. Four transgenic lines containing the *gafp-1* gene were obtained via *A. tumefaciens*-mediated transformation. Three lines were chosen for further experimentation and were designated 4J, 4I, and 5D. The fourth line was excluded from disease assays due to weak growth and limited propagation success.

DNA blotting

DNA was isolated from young, fully expanded plum leaves of transgenic and non-transformed plum plants following the procedures of Kobayashi *et al.* (1998). Briefly, DNA (13

µg) was digested with the restriction enzyme *Bam*HI (New England Biolabs, Ipswich, MA, USA), separated on a 1 % (w/v) agarose gel and blotted to a positively charged nylon membrane (Roche Diagnostics Corporation, Indianapolis, IN, USA). The filter was hybridized with a Digoxigenin-11-dUTP alkali-labile labeled probe (Roche) coding for *gafp-1* cDNA. The probe was generated by PCR using the *gafp-1* specific primers described above.

Detection of GAFP-1 in transgenic lines

GAFP-1 synthesis was confirmed in transgenic lines by immunoblot analysis of root tissue protein extracts. Total cellular protein was extracted from young root tissue (100 mg) of 1-year-old trees using 700 µL TRIzol Reagent© (Invitrogen Corporation, Carlsbad, CA, USA) according to the methods of Chomczynski, 1993. Total cellular protein (10 µL) was separated on an 18% Tris-HCl gel by SDS-PAGE and transferred to a PVDF membrane overnight (30 V) at 4 ^{o}C. Membranes were rinsed 3 times in de-ionized (dI) water and air-dried for 1 h to fix peptides to the membrane. Prior to blocking, membranes were re-wet in methanol and rinsed in water. Membranes were incubated with affinity-purified, polyclonal GAFP-1 antibodies (1:1000 dilution) developed by Zymed® Laboratories (Invitrogen) and alkaline phosphatase-conjugated secondary antibodies (1:2500 dilution) (Promega Corp., Madison, WI, USA) according to standard methods (Gallagher *et al.*, 1997). GAFP-1 was detected on membranes with BCIP/NBT (Sigmafast^{TM}; Sigma Aldrich, St. Louis, MO, USA). Recombinant GAFP-1 purified from *E. coli* and cleaved from a maltose-binding protein fusion with Factor Xa according to the parameters of Wang et al., 2001 was used as a standard. Protein extraction and GAFP-1 detection were performed twice for root tissues from each line.

Morphological data

Growth and morphological characteristics were evaluated for 2-year old trees from transgenic and non-transformed control lines. Being roughly elliptical in shape, leaf areas were estimated using the formula $A = \pi LW$, where L and W represent half the length and half the width of the leaf, respectively. Counting backwards from the apical meristem, leaf area was measured for leaves at positions 1, 3, 5, 7, and 9 on a single branch. Internodes were counted on a 30 cm branch section beginning at position 1. Position 1 corresponded to the first expanded leaf at the branch tip to exhibit non-curled edges. Average values and standard deviations for leaf area and internode number were determined from nine branches per line.

Plant materials and treatments

Plants for disease assays were clonally propagated from original transformed or control plum lines (T_0 generation). T_0 trees were pruned every three months to encourage shoot growth. When newly flushed shoots were approximately 12 to 15 cm long, they were cut and pruned to a length of 10 cm and gently scored (5 mm in length) along the base of the shoot with a razor blade. The scored area was dipped briefly in 10% indole 3-butyric acid (IBA) (Miracle-Gro "Fast Root" rooting hormone; Miracle-Gro Lawn Products, Inc., Marysville, OH, USA]. Shoots were placed approximately 3 cm deep in 15 cm^3 sterile vermiculite under humidity domes to prevent dehydration. Domes were removed 1-2 weeks after transplanting. The healthiest rooted cuttings were selected for disease screening at the end of 90 d. All T_0 lines, rooted cuttings, and disease trials were kept in a biosafety level 2 greenhouse under constant temperature (27 ± 5 °C) and light (16/8 h day/night) conditions. Plants were watered, fertilized, and pruned as necessary.

Disease resistance screening

All disease assays were performed twice with 5 to 10 single tree replicates per disease treatment. Inoculated, non-transformed plum lines were used as positive controls for decline due to pathogen infection. An additional 5 to 10 tree replicates from each transgenic line and the control line were left uninoculated during disease assays and served as the negative control groups. Inoculated and uninoculated experimental plants were arranged in randomized complete blocks on greenhouse benches.

Plum lines were challenged with *Phytophthora cinnamomi* (isolate 05-1127) isolated from naturally infected peach (*Prunus persica*) (Clemson, SC). *P. cinnamomi* cultures were maintained on plates (8.5 cm) containing PARP selective medium [per liter H_2O: 5% by volume clarified V8-juice concentrate, 15 g agar, 10 mg pimarcin, 250 mg ampicillin, 10 mg rifmycin, 66.7 mg pentachloronitrobenzene (PCNB)] (Jeffers and Martin, 1986) dark (22 ºC). Five plugs (6 mm in diameter) were taken from the periphery of 3-d-old active cultures and added to Erlenmeyer flasks (1000 mL) containing 300 mL of a sterile, V8-juice:vermiculite (1:2 v/v) mixture. Inoculated flasks were incubated in the dark at 22 ºC for 8 weeks with periodic shaking. After 8 weeks, small pieces of infested vermiculite were incubated on potato dextrose agar (PDA) for 5 d in the dark to confirm the purity of the inoculum.

Plants (90-d-old) were transplanted to plastic torpedo pots (diameter = 5 cm) containing approximately 400 cm^3 sterile potting soil mixed with infested V8-juice:vermiculite (2% by volume). Plants from negative control treatments were transplanted into soil mixed with uninfested, sterile V8-juice:vermiculite. Pots were suspended in plastic racks (10 pots per rack) and placed in 10 gallon plastic bins. Plants were watered as needed and after 1 week were flooded

for 48 h to promote infection. Symptoms of *P. cinnamomi* infection, such as wilting, chlorosis, and necrosis of leaf and stem tissues, were evaluated every other day. Symptoms were rated as follows: 0 = healthy plant with no affected tissues, 1 = wilting and less than 25% of the plant exhibiting symptoms of chlorosis and necrosis, 2 = between 26 and 50% of the plant exhibiting symptoms of chlorosis and necrosis, 3 = between 51 and 75% of the plant exhibiting symptoms of chlorosis and necrosis, 4 = greater than 75% of the plant exhibiting symptoms of chlorosis and necrosis. Experiments were concluded after 20 d, when the majority of inoculated control plants had died. Fresh root weight was recorded for inoculated seedlings. Random root pieces were sampled from inoculated seedlings and were incubated on PARPH [PARP + 50 mg 5-methylisoxazol-3-ol (hymexazol)] selective medium to confirm infection by *P. cinnamomi*.

Plum lines were challenged with *M. incognita* (Kofoid & White) Chitwood originally isolated from infected peach (Byron, GA). RKN were maintained on 60-d-old tomato plants (cv. 'Rutgers') and re-cultured every 60 d. Plants (90-d-old) were transplanted into plastic pots (diameter = 20 cm) containing 1000 cm^3 of sterile sand:vermiculite (1:1 v/v). RKN eggs were extracted from infected tomato roots using a 10% NaOCl solution diluted in water (Hussey and Barker, 1973). Eggs were washed thoroughly in tap water and added (6000 count) to the soil around the base of the plants via three holes (~1 cm deep) created in the soil. Negative control plants were inoculated with tap water in the same manner.

Infection was allowed to proceed for 60 d, after which time the plum roots were excavated and the root systems were rated for susceptibility to RKN. Root systems were harvested, washed with water and dried to a damp condition. Egg masses on the root systems were stained with Phloxine B for 20 min and counted (Dickson and Struble, 1965). One minute of counting time was allowed per root system in an effort to standardize the mass counts. Root systems were then rated for galls according to the following scale: 0 = no detectable infection, 1 =

trace infection or less than 10% of the root system galled, 2 = between 10 and 25% of the root system galled, 3 = between 26 and 50% of the root system galled, 4 = between 51 and 75% of the root system galled, 5 = greater than 75% of the root system galled (Barker, 1985). Wet root weight was determined for each root system after drying with a paper towel to remove excess stain. Eggs were extracted from plum roots with a 10% NaOCl solution and quantified on a nematode counting slide. Raw egg counts were normalized against fresh root weight.

Statistical analysis

All calculations were performed using SAS (SAS version 9.1; SAS Institute Inc., Cary, NC, USA) and a significance level of $\alpha = 0.05$. Qualitative scores (symptom severity scores for *P. cinnamomi* and gall ratings for *M. incognita*) were analyzed as follows. Frequency distributions were created for each line based on the percentage of plants on the last day of the trial that fell into a scored category. Replication effects between the two independent experiments were tested for each line using Cochran-Mantel-Haenszel (CHM) statistics. Since replication effects were not found to be significant for any line in any trial (see Results), the data sets from corresponding trials were combined. Overall line effect and pair-wise line differences were tested within the PROC FREQ procedure (SAS) using χ^2 analysis and Fischer's exact test for low sample sizes.

Quantitative data were processed as follows. Prior to statistical analysis, *M. incognita* egg count values (eggs per g root fresh weight) were $\log_{10}(x+1)$ transformed. Data transformation was performed to allow for the skewed egg count distribution which is generally observed in nematode populations due to variations in individual fecundity. Mean egg mass and transformed egg count values were determined for each line. Replication effects between the two experiments were tested using ANOVA. Because replication effects for mean egg mass and egg count values

were not significant, the data means were combined, overall line effects were tested using ANOVA, and Tukey's Studentized Range (HSD) test was employed for post-hoc multiple comparison analysis. Mean root mass values for each line were determined from *P. cinnamomi* and *M. incognita* disease trials. Average values for root mass were compared between inoculated control and transgenic plum lines in both trials using ANOVA and Fisher's Least Significant Difference (LSD).

RESULTS

Transformation of plum

Morphological characteristics were compared between the non-transformed control line and transgenic lines 4J, 4I, and 5D (T_0 generation). Transgenic lines 4J and 4I were indistinguishable from the non-transformed control line with respect to vigor and growth habit. Morphological variation in line 5D was pronounced, however. Trees from this line displayed smaller leaves, which were clustered more closely on the branch (Figs. 2.1 A-C). 5D trees also exhibited increased lateral branching, maintaining a low, bushy habit (data not shown). The three transgenic lines used in the study were siblings since they all originated from 'Stanley' seeds, however each was line was genetically unique. Trees from the non-transformed control line originated from 12 'Stanley' seedling lines and were expected to represent a range of genetic variation for inherent disease resistance within the 'Stanley' cultivar.

DNA and immunoblot analysis

Insertion of the *gafp-1*-containing construct (Fig. 2.2 A; performed by Dr. Cesar Petri), and subsequent GAFP-1 expression, were confirmed in all lines by DNA blotting and immunoblot analysis. DNA blotting with a *gafp-1* specific probe demonstrated 1, 2, and 4 copies of the transgene insertion in lines 4J, 4I, and 5D, respectively (Fig. 2.2 B; performed by Dr. Cesar Petri). Moreover, all lines produced the GAFP-1 lectin (expected size 12 kDa) in root tissues (Fig. 2.2 C). *Gafp-1* probe and antibody hybridization were absent when root tissue DNA and protein extracts from the non-transformed control line were analyzed by DNA and immunoblotting, respectively.

Disease resistance screening

After 20 d of infestation, all lines were assessed for their susceptibility to *P. cinnamomi* by rating qualitative symptoms of *Phytophthora* infection. Diagnostic symptoms, such as wilting, chlorosis, and necrosis of the leaves and stem (Fig. 2.3), were observed to some extent in plants from all infected lines. In both independent experiments, the non-transformed control line and transgenic lines 4J and 4I developed characteristic symptoms associated with PRR 8 to10 d after inoculation with *P. cinnamomi*. An accelerated onset of disease symptoms was observed in line 5D, with symptoms becoming apparent as early as day 2 (data not shown). Plants from uninoculated, negative control groups remained unaffected by necrotic symptoms. A small number of negative control plants, however, displayed symptoms of water logging after the flooding period. Leaves from the non-infected, water-logged plants became chlorotic and eventually abscised, but these same plants recovered before the end of the experiment, flushing new leaves and displaying healthy growth whereas infected plants continued to decline over the

entire period. Rather than abscising, necrosed leaves from *Phytophthora*-infested plants remained attached to the stem. In neither experimental trial did the average final root mass of the inoculated control line differ significantly from the average root mass of any of the transgenic lines (Fig. S2.1).

Replication effects were not found to be significant between *P. cinnamomi* experiments by CHM analysis (P = 0.97). By the end of the 20 d incubation period, most plants from the inoculated, non-transformed control and 5D lines were severely diseased and primarily distributed in scored categories 3 and 4 (Table 2.1). In contrast, most plants from transgenic lines 4J and 4I developed weaker symptoms and fell into scored categories 1 and 2. Frequency distributions for lines 4J and 4I were significantly shifted compared to that of the inoculated control line (P = 0.02), but did not differ significantly from each other by χ^2 analysis (P = 0.77). The 5D line distribution was not significantly shifted compared to the distribution of the inoculated control line (P = 0.20).

All lines were assessed for their susceptibility to *M. incognita* by evaluating root galling, egg mass deposition, and nematode reproduction (egg counts) in infected roots after 60 d. Replication effects between independent experiments were not found to be significant with respect to gall ratings (CHM; P = 0.16), egg mass deposition (ANOVA; P = 0.27), or transformed egg counts (ANOVA; P = 0.92). Tomato seedlings used for nematode culture were severely galled at the time of nematode extraction, verifying the viability of the inoculum. Lines 4J and 4I exhibited a lower degree of root galling compared to line 5D and the inoculated, non-transformed control line (Table 2.2). The majority of plants from lines 4J and 4I fell into scored categories 0 and 1, and distributions were found to be significantly different from the inoculated control line (P = 0.004 and P = 0.0003, respectively) but not significantly different from each other by χ^2

analysis (P = 0.17). The line 5D distribution was not significantly shifted compared to the inoculated control line (P=0.06).

Egg mass deposition was significantly reduced in lines 4J and 4I compared to the inoculated control line (Fig. 2.4 A), consistent with the decreased galling observed in these same lines. While values for transformed egg counts were depressed in lines 4I and 5D compared to the inoculated control line, only line 4J demonstrated a significantly reduced number of eggs produced per gram root tissue (Fig. 2.4 B). In neither experimental trial did the average final root mass of the inoculated control line significantly differ from the average final root mass of any of the transgenic lines (Fig. S2.2). Plants from uninoculated, negative control groups remained healthy for the duration of the experiment. Taking into account an inoculum density of 6000 eggs/plant, the degree of infection observed in the inoculated control line was comparable to other studies conducted on *Prunus* species with root-knot nematodes (Lu *et al*., 2000; Rubio-Cabetas *et al.*, 2001).

The initial size of 90-d-old rooted cuttings varied within all lines due to differences in propagation and planting date. Therefore, parameters related to seedling size, such as root mass, were not used as measures of disease susceptibility. Rather, evaluations were based on the percentage of root system affected, or measurements were normalized against root mass in order to reduce the effects of root size variability.

DISCUSSION

In this study expression of *gafp-1* was correlated with increased tolerance to *P. cinnamomi* in the two morphologically consistent lines, 4J and 4I. These same lines were less affected by symptoms of *M. incognita* infestation, displaying significantly reduced root galling

severity, egg mass deposition, and, in line 4J, a significantly lower degree of reproduction. These results are consistent with an earlier study describing reduced PRR and RKN symptom severity in tobacco seedlings expressing *gafp-1* (Cox *et al*. 2006). Because production of GAFP-1 is associated with increased tolerance to stramenopile and nematode pathogens in two independently transformed systems, it seems likely that this protein might be able to target selected non-fungal as well as fungal organisms.

As was the case in this study, increased gene copy number and/or transcript expression levels do not necessarily correlate to an increased resistance phenotype in transgenic plant lines (Dandekar *et al.*, 1998; Ripoll *et al*., 2003). DNA blotting revealed multiple *gafp-1* gene copies in line 5D, whose leaf morphology and growth patterns were altered compared to the other lines. Plants from line 5D were the most severely affected in *P. cinnamomi* disease assays despite production of GAFP-1 in root tissues. Although some reduction in RKN symptom severity was observed in line 5D, results were not as dramatic as those exhibited by lines 4J and 4I. The divergent morphology of the 5D line likely indicates a physiological defect resulting from the transformation procedure. The occurrence of multiple transgene copies raises the possibility of a problematic insertion event, or this line may be a somaclonal variant negatively affected by the regeneration process. All transgenic plum lines represent separate genotypes as all transformants were generated from different seeds of the 'Stanley' cultivar. It is therefore possible that any inherent variation in traits controlling pathogen resistance in line 5D may also be contributing to its weaker performance. Lastly, being of a slightly different genetic background, it may be the case that this line is more susceptible to pleiotropic effects of GAFP-1 production, resulting in negative physiological impacts.

The mechanism by which GAFP is able to inhibit growth of fungal hyphae has not yet been elucidated. As a member of the MMBL family it has been hypothesized that GAFP binds to

mannose-containing glycans or glycoproteins embedded in the fungal cell wall matrix, possibly interfering with the dynamics of cell wall development or expansion (Wang *et al*., 2003). Supporting this is a recent study which demonstrated GAFP localization in the apices and septa of actively growing hyphae of *Trichoderma viride* (Xu *et al*., 2003). In addition to mannose, the GAFP lectin was also able to associate with single residues and chains of N-acetylglucosamine *in vitro* (Xu *et al*., 1998). The ability to bind a glucose derivative is rare among the monocot-mannose binding lectins, which are diagnostic for their specificity towards mannose (Barre *et al*., 2001; Liu *et al*., 2005; Van Damme *et al*., 1998). If GAFP is able to accommodate chitin, this could theoretically contribute to its activity in fungi. The mechanism of GAFP-1 action on stramenopile and nematode pathogens (Cox *et al*., 2006; this study) is unknown. *Phytophthora* species are cell wall-enclosed mycelial organisms, therefore GAFP-1 may act on stramenopiles in a manner similar to fungi. As for the root knot nematode, insecticidal MMBLs such as GNA are able to target RKN by binding mannose-type glycoconjugates within the mid-gut region of the insect (Ripoll *et al*., 2003). GAFP-1 may have analogous activity within *M. incognita,* perhaps binding to surface glycans on receptors of the endo-parasite to create a toxic effect or otherwise impeding egg hatch.

A transgenic, woody rootstock with increased tolerance to soil-borne pathogens would be of great benefit for the stone-fruit industry. Virtually all the major tree fruit crops are propagated by grafting onto rootstocks, and if it can be shown that the *gafp-1* gene products cannot traverse the graft union, a transgenic rootstock combined with a non-transgenic scion may cause less public concern because pollen and fruit would be produced on the non-transgenic parts of the plant. GAFP-1 significantly decreased the effects of infection by *P. cinnamomi* and *M. incognita* in our morphologically invariant plum lines. Future work will help us determine if *gafp-1* expression is able to slow infection by *Armillaria tabescens*, the causal agent of Armillaria Root

Rot and a species related to GAFP's target pathogen, *A. mellea.* Multi-year tests will be necessary to investigate this transgenic system under field-infection conditions.

FIGURES AND TABLES

A

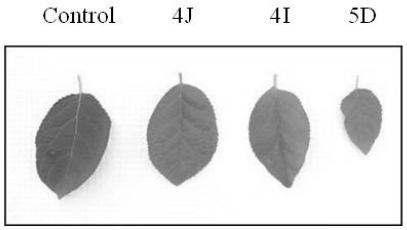
Control
4J
4I
5D

B

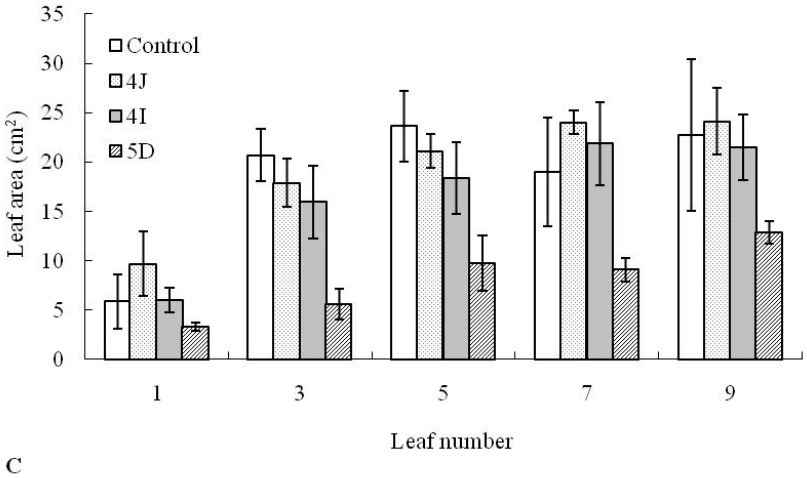
Control
4J
4I
5D
Leaf area (cm²)
Leaf number
0
5
10
15
20
25
30
35
1
3
5
7
9

C

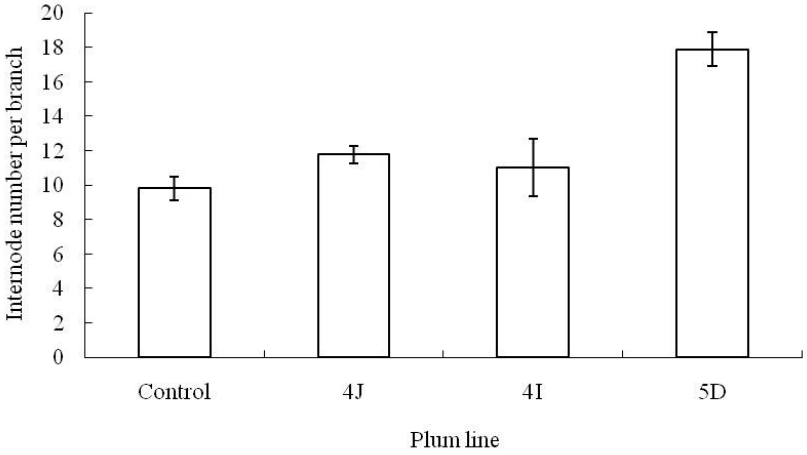
Internode number per branch
Plum line
Control
4J
4I
5D
0
2
4
6
8
10
12
14
16
18
20

Figure 2.1. Morphological characteristics of 2-year-old trees (T_0) from non-transformed control and transgenic plum lines 4J, 4I, and 5D. (A) Representative leaves from position 8. (B) The average area of leaves taken from positions 1, 3, 5, 7 and 9. (C) The average number of internodes on 30 cm branch sections starting at position 1. For (A-C), position 1 corresponds to the first expanded leaf below the apical meristem. Values are means and standard deviations calculated from nine branches per line.

A

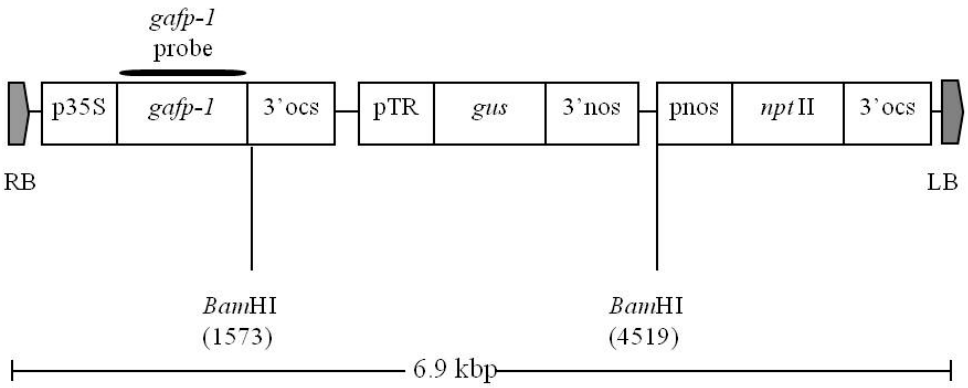
gafp-1
probe
p35S
gafp-1
3'ocs
pTR
gus
3'nos
pnos
nptII
3'ocs
RB
LB
BamHI
(1573)
BamHI
(4519)
6.9 kbp

B

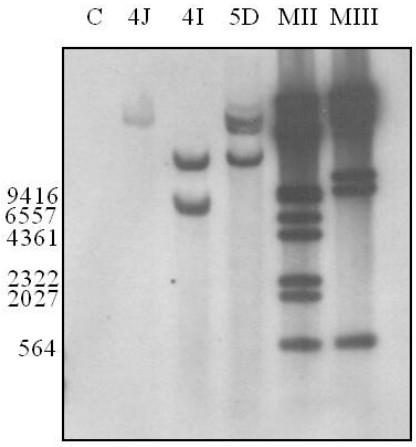
C
4J
4I
5D
MII
MIII
9416
6557
4361
2322
2027
564

C

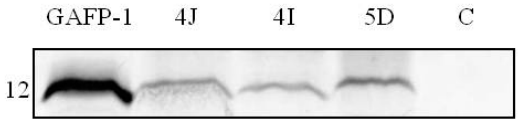
GAFP-1
4J
4I
5D
C
12

Figure 2.2. GAFP -1 is expressed within transgenic plum lines 4J, 4I, and 5D, but not within the non-transformed control (C) line. (A) The pAVNF T-DNA insert representing *BamH*I restriction sites and the position of the *gafp-1* specific probe. The open reading frame of the *gafp-1* gene is flanked by the 35S promoter (p35S) and a 3' opine termination/polyadenylation signal (3'ocs). The scorable marker β-glucuronidase (*gus*) and a selector for kanamycin resistance (*nptII*), both under the control of 5' (pTR and pnos) and 3' (3'ocs and 3'nos) opine promoter/terminator sequences, are also represented. (B) DNA blotting of non-transformed control and transgenic plum lines. MII and MIII are DIG-labeled DNA molecular weight markers II and III, respectively (Roche). Fragment sizes (bp) for the MII marker are indicated to the left of the figure. (C) Immunoblot analysis of protein extracts from root tissues of non-transformed and transgenic lines. The first lane contains recombinant GAFP-1-VNF (GAFP-1; expected size 12 kDa) cleaved from a maltose-binding protein fusion as a standard (140 ng total protein).


Score 0

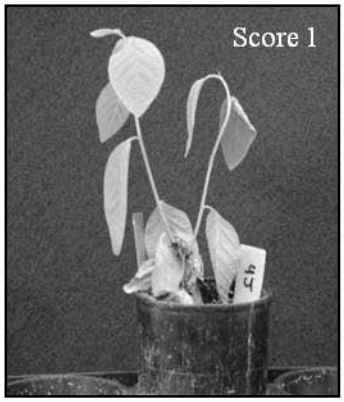
Score 1

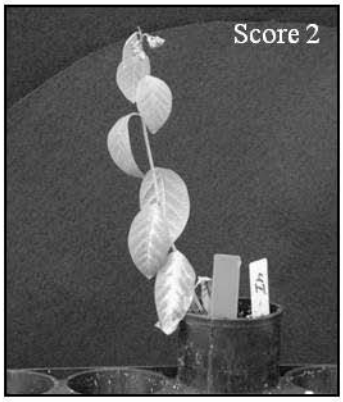
Score 2


Score 3


Score 4

Figure 2.3. Plants representative of the scores used to rate disease symptoms resulting from *P. cinnamomi* infection in 90-d-old plum. Score 0 = healthy plant with no affected tissues, Score 1 = wilting and < 25% plant affected, Score 2 = 26 - 50% of the plant affected, Score 3 = 51 - 75% of the plant affected, Score 4 = > 75% of the plant affected.

Table 2.1. Percentage of plants manifesting symptoms of *P. cinnamomi* infection after 20 d.

Line	Observations[y]	Symptom severity score[z]				
		0	1	2	3	4
Control a[x]	19	5.3%	0.0%	15.8%	31.6%	47.4%
4J b	13	7.7%	30.8%	38.5%	15.4%	7.7%
4I b	16	0.0%	31.3%	31.3%	25.0%	12.5%
5D a	14	0.0%	0.0%	0.0%	21.4%	78.6%

[z]Symptom severity scores are depicted in Fig. 2.3.

[y]Total number of inoculated plants across two independent experiments.

[x]Frequency distributions for lines followed by the same letter were not significantly different ($\alpha = 0.05$).

Table 2.2. Percentage of plants manifesting *M. incognita* galling symptoms after 60 d.

Line	Observations[y]	Symptom severity score[z]						
		0	1	2	3	4	5	D
Control a[x]	20	0%	25%	30%	35%	5%	0%	5%
4J b	20	15%	70%	15%	0%	0%	0%	0%
4I b	20	30%	65%	0%	0%	0%	0%	5%
5D a	20	5%	40%	50%	0%	0%	0%	5%

[z]Gall ratings were assigned based on the scale outlined in the Materials and Methods. The percentage of plants that died (D) during the experiment are also represented.

[y]Total number of inoculated plants across two independent experiments.

[x]Frequency distributions for lines followed by the same letter were not significantly different ($\alpha = 0.05$).

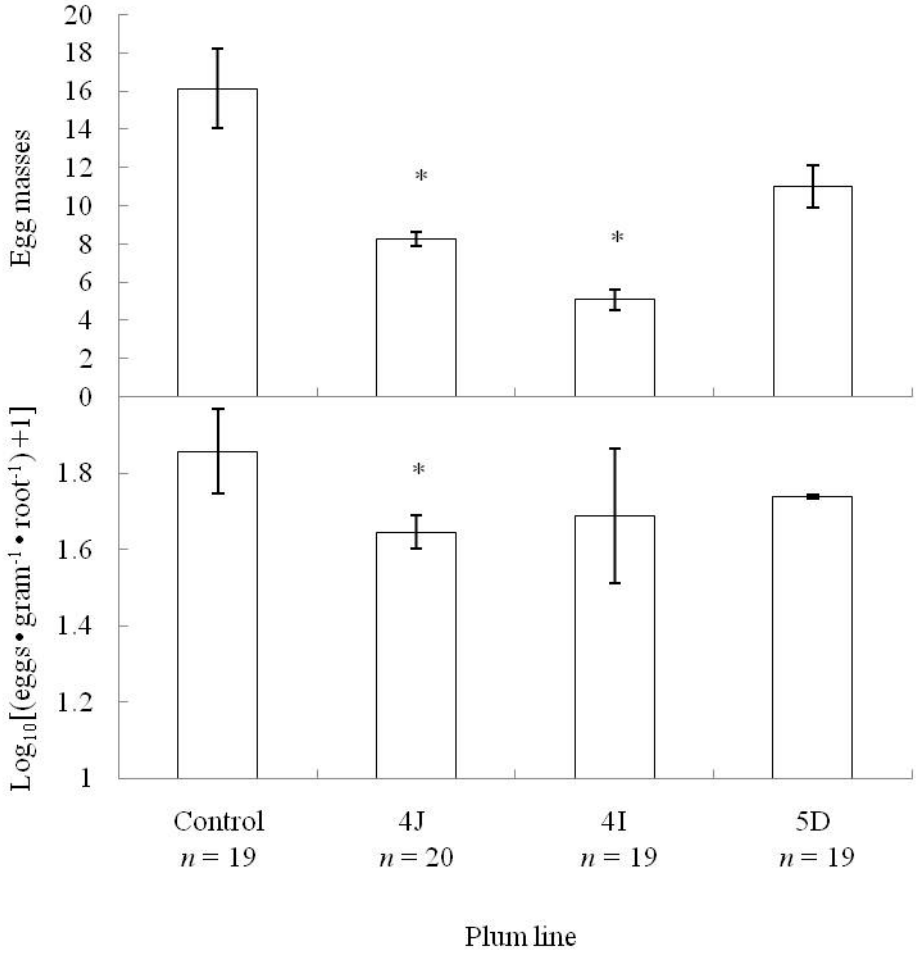
Egg masses
20
18
16
14
12
10
8
6
4
2
0
*
*
Log10[(eggs • gram-1 • root-1)+1]
1.8
1.6
1.4
1.2
1
*
Control
n = 19
4J
n = 20
4I
n = 19
5D
n = 19
Plum line

Figure 2.4. Egg mass deposition (top) and nematode reproduction (bottom) were analyzed for root systems of the non-transformed control line and transgenic lines 4J, 4I, and 5D 60 d after inoculation with eggs of *M. incognita*. Values for the number of eggs produced per gram fresh root tissue (egg counts) were used to assess reproduction in all lines. Egg count values were $\log_{10}(x+1)$ transformed prior to statistical analysis. Values are means and standard deviations calculated from *n* plants per line across two independent experiments. Plants that died (Table 2.2) were excluded from statistical analysis. Values with an asterisk (*) are significantly different from that of the inoculated control line ($\alpha = 0.05$).

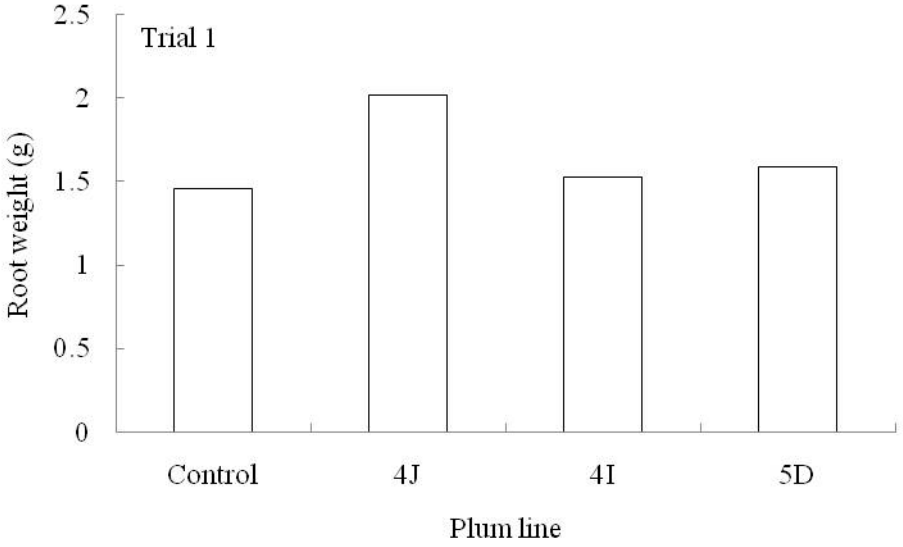
Trial 1
Root weight (g)
2.5
2
1.5
1
0.5
0
Control
4J
4I
5D
Plum line

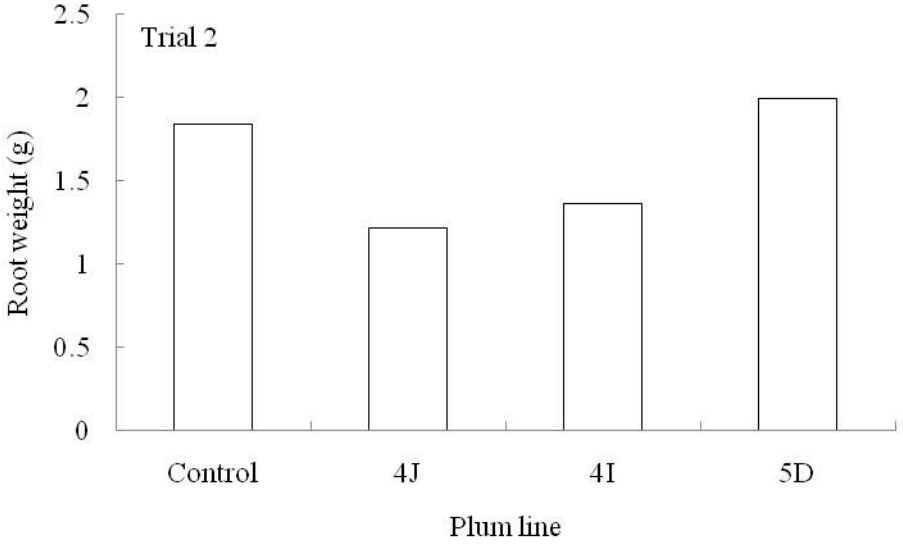
Trial 2
Root weight (g)
2.5
2
1.5
1
0.5
0
Control
4J
4I
5D
Plum line

Supplemental Figure 2.1. Mean fresh root weight of seedlings from non-transformed control and transgenic plum lines 4J, 4I, and 5D 20 d after infection with *P. cinnamomi*. In neither trial did the average root mass of the non-transformed control line significantly differ from that of any transgenic line by Fischer's Least Significant Difference (LSD) ($\alpha = 0.05$).

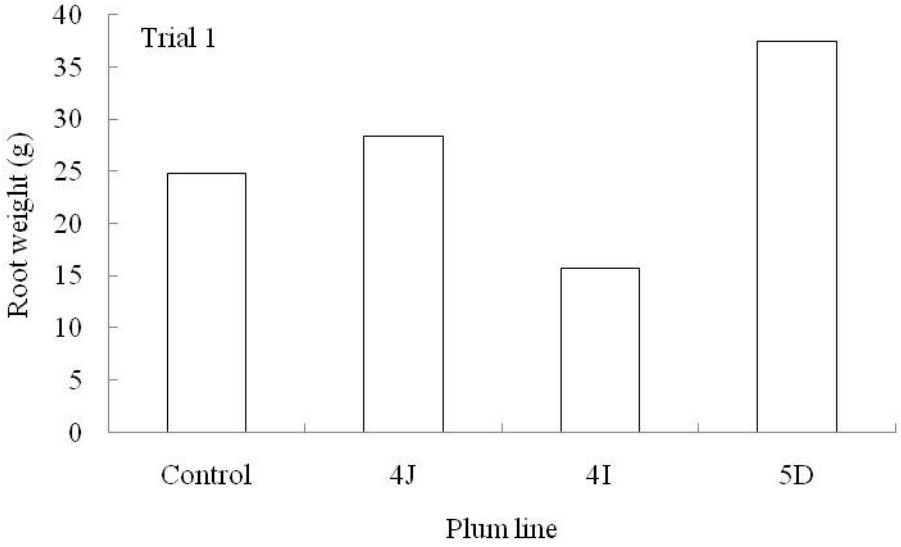
Trial 1
Root weight (g)
40
35
30
25
20
15
10
5
0
Control
4J
4I
5D
Plum line

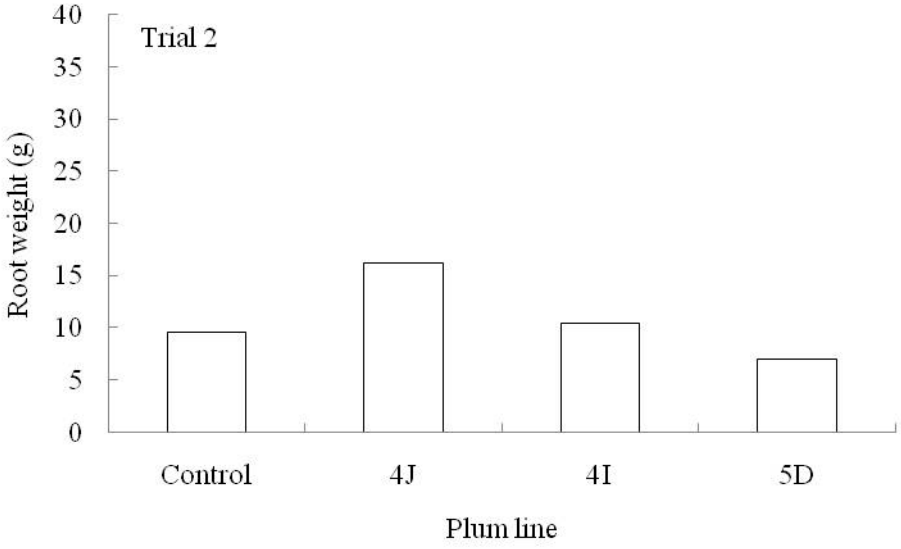
Trial 2
Root weight (g)
40
35
30
25
20
15
10
5
0
Control
4J
4I
5D
Plum line

Supplemental Figure 2.2. Mean fresh root weight of seedlings from non-transformed control and transgenic plum lines 4J, 4I, and 5D 60 d after infection with *M. incognita*. In neither trial did the average root mass of the non-transformed control line significantly differ from that of any transgenic line by Fischer's Least Significant Difference (LSD) ($\alpha = 0.05$).

LITERATURE CITED

Barker, K.R. 1985. Design of greenhouse and microplot experiments for evaluation of plant resistance to nematodes, p. 103-113. In: Zuckerman, B.M., Mai, W.F., and M.B. Harrison (eds.). Plant Nematology Laboratory Manual. University of Massachussets Agriculture Experiment Station, Amherst, M.A.

Barre, A., Y. Bourne, E.J.M. Van Damme, W.J. Peumans, and P. Rougé. 2001. Mannose-binding plant lectins: Different structural scaffolds for a common sugar-recognition process. Biochemie 83:645−651.

Brown, G.T. and S.M. Mircetich. 1995. Phytophthora Root and Crown Rots, p. 38-40. In: Ogawa, J.M., E.I. Zehr, G.W. Bird, D.F. Ritchie, K. Uriu, and J.K. Uyemoto (eds.). Compendium of stone-fruit diseases. Amer. Phytopathol. Soc. Press, St. Paul, M.N.

Chen, H., R. Nelson, and J. Sherwood. 1994. Enhanced recovery of transformants of *Agrobacterium tumefaciens* after freeze-thaw transformation and drug selection. Biotechniques 16:664-668.

Chomczynski, P. 1993. A reagent for the single-step simultaneous isolation of RNA, DNA, and proteins from cell and tissue samples. Biotechniques 15:532-537.

Cox, K., D. Layne, R. Scorza, and G. Schnabel. 2006. Gastrodia anti-fungal protein from the orchid *Gastrodia elata* confers disease resistance to root pathogens in transgenic tobacco. Planta 224:1373-1383.

Dandekar, A.M., G.H. McGranahan, P.V. Vail, S.L. Uratsu, C. Leslie, and J.S. Tebbets. 1998. High levels of expression of full length cryIA(c) gene from *Bacillus thuringiensis* in transgenic somatic walnut embryos. Plant Sci. 131:181-193.

Dickson, D.W. and F.B. Struble. 1965. A sieving-staining technique for extraction of egg masses of *Meloidogyne incognita* from soil. Phytopathology. 55:497.

Gallagher, S., S. Winston, S. Fuller, and J. Hurrell. 1997. Immunoblotting and immunodetection, p. 10.8.1-10.8.21. In: F. Ausubel, R. Bent, R. Kingston, D. Moore, J. Seidman, J. Smith, and K. Struhl (eds.). Current protocols in molecular biology. Wiley, Hoboken, N.J.

Hu, Z., Z. Yang, and J. Wang. 1988. Isolation and partial characterization of an antifungal protein from *Gastrodia elata* corm. Acta Botanica Yunnanica. 10:373-380.

Hussey, R.S. and K.R. Barker. 1973. A comparison of methods of collecting inocula of *Meloidogyne sp.*, including a new technique. Plant Dis. Rptr. 57:1025-1028.

IPM: Integrated Pest Management. 1999. Crop profile for peaches in Pennsylvania. Regional IPM Centers, U.S. Dept. Agr. 10 December 2007. <http://www.ipmcenters.org/cropprofiles/docs/papeaches.html/>.

Jeffers, S.N. and S.B. Martin. 1986. Comparison of two media selective for *Phytophthora* and *Pythium* species. Plant Dis. 70:1038-1043.

Kobayashi, N., T. Horikoshi, H. Katsuyama, T. Handa, and K. Takayanagi. 1998. A simple and efficient DNA extraction method for plants, especially woody plants. Plant Tissue Cult. and Biotechnol. 4:76-80.

Liu, W., N. Yang, J. Ding, R. Huang, Z. Hu, and D. Wang. 2005. Structural mechanism governing the quaternary organization of monocot-mannose binding lectin revealed by the novel monomeric structure of an orchid lectin. J. Biol. Chem. 280:14865-14876.

Lu, Z.X., G.L. Reighard, A.P. Nyczepir, and T.G. Beckman. 2000. Inocula and media affect root-knot nematode infection of peach seedling roots. J. Amer. Pomol. Soc. 54:76-81.

Nyczepir, A. P. 1991. Nematode management strategies in stone fruits in the United States. J. Nematol. 23:334-341.

Nyczepir, A.P., R. W. Miller, and T. G. Beckman. 1997. Root-knot nematodes on peach in the southeastern United States: An update and advances. African Plant Protection. 3:115.

Padilla, I.M.G., K. Webb, and R. Scorza. 2003. Early antibiotic selection and efficient rooting and acclimatization improve the production of transgenic plum plants (*Prunus domestica* L.). Plant Cell Rep. 22:38-45.

Ripoll, C., B. Favery, P. Lecomte, E. Van Damme, W. Peumans, P. Abad, L. Jouanin. 2003. Evaluation of the ability of lectin from snowdrop (*Galanthus nivalis*) to protect plants against root-knot nematodes. Plant Sci. 164:517-523.

Rubio-Cabetas, M.J., J.C. Minot, R.Voisin, and D. Esmenjaud. 2001. Interaction of root-knot nematodes (RKN) and the bacterium *Agrobacterium tumefaciens* in roots of *Prunus cerasifera*: evidence of the protective effect of the *Ma* RKN resistance genes against expression of crown gall symptoms. European J. Plant Pathol. 107:433-441.

Sharpe, R. R., P. L. Pusey, A. P. Nyczepir, and W. J. Florkowski. 1993. Yield and economics of intervention with peach tree short life disease. J. Prod. Agr. 6:241-244.

Van Damme, E.J.M., W.J. Peumans, A. Barre, and P. Rouge. 1998. Plant lectins: a composite of several distinct families of structurally and evolutionary related proteins with diverse biological roles. Critical Rev. in Plant Sci. 17:575–692.

Wang, X., G. Bauw, E.J.M. Van Damme, W.J. Peumans, Z.-L. Chen, M. Van Montagu, G. Angenon, and W. Dillen. 2001. Gastrodianin-like mannose-binding proteins: a novel class of plant proteins with antifungal properties. Plant J. 25:651:661.

Wang, P., Y. Wang, Q. Sa, W. Li, and Y. Sun. 2003. The site-directed mutagenesis of *Gastrodia* antifungal protein mannose-binding sites and its expression in *Escherichia coli*. Protein and Peptide Lett. 10:599-606.

Xu, Q., Y. Liu, X. Wang, H. Gu, and Z. Chen. 1998. Purification and characterization of a novel anti-fungal protein from *Gastrodia elata*. Plant Physiol. Biochem. 36:899-905.

Xu, R.H., and Z.X. Liu. 2003. Action site of Gastrodia antifungal protein on *Trichoderma* hyphae. Acta Botanica Yunnanica 25:573-578.

CHAPTER THREE

THE *GASTRODIA* ANTIFUNGAL PROTEIN (GAFP-1) AND ITS TRANSCRIPT ARE ABSENT FROM SCIONS OF CHIMERIC-GRAFTED PLUM

This work has been published:

Nagel, A.K., H. Kalariya, and G. Schnabel. 2010. The *Gastrodia* anti-fungal protein (GAFP-1) and its transcript are absent from scions of chimeric-grafted plum. HortSci. 44:188-192.

ABSTRACT

The *Gastrodia* anti-fungal protein (GAFP-1) is a monocot mannose-binding lectin from the Asiatic orchid *Gastrodia elata*. Transgenic plum (*Prunus domestica* var. 'Stanley') lines expressing GAFP-1 exhibit enhanced tolerance to the stramenopile pathogen *Phytophthora cinnamomi* and the root-knot nematode *Meloidogyne incognita*. Rootstocks created from transgenic lines might be more readily accepted by consumers if it can be shown that foreign gene products are not migrating into a grafted, non-transgenic scion on which fruit is produced. In this study, wild-type (WT) plum tissue was budded onto transgenic plum lines to create chimeric-grafted trees. Tissues from chimeric-grafted trees were analyzed for *gafp-1* transcripts (leaf and root) and protein (leaf, soft shoot, and root) by RT-PCR and immunodetection, respectively. Transcripts of *gafp-1* were detected consistently in the root tissues but not within the leaves of the grafted, WT scions. Similarly, the GAFP-1 lectin was identified within the roots, but not in the soft shoot or leaf tissues of the grafted, WT scions. These results suggest that *gafp-1* mRNA and protein are not moving into the WT scion tissues of chimeric-grafted plum trees.

INTRODUCTION

Development of genetically modified (GM) agricultural crops has given producers new weapons to combat pests and diseases. These transgenic options can be limited, however, depending on the type of crop and the nature of the affliction. For instance, despite the important economic impacts that root diseases can have on fruit production, few GM fruit tree species have been engineered for resistance to root-associated pathogens (Petri and Burgos, 2005). Transgenic plum (*Prunus domestica* var. 'Stanley') lines (designated 4J and 4I) expressing an isoform of the *Gastrodia* anti-fungal protein, GAFP-1-VNF (hereafter referred to as GAFP-1), are one example of such an engineered fruit tree system (Nagel *et al*., 2008). These lines displayed significantly reduced symptom severity when challenged with the stramenopile pathogen *Phytophthora cinnamomi* and both lines trended towards increased tolerance to the root-knot nematode *Meloidogyne incognita*.

The presence of foreign gene products in consumables is a controversial issue. It has been shown that perceptions about the safety of GM food are a factor in the consumer's willingness to purchase such items (Boccaletti and Moro, 2000; Bukenya and Wright, 2007; Burton *et al*., 2001). Grafting cultivar scions to rootstocks with desirable attributes is already common practice in fruit tree propagation. Therefore a potentially more consumer-friendly way to utilize GM technology would be to combine a transgenic, disease-resistant rootstock with a non-transgenic scion. Ideally, foreign gene products expressed in the root tissues would remain in the rootstock and not enter the fruit produced on a grafted scion. Whether the GAFP-1 lectin or its transcripts can move across a graft union into non-transformed scion tissues is not known.

The goal of this study was to determine if *gafp-1-vnf* (hereafter referred to as *gafp-1*) transcripts and/or protein are moving into grafted, WT scion tissues. Chimeric-grafted plum trees were created, consisting of wild-type (WT) scion tissue budded onto *gafp-1* expressing rootstocks. Root and scion tissues were analyzed for *gafp-1* mRNA and protein.

MATERIALS AND METHODS

["Detection of GAFP-1" was performed by Hetal Kalariya, affiliated with the lab of Dr. Guido Schnabel (Department of Entomology, Soils, and Plant Sciences at Clemson University, SC).]

Generation of chimeric-grafted and auto-grafted trees

Transgenic plum (*Prunus domestica* var. 'Stanley') lines 4J and 4I (Nagel *et al*., 2008) and non-transformed WT plum lines were used in this study. Both transgenic 4J and 4I lines express the *gafp-1* gene under the control of the CaMV-35S promoter sequence (Plant Genetic Systems N. V., Gent, Belgium). Trees from 4J and 4I lines were clonally propagated from their respective mother (T_0) lines. WT trees, however, originated from different 'Stanley' seeds, and thus represented some, albeit limited, inherent genetic variation within the WT population.

WT scion tissue was chip-budded (hereafter referred to as 'budded') onto three transgenic 4J and 4I trees and three non-transformed WT trees (Fig. 3.1). Briefly, dormant bud tissue was excised from the scions of donor (WT) and recipient (4J, 4I, or WT) rootstocks. The donor bud was then placed onto the chipped area of the recipient rootstock stem. Buds from 1-year-old WT scions were budded onto the stems of 1-year-old 4J and 4I lines to create chimeric-grafted (CG)

trees. Buds from 1-year-old WT plum were budded onto stems of 1-year-old WT plum (originating from different seeds) to create auto-grafted (AG) trees. AG trees served as negative controls for the detection of *gafp-1* mRNA and protein. Three tree-replicates received 2 buds each for a total of 6 budding attempts per line. Buds were wrapped in Parafilm® for 2 weeks. After this time the Parafilm® was removed. Four weeks after the budding event the WT scion was truncated just above the uppermost bud graft. If two buds flushed on the same tree, they were both allowed to develop on the stem. Non-transformed and transgenic ungrafted (UG) trees were kept as additional controls for the detection of *gafp-1* molecular products in tissues. Trees were maintained in a biosafety level 2 greenhouse under constant temperature (27 ± 5°C) and light conditions (16/8 h day/night).

Tissue sampling

Leaf, shoot and root tissues were sampled from CG, AG and UG trees for molecular analysis. Sampling of both grafted and ungrafted tissues continued over a 24 month period. During this time, trees were pruned every six months. The grafted scions were truncated about 3-5 inches above the graft union.

Newly-emerged leaves were sampled from just below the apical meristem beginning 2 weeks after maintenance pruning, and partially lignified root tissue was sampled from the tips of the plum tree roots. Unlignified, soft shoots were sampled from trees between 2 and 6 weeks after maintenance pruning. Two weeks was the minimum amount of time it took for axillary buds to flush new, expanded leaves exhibiting non-curled edges. For each line, leaf tissues were taken from a total of three grafted scions on at least two different CG and AG trees. Root tissues were sampled from corresponding trees. When possible, leaf tissue was sampled from grafted scions on

separate trees. Leaf and root tissues were also sampled from three UG 4J, three UG 4I, and three UG WT trees. Soft shoots were sampled from two grafted scions on separate CG, AG, and UG trees from each line.

Detection of gafp-1 *mRNA*

The reverse transcriptase polymerase chain reaction (RT-PCR) was used to determine if *gafp-1* transcripts were present in leaf and root tissues of CG, AG, and UG trees. Plant tissues (100 mg) were collected directly into liquid nitrogen and homogenized. Total RNA was extracted using the RNeasy® Plant Mini Kit (Qiagen, Valencia, CA) according to the manufacturer's instructions. Total RNA (1 μg) was reverse-transcribed to cDNA using the SuperScript™ First-Strand Synthesis System (Invitrogen Corporation, Carlsbad, CA) according to the manufacturer's instructions. Control reactions were performed for all samples in which dIH_20 (de-ionized water) was substituted for the RT enzyme. These were included to verify that genomic DNA contamination was not present. Otherwise parameters for cDNA synthesis remained the same. RNA concentration was determined using a GeneQuant *pro* spectrophotometer at 260 nm. The RT procedure is documented to produce cDNA from as little as 1 ng of total RNA (Invitrogen).

Root and leaf tissue-derived cDNAs were selectively amplified using gene specific primers (Table 3.1). Tissues were analyzed for *gafp-1* transcripts by amplifying cDNA (5 ul first-strand synthesis) with primers 1 and 2, which are specific to the *gafp-1* transcript sequence (NCBI accession number AJ277786). As *gafp-1* transcripts were expected to be absent in WT tissues, additional reactions had to be conducted to verify proper cDNA amplification. Leaf tissue cDNA synthesis was confirmed by PCR amplification with primers 3 and 4, which are specific to the *catalase 2* (*cat2*) transcript sequence from peach (*Prunus persica*) (Accession number

AJ496419). Root tissue cDNA was PCR amplified with primers 5 and 6, specific to the *α-tubulin* (*α-tub*) transcript sequence from almond (*Prunus dulcis*) (NCBI accession number X67162). PCR amplification of all samples was performed with a Bio-Rad iCycler Version 4.006 (Bio-Rad Laboratories, Hercules, CA, USA). Cycling parameters were as follows: initial denaturation at 95ºC for 2 min, 35 cycles of 94ºC for 30 s, 65ºC for 30 s, and 72ºC for 40 s; final elongation was at 72ºC for 10 min. The entire procedure (mRNA isolation and RT-PCR analysis) was repeated for all tissues.

Detection of GAFP-1

Immunoblot analysis was used to determine if the GAFP-1 lectin (expected size 12 kDa) was present in leaf and root tissues of CG, AG, and UG trees. Total protein was extracted from leaf, shoot, and root tissues. Plant tissues (300 mg) were sampled and kept on ice until homogenizing in liquid nitrogen. Total cellular protein was extracted with TRIzol Reagent© (Invitrogen) according to standard methods (Chomczynski, 1993). Soluble protein was dissolved in 1% sodium dodecyl sulfate (SDS). The total protein concentration for each sample was determined with the DC (Detergent Compatible) Protein Assay (Bio-Rad) according to manufacturer's instructions. Bovine serum albumin was used as a standard. Sample absorbance was quantified at 650 nm using an Emax® precision microplate reader.

Total protein (20 µg) was loaded onto a 15% Tris-HCl gel and separated by SDS-PAGE. Protein molecular weight markers were included in all analyses (Precision Plus Protein™ duel color standard, Bio-Rad). Proteins were tank-transferred to a PVDF membrane for 18 h at 30 V. Membranes were blocked with 5% dry non-fat milk in TBST [(20 mM Tris-HCl, 140 mM NaCl, pH 7.5) + 0.1% Tween 20], rinsed twice, and then incubated with purified, polyclonal

GAFP-1 antibodies (1:1000 dilution) in 1% dry non-fat milk + TBST. Membranes were rinsed three times and then incubated with goat, anti-rabbit alkaline-phosphatase (AP) -conjugated secondary antibodies (1:2500 dilution) (Promega Corp., Madison, WI) in 1% dry non-fat milk + TBST. Membranes were developed with BCIP/NBT solution (Sigmafast™, Sigma Aldrich, St. Louis, MO, USA). The entire procedure (protein isolation and immunoblot analysis) was repeated for all tissues. The AP-conjugated secondary antibody is documented to detect as little as 10 pg of protein (Bio-Rad).

RESULTS

With one exception, at least one out of the two budding attempts became successfully established on each replicate tree. One individual from line 4J failed to yield any successful bud-grafts. Successfully grafted buds began to flush about 3 to 4 weeks after budding.

The expected 367-bp *gafp-1* and 498-bp *α-tub* fragments were successfully amplified from root tissue cDNAs of CG 4J and CG 4I trees (Fig. 3.2 A). However, even after 35 cycles of amplification we were not able to detect *gafp-1* transcripts by RT-PCR in leaf tissues taken from WT scions of CG 4J or CG 4I trees (Fig. 3.2 B). Successful amplification of the expected 572-bp *cat2* fragment confirmed the quality of the mRNA extracted from these leaf tissues (Fig. 3.2 B). Transcripts of *gafp-1* were not detected in the leaf or root tissues of UG WT or AG trees, but *gafp-1* fragments were consistently amplified from leaf and root tissue cDNAs of transgenic UG 4J and UG 4I trees (Table 3.2). *Cat2* and *α-tub* transcripts were detected in leaf and root tissues, respectively, from all CG, AG, and UG trees. Duplicates of every sample were created at the RNA extraction stage and subjected to the entire procedure without the inclusion of the RT

enzyme. This confirmed that cDNA-derived amplicons were not a result of genomic DNA contamination (Figs. 3.2 A and B).

GAFP-1 (expected size 12 kDa) was detected in roots of CG 4J and CG 4I trees but not in the leaf or soft shoot tissues of grafted, WT scions (Figs. 3.3 A and B; performed by Hetal Kalariya). In contrast, the lectin was detected consistently in the leaf and root tissues of UG 4J and UG 4I trees (Fig. 3.3 C; performed by Hetal Kalariya). A GAFP-1 signal was not detected in leaf, soft shoot, or root tissues from UG WT or AG trees (Table 3.2, Figs. 3.3 A-C). Lignified tissues from grafted, WT scions of CG trees were not analyzed for *gafp-1* products in this study.

GAFP-1 antibodies showed cross-reactivity with other proteins on the immunoblots, however cross-reaction was not observed at the 12 kDa position. Antibody cross-reaction occurred with an unknown 14 kDa protein in protein extracts taken from leaf, shoot and root tissues, and with a 15 kDa protein in protein extracts from shoot and root tissues. While the binding specificity of the GAFP-1 polyclonal antibody may have been optimized by loading a smaller amount of protein on the gels, we chose to load higher amounts of total protein (20 μg) in an effort to resolve small amounts of GAFP-1 that may have been moving from the rootstock into the leaf tissues of the grafted, WT scion. On the immunoblots the intensity of GAFP-1 bands varied among protein samples taken from different tissues. This occurred despite the fact that the amount of total protein loaded on the gel remained constant. This variation in band density was likely due either to inconsistencies in the homogenization of the fibrous plant tissues or possible differences in expression levels among the transgenic lines.

DISCUSSION

Many phloem-mobile macromolecules have been shown to traverse a graft union formed between compatible plant tissues. *In situ* RT-PCR studies demonstrated that pumpkin-derived *CmNACP* mRNA was present within the functional sieve elements (SE) of grafted cucumber scions (Ruiz-Medrano *et al*., 1999). Gomez *et al*. (2005) showed that an RNA-binding phloem lectin from melon, CmmLec17, could be detected within the phloem-exudate of heterografted pumpkin tissues. Grafting experiments between transgenic and WT tissues have demonstrated that transcripts may move through graft junctions and elicit responses in plant cells that do not contain the causal gene. Transcripts of the tomato *PFP-LeT6* gene, a sequence fusion found exclusively in the dominant mutant *Mouse ears,* were able to move across a graft union and induce changes in leaf pinnation in WT tissues (Kim *et al*., 2001). *BEL5* transcripts from *Solanum tuberosum* were translocated across grafts made between potato over-expression lines and WT rootstocks. Localization of St *BEL5* in stolon tips resulted in a two-fold increase in tuber yields (Banerjee *et al*., 2006). Macromolecules have even been observed to move across graft unions established in host-parasite relationships. After colonization of transgenic tobacco by the adventitious plant species *Cuscuta reflexa*, green-fluorescent protein expressed within tobacco companion cells was detectable within the SE's of the associated parasite (Haupt *et al*., 2001).

This study provides evidence that *gafp-1* transcripts and protein may not be moving into the grafted, WT scions of a CG tree species, contradicting previous research that supports the phloem mobility of GAFP within its host, the achlorophyllic orchid *Gastrodia elata*. Immunofluorescence studies demonstrated that the GAFP lectin is present within the vascular tissue of terminal corms, and it was proposed that the lectin is transported from the primary (nutritive) to the secondary (terminal) corm of the orchid, as well as into the developing flower stem, via the SE's (Hu and Huang, 1994). There are no data, however, to indicate that the lectin is

expressed in the terminal corm, as opposed to being transported, or to suggest that *gafp* transcripts themselves are phloem-mobile in *G. elata*.

As emerging leaves develop on the scion they make the transition from 'sink' to 'source,' and at this point they begin to contribute phloem-assimilates to the scion translocation stream (Haywood *et al*., 2005). By routinely pruning the trees we strived to keep the grafted scions in a 'sink' state. There was not a single instance in which our detection procedures gave any indication of *gafp-1* mRNA or protein in the grafted, WT leaf tissues of CG trees, even when tissues were sampled shortly (2 weeks) after maintenance pruning. Similarly, soft shoots, which were sampled from scions of CG trees between 2 and 6 weeks post-pruning, never showed a protein signal at the 12 kDa position. Immunoblots performed on protein extracts from WT leaves of CG 4J and CG 4I trees eight weeks after budding (four weeks post-bud flush) did not show GAFP-1 protein signals (data not shown).

We began to sample leaves and soft shoots for the detection of *gafp-1* mRNA and protein 2 weeks after maintenance pruning. This should have been an adequate amount of time for the hypothetically phloem-mobile *gafp-1* molecular products to move into grafted tissues. Several studies have demonstrated that macromolecules utilizing phloem channels will spread relatively quickly within the plant. It has been reported that phloem-mobile gene silencing signals are distributed systemically within a few days in tomato (Voinnet *et al*., 1998). In herbaceous heterografts, three weeks has been sufficient for the detection of various, imported phloem-mobile transcripts and proteins (Gomez *et al*., 2005; Haywood *et al*., 2005; Ruiz-Medrano *et al*., 1999). Certain phloem-mobile plant viruses, which are thought to travel through the translocation stream as ribonucleoprotein complexes (Santa Cruz, 1999), are capable of spreading systemically in a matter of hours (Capoor, 1949; Ismail *et al*., 1987) or days (Bennett, 1940; Gal-On *et al.*, 1994; Helms and Wardlaw, 1976; Más and Pállas, 1996) in herbaceous species. Most grafting

studies conducted with woody plant material do not determine on a molecular level the amount of time it takes for phloem-mobile virus particles to move into budded tissues (S. Scott, personal communication). However, it has been shown in herbaceous systems that manifestation of disease symptoms in grafted tissues is preceded by the delivery of virus RNA to target cells (Más and Pállas, 1996). If symptom emergence is therefore indicative of virus movement, fruit tree seedling double-budding experiments have shown that virus particles can move from infected to non-infected tissues in 4 weeks (Fridlund, 1980).

It is possible that the GAFP-1 lectin may not be compatible with the phloem transportation machinery of *P. domestica*. Being in a different genetic background, the GAFP-1 lectin may move into the translocation stream only to be quickly degraded, or the protein may not be entering the translocation stream at all. In higher plants, the non-cell-autonomous activity of signaling proteins and transcripts has a significant impact on the coordination of complex developmental and physiological events (Nakajima *et al*., 2001; Palauqui *et al*., 1997; Ruiz-Medrano *et al*., 1999; Yoo *et al*., 2004; Xoconostle-Cázares *et al*., 1999), and is likely subject to a certain degree of regulation. Indeed, targeted transport of macromolecules, as well as non-specific diffusion, has been observed within symplasmically-connected cells and SE's (Crawford *et al*., 2000; Itaya *et al*., 2002; Lucas *et al*., 1995; Stadler *et al*., 2005). The concept of a surveillance system controlling the movement of transcripts into specific tissues has been supported by studies on the selective entry of virus-derived post-transcriptional gene silencing signals into the plant shoot apex (Foster *et al*., 2002). Likewise, Haywood *et al*. (2005) showed that expressed cucurbit *Cmgaip* transcripts were able to move into the WT leaf and flower tissues of CG tomato, but not into the fruits produced on the WT scions. Analogous mechanisms likely exist for regulating the delivery of phloem-associated proteins to plant tissues. This statement is congruent with the observation that phloem proteins from *Cucurbita maxima* have the ability to interact with and

increase the size exclusion limit of the plasmodesmata in cotyledon mesophyll cells (Balachandran *et al*., 1997). Also, the melon RNA-binding phloem protein CmmPP2 was not detected in scion phloem exudates of grafted pumpkin tissues, despite the successful translocation of other phloem-mobile melon proteins such as CmmLec17 (Gomez *et al*., 2005).

Our results suggest that *gafp-1* transcripts and protein are not phloem-mobile in CG plum. It remains to be determined whether *gafp-1* products expressed in transgenic rootstocks can accumulate in non-transgenic branches and leaves after several years of establishment in the field, or in flowers or fruits following significant physiological changes such as the onset/breaking of dormancy and fruiting. Most fruit tree crops are propagated by grafting cultivar tissue onto rootstocks with desirable attributes, such as enhanced tolerance to root diseases. Thus, a CG strategy such as we have described could have broader applications for a range of plant systems engineered for root-associated disease resistance. The ability of different GM rootstocks to retain foreign gene products would depend highly on the nature of the expressed protein or transcript and its compatibility with the translocation machinery of the host plant species to which transgenic resistance was being applied.

FIGURES AND TABLES

A

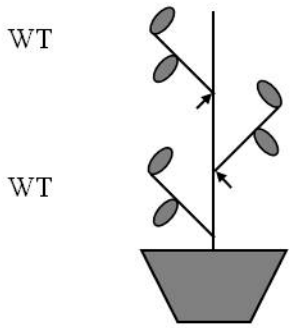

AG tree

B

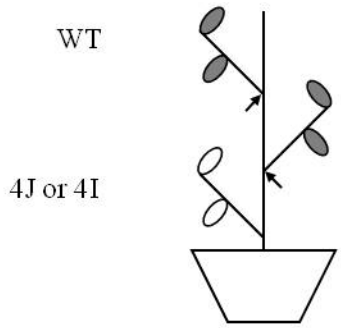

CG tree

Figure 3.1. A schematic diagram of the trees used in grafting experiments. (A) Wild-type (WT) plum tissue was budded onto WT rootstocks to create auto-grafted (AG) trees. AG trees served as negative controls. (B) WT plum tissue was budded onto rootstocks from transgenic plum lines 4J and 4I to create chimeric-grafted (CG) trees. WT rootstock and scion tissues are indicated in grey, transgenic tissues are indicated in white. Two buds were budded per rootstock. Black arrows indicate the graft junction occurring on the rootstock stem.

Table 3.1. Primers used for amplification of cDNAs from leaf and root tissues.

Primer	Target	Size (bp)	Orientation[z]	Sequence
1	*gafp-1*	367	F	5'CCTGTTCTTTCGCGTGACAACAG3'
2	*gafp-1*		R	5'GTGTGGGTTGCCCAAATCGCATT3'
3	*cat2*	572	F	5'AGGCACATGGAAGGCTCTAGTGTT3'
4	*cat2*		R	5'ACCTCCTCATCCCTGTGCATGAAA3'
5	α-*tub*	498	F	5'TTGACATTGAGCGACCCACCTACA3'
6	α-*tub*		R	5'TGGTCGAGTTGGAGATCATGCACA3'

[z]Orientation of forward (F) and reverse (R) primers (5' to 3').

A

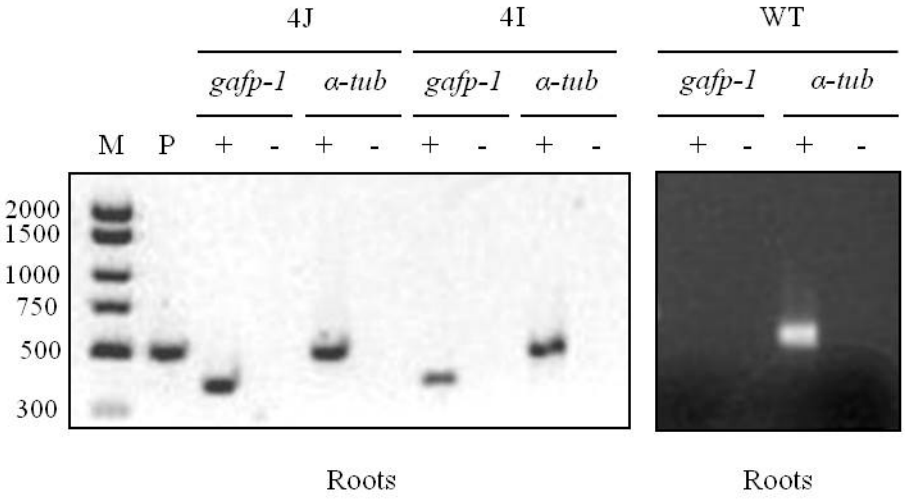
4J
4I
WT
gafp-1
α-tub
gafp-1
α-tub
gafp-1
α-tub
M P + - + - + - + - + - + -
2000
1500
1000
750
500
300
Roots
Roots

B

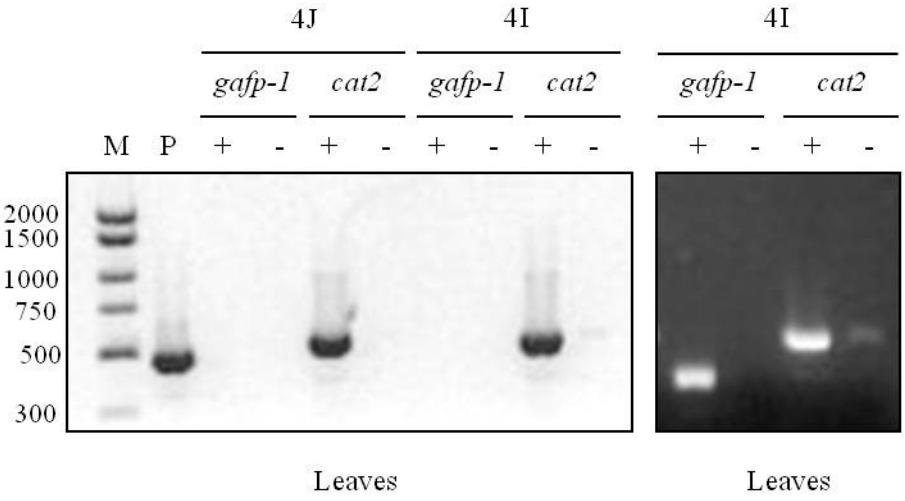
4J
4I
4I
gafp-1
cat2
gafp-1
cat2
gafp-1
cat2
M P + - + - + - + - + - + -
2000
1500
1000
750
500
300
Leaves
Leaves

Figure 3.2. RT-PCR analysis (35 cycles) of cDNA prepared from chimeric-grafted (CG) and ungrafted (UG) (A) leaf and (B) root tissues. (A) Amplicons from root tissues of CG 4J and 4I trees (left-side panel) and a UG wild-type (WT) tree (right-side panel). (B) Amplicons from leaf tissues of WT grafts on CG 4J and 4I trees (left-side panel) and a UG 4I tree (right-side panel). *Gafp-1* (expected size 367-bp) and *α-tubulin* (*α-tub*; expected size 498-bp) or *catalase* (*cat2*; expected size 572-bp) transcripts were reverse-transcribed and PCR-amplified with sequence-specific primers. A plus (+) or minus (-) sign indicates the inclusion or exclusion, respectively, of the reverse transcriptase enzyme during cDNA synthesis. Chloramphenicol acetyltransferase (P; expected size 500-bp) RNA was reverse-transcribed and amplified with gene-specific primers (provided by SuperScript™ First-Strand Synthesis System, Invitrogen) as a positive control for cDNA synthesis and amplification. The numbers to the left of the figures indicate the size of the DNA markers (M) in base pairs (exACTGene® Low Range DNA Ladder, Fisher Scientific, Pittsburgh, PA, USA).

A

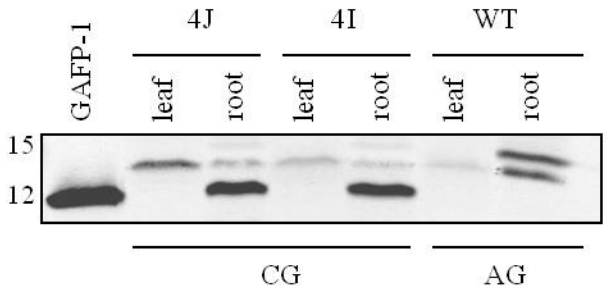
GAFP-1
4J
4I
WT
leaf
root
leaf
root
leaf
root
15
12
CG
AG

B

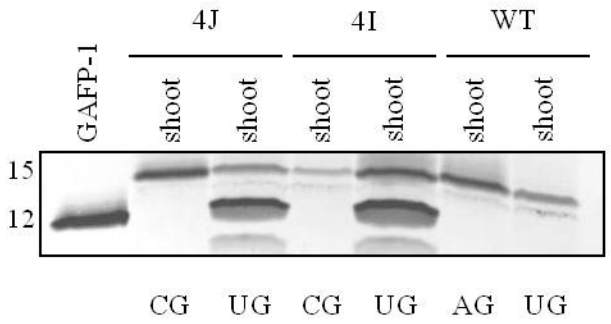
GAFP-1
4J
4I
WT
shoot
shoot
shoot
shoot
shoot
shoot
15
12
CG
UG
CG
UG
AG
UG

C

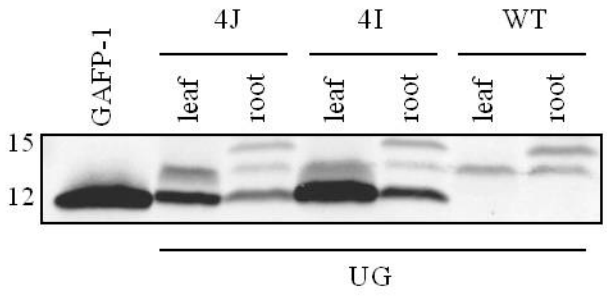
GAFP-1
4J
4I
WT
leaf
root
leaf
root
leaf
root
15
12
UG

Figure 3.3. Immunoblot analysis of protein extracts from chimeric-grafted (CG), auto-grafted (AG), and ungrafted (UG) trees. (A) Leaves and roots from CG and AG trees, (B) soft shoots from CG, UG, and AG trees, and (C) leaves and roots from UG trees were analyzed for the presence of the GAFP-1 lectin. Recombinant GAFP-1-VNF (GAFP-1; expected size 12 kDa) cleaved from a maltose-binding protein fusion was included as a standard (140 ng total protein). Protein extracts from leaf and root tissues of AG and UG wild-type (WT) trees served as negative controls. The numbers to the left of the figures indicate the size of the protein bands in kilodaltons.

Table 3.2. Detection of *gafp-1* mRNA and protein in tissues of auto-grafted (AG), ungrafted (UG), and chimeric-grafted (CG) trees.

Tree			Plant Tissue[z]				
			Leaf		Root		Shoot
Rootstock	Graft type	Observations[y]	mRNA	Protein	mRNA	Protein	Protein
WT	UG	n = 3/3: 2	-	-	-	-	-
WT	AG	n = 2/2: 2	-	-	-	-	-
4J	UG	n = 3/3: 2	+	+	+	+	+
4J	CG	n = 2/2: 2	-	-	+	+	-
4I	UG	n = 3/3: 2	+	+	+	+	+
4I	CG	n = 3/3: 2	-	-	+	+	-

[z]Leaf, shoot, and root tissues were analyzed twice for the presence (+) or absence (-) of *gafp-1* transcripts or protein.

[y]Number of trees from which leaf/root:shoot tissues were sampled.

LITERATURE CITED

Balachandran, S., Y. Xiang, C. Schober, G.A. Thompson, and W.J. Lucas. 1997. Phloem sap proteins from *Cucurbita maxima* and *Ricinus communis* have the capacity to traffic cell to cell through plasmodesmata. Proc. Natl. Acad. Sci. 94:14150-14155.

Banerjee, A.K., M. Chatterjee, Y. Yu, S. Suh, W.A. Miller, and D.J. Hannapel. 2006. Dynamics of a mobile RNA of potato involved in a long-distance signaling pathway. Plant Cell 18:3443-3457.

Bennett, C.W. 1940. Relation of food translocation to movement of virus of tobacco mosaic. J. Agric. Res. 60:361-390.

Boccaletti, S. and D. Moro. 2000. Consumer willingness-to-pay for GM food products in Italy. AgBioForum. 3:259-267. 1 July 2009. <http://www.agbioforum.org>.

Bukenya, J.O. and N.R. Wright. 2007. Determinants of Consumer Attitudes and Purchase Intentions with Regard to Genetically Modified Tomatoes. Agribusiness 23:117-130.

Burton, M., D. Rigby, T. Young, and S. James. 2001. Consumer attitudes to genetically modified organisms in food in the UK. European Rev. Agr. Econ. 28:479-498.

Capoor, S.P. 1949. The movement of tobacco mosaic viruses and potato virus X through tomato plants. Ann. of Applied Biol. 36:307-319.

Chomczynski, P. 1993. A reagent for the single-step simultaneous isolation of RNA, DNA, and proteins from cell and tissue samples. Biotechniques 15:532-537.

Crawford, K.M. and P.C. Zambryski. 2000. Subcellular localization determines the availability of non-targeted proteins to plasmodesmatal transport. Current Biol. 10:1032-1040.

Foster, T.M., T.J. Lough, S.J. Emerson, R.H. Lee, J.L. Bowman, R.L.S. Forster, and W.J. Lucas. 2002. A surveillance system regulates selective entry of RNA in the shoot apex. The Plant Cell 14:1497-1508.

Fridlund, P.R. 1980. Glasshouse indexing for fruit tree viruses. Acta Phytopathologica Academiae Scientiarum Hungaricae. 15:1-4.

Gal-On, A., I. Kaplan, M.J. Roossinck, and P. Palukaitis. 1994. The kinetics of infection of zucchini squash by cucumber mosaic virus indicate a function for RNA 1 in virus movement. Virology. 205:280-289.

Gomez, G., H. Torres, and V. Pallas. 2005. Identification of translocatable RNA-binding phloem proteins from melon, potential components of the long-distance RNA transport system. Plant J. 41:107-116.

Haupt, S., K.J. Oparka, N. Sauer, and S. Neumann. 2000. Macromolecular trafficking between *Nicotiana tabacum* and the holoparasite *Cuscuta reflexa*. J. Expt. Bot. 52:173-177.

Haywood, V., T.-S. Yu, N.-C. Huang, and W.J. Lucas. 2005. Phloem long-distance trafficking of *GIBBERELLIC-ACID_INSENSITIVE* RNA regulates leaf development.

Helms, K. and I.F. Wardlaw. 1976. Movement of viruses in plants: long distance movement of tobacco mosaic virus in *Nicotiana glutinosa*, p. 283-293. In: I.F. Wardlaw and J.B. Passioura (eds.). Transport and Transfer Processes in Plants. Academic Press, New York.

Hu, Z. and Q.Z. Huang. 1994. Induction and accumulation of the antifungal protein in *Gastrodia elata*. Acta Botannica Yunnanica 16:169-177.

Ismail, I.D., I.D. Hamilton, E. Robertson, and J.J. Milner. 1987. Movement and intracellular location of sonchus yellow net virus within infected *Nicotiana edwardsonii*. J. Gen. Virol. 68:2429-2438.

Itaya, A., F. Ma, Y. Qi, Y. Matsuda, Y. Zhu, G. Liang, and B. Ding. 2002. Plasmodesma-mediated selective protein traffic between “symplasmically-isolated” cells probed by a viral movement protein. Plant Cell. 14:2071-2083.

Kim, M., W. Cannio, S. Kessler, N. Sinha. 2001. Developmental changes due to long-distance movement of a homeobox fusion transcript in tomato. Science 293:287-289.

Lucas, W.J., S. Bouche-Pillon, D.P. Jackson, L., Nguyen, L. Baker, B. Ding, and S. Hake. 1995. Selective trafficking of KNOTTED1 homeodomain protein and its mRNA through plasmodesmata. Science. 270:1980–1983.

Más, P. and V. Pállas. 1996. Long-distance movement of cherry leaf roll virus in infected tobacco plants. J. Gen. Virol. 77:531-540.

Nagel, A.K., R. Scorza, C. Petri, and G. Schnabel. 2008. Generation and characterization of transgenic plum lines expressing the *Gastrodia*-Anti Fungal Protein. HortSci 43:1514–1521.

Nakajima K., G. Sena, T. Nawy, and P.N. Benfey. 2001. Intercellular movement of the putative transcription factor SHR in root patterning. Nature 413:307–311.

Palauqui, J.C., T. Elmayan, J.M. Pollien, and H. Vaucheret. 1997. Systemic acquired silencing: transgene-specific post-transcriptional silencing is transmitted by grafting from silenced stocks to non-silences scions. EMBO J. 16:4738-4745.

Petri, C. and L. Burgos. 2005. Transformation of fruit trees: useful breeding tool or continued future prospect? Transgenic Res. 14:15-26.

Ruiz-Medrano, R., B. Xoconostle-Cázeres, and W.J. Lucas. 1999. Phloem long-distance transport of CmNACP mRNA: implications for supracellular regulation in plants. Development 126:4405-4419.

Santa Cruz, S. 1999. Perspective: phloem-transport of viruses and macromolecules – what goes in must come out. Trends in Microbiol. 7:237-241.

Stadler, R., K.M. Wright, C. Lauterbach, G. Amon, M. Gahrtz, A. Feuerstein, K.J. Oparka, and N. Sauer. 2005. Expression of GFP-fusions in Arabidopsis companion cells reveals non-specific protein trafficking into sieve elements and identifies a novel post-phloem domain in roots. Plant J. 41:319-331.

Voinnet, O., P. Vain, S. Angell, and D.C. Baulcombe. 1998. Systemic spread of sequence-specific transgene RNA degradation in plants is initiated by localized introduction of ectopic promoterless DNA. Cell. 95:177-187.

Xoconostle-Cázares, Y. Xiang, R. Ruiz-Medrano, H.L. Wang, J. Monzer, B.C. Yoo, K.C. McFarland, V.R. Franceschi, and W.J. Lucas. 1999. Plant paralog to viral movement protein that potentiates transport of mRNA into the phloem. Science. 283:94.

Yoo, B.C., F. Kragler, E. Varkonyi-Gasic, V. Haywood, S. Archer-Evans, Y.M. Lee, T.J. Lough, and W.J. Lucas. 2004. A systemic small RNA signaling system in plants. Plant Cell 16:1979–2000.

CHAPTER FOUR

GASTRODIA ANTI-FUNGAL PROTEIN (GAFP-1) ACTIVITY AND LOCALIZATION IN *PHYTOPHTHORA SP.* AND *MELOIDOGYNE INCOGNITA*

ABSTRACT

The *Gastrodia* anti-fungal protein (GAFP) is a monocot mannose-binding lectin (MMBL) which is able to inhibit the growth of multiple species of plant pathogenic fungi *in vitro*. Additionally, expression of the lectin *in vivo* imparts protective effects against stramenopile, root-knot nematode (RKN), and fungal pathogens. In this study, GAFP-1 was isolated from transgenic tobacco line pAVNF-3 and purified by ion exchange, affinity, and size exclusion chromatography. *Phytophthora cinnamomi*, *P. nicotianae*, and the RKN *Meloidogyne incognita* were then challenged with purified GAFP-1 to confirm the direct effect of the anti-fungal lectin on non-fungal stramenopile and RKN pathogens. Purified GAFP-1 inhibited growth of the *P. cinnamomi* and *P. nicotianae* mycelium in a concentration dependent manner. However, contact with the lectin did not impair J2 mobility or egg hatch in *M. incognita* over 96 h. The mycelia of *P. cinnamomi* and the fungus *Trichoderma viride* were next challenged with GAFP-1 for 60 min and then subjected to cellular fractionation. Immunoblotted soluble fractions prepared from tissues of both species contained the majority GAFP-1 signal. Pre-treatment of the mycelium with the endocytic inhibitor nocodazole did not alter the localization of GAFP-1 to the soluble fractions of either species, despite inhibitory effects of nocodazole on vesicle trafficking demonstrated by the reduced rate of FM4-64 internalization. Consistent with previous studies in fungi, however, GAFP-1 was able to strongly associate with cell wall pellets prepared from *T.*

viride as well as *P. cinnamomi*. This study demonstrates the ability of GAFP-1 to directly inhibit the oomycete pathogens *P. cinnamomi* and *P. nicotianae* and provides evidence that GAFP-1 can bind the cell wall components of stramenopiles in addition to fungi. Cellular fractionation results from nocodazole pre-treated tissues suggest that GAFP-1 is not being taken up by the cells via microtubule-mediated endocytosis.

INTRODUCTION

It has been demonstrated recently that the expression of the *Gastrodia* anti-fungal protein (GAFP-1) in tobacco and plum confers enhanced tolerance to Phytophthora root rot (PRR), caused respectively by the stramenopile pathogens *Phytophthora nicotianae* and *P. cinnamomi*, and the root-knot nematode (RKN) *Meloidogyne incognita* (Cox *et al.*, 2006; Nagel *et al.*, 2008). Transgenic lines from both systems displayed significantly reduced symptoms of infection by the stramenopiles and reduced galling by the RKN. Additionally, *gafp-1* expressing plum lines demonstrated a significantly lower degree of egg deposition and trended towards decreased RKN reproduction. Although these studies are the first to suggest that the monocot mannose-binding lectin (MMBL) GAFP-1 can target non-fungal oomycete and metazoan organisms, the direct action of the lectin on these pathogens has not yet been investigated.

GAFP possesses strong inhibitory activity against many species of plant parasitic fungi, including *Armillaria mellea*, *Trichoderma viride, Rhizoctonia solani, Valsa ambiens, Gibberella zeae, Ganoderma lucidum,* and *Botrytis cinerea* (Hu and Huang, 1994; Xu *et al.*, 1998). The protective mechanism of GAFP-1 against plant pathogenic fungi has not yet been elucidated, however, making prediction of a putative mode-of-action of the lectin against stramenopile and metazoan pathogens more difficult. Xu and Liu (2003) hypothesized that the lectin interferes with

the dynamics of fungal cell wall expansion after fluorescently-labeled GAFP was found to localize within cell walls of the fungus *Trichoderma viride. Phytophthora* species, which also possess a cell wall, may be targeted by the lectin in a similar manner. Inhibition from both feeding and contact with plant lectins has been observed in RKN of the genus *Meloidogyne* (Marban-Mendoza *et al*., 1987; Sharon *et al*., 2002). RKN are sedentary endoparasites which establish themselves in the vascular bundle of the root and might theoretically be exposed to GAFP-1 through both feeding and contact from cell breakage. GAFP-1 expressing plum lines, however, did not support lower populations of the ecto-parasitic ring nematode, *Mesocriconema xenoplax* (Nyczepir *et al*., 2009). *M. xenoplax* would likely be vulnerable to the lectin only through feeding since they carry out their life-cycle in the surrounding soil, increasing the possibility that GAFP-1 inhibits RKN through contact effects. The purpose of this study was to investigate direct action of GAFP-1 on stramenopile pathogens *P. cinnamomi, P. nicotianae* and the RKN *M. incognita,* as was lectin localization in *T. viride* and *P. cinnamomi*.

MATERIALS AND METHODS

Cultures and plant material

Stramenopile pathogens *Phytophthora cinnamomi*, *P. nicotianae*, and the root-knot nematode *Meloidogyne incognita* were assayed for their susceptibility to GAFP-1. The basidiomycete fungus *Trichoderma viride* was assayed for its susceptibility to GAFP-1 as a positive control for activity of the purified lectin (Yang and Hu, 1990; Xu *et al*., 1998). Active cultures of *T. viride* (isolated from soil, Cave Junction, OR) and *Phytophthora sp*. [*P. cinnamomi,* isolate 05-1127 from peach (*Prunus persica*); *P. nicotianae*, isolate 011P from

tobacco (*Nicotianae tabacum*); Clemson, SC] were maintained on potato dextrose agar (PDA; EMD Chemicals Inc., Gibbstown, NJ, USA) and V8-Amp medium (5% by volume clarified V8-juice concentrate, 1.5% agar, 0.25 mg/mL ampicillin), respectively, in the dark (22 ºC). Populations of *M. incognita* (Blackville, SC) were maintained on roots of tomato (*Solanum lycopersicum* cv. 'Brandywine) in sand:vermiculite (1:1 v/v). Tobacco line pAVNF-3 was used for GAFP-1 isolation (Cox *et al*., 2006). Tobacco and tomato plants were maintained in a Biosafety level 2 greenhouse under constant temperature (27 ± 5 ºC) and light (16/8 h day/night) conditions. Plants were watered, fertilized, and pruned as necessary.

Isolation and purification of GAFP-1

Total protein was isolated from leaf tissues (excluding the central vein) of non-transformed control (NC) and pAVNF-3 (G3) tobacco lines (Cox et al., 2006). Two methods were employed for the isolation of total protein over the course of this study. In both procedures leaf tissues (100 g) were homogenized in liquid nitrogen. Isolation of protein by ammonium sulfate [$(NH4)_2SO_4$] precipitation was performed according to the methods of Wang et al., 2004. Briefly, the leaf homogenate was re-suspended in 300 mL cold cell lysis buffer (40 mM NaH_2PO_4, 200 mM NaCl, pH 6.0) with 1 mL of a 10% protease inhibitor cocktail (Sigma Aldrich, St. Louis, MO, USA). The tissue slurry was filtered through four-layers of sterile cheesecloth and centrifuged at 16,000 x g for 15 min (4 ºC). The resulting supernatant was vacuum-filtered through Whatman® No. 2 filter paper and adjusted to 80% saturation with solid $(NH_4)_2SO_4$. The solution was stirred overnight (4 ºC) and the precipitate was collected by centrifuging at 16,000 x g for 30 min (4 ºC). Precipitated protein was re-suspended in 40 mL phosphate buffer (50 mM K_2HPO_4, pH 6.1). Re-suspended samples were dialyzed against

phosphate buffer (200% by volume) at 4 ℃ in Fisherbrand regenerated-cellulose dialysis tubing (6000-8000 Da MWCO; Thermo Fisher Scientific, Waltham, MA, USA), exchanging a total of three phosphate buffer volumes over 36 hours. Insoluble protein was removed from the dialyzed samples by centrifuging at 16,000 x g for 15 min (4 ℃). The supernatant (crude lysate, pH 6.1) was loaded directly onto Q-sepharose resin (Sigma) (see below). A second isolation procedure based on the methods of Wang et al. (2001) typically resulted in a greater yield of soluble GAFP-1. After grinding of the tissues, the leaf homogenate was re-suspended in 300 mL cold ascorbic acid (1 g/L) with 1 mL of a 10% protease inhibitor cocktail (Sigma) and filtered through sterile cheesecloth. The pH of the solution was adjusted to 2.8 with 1N HCl and centrifuged at 3000 x g for 5 min (4 ℃). The supernatant (crude lysate, pH 2.8) was vacuum-filtered through Whatman™ No. 2 filter paper and loaded directly onto SP-sepharose resin (Sigma).

Crude lysates from leaves of NC or G3 lines were purified in parallel using ion exchange, affinity, and size-exclusion chromatography at 4 ℃ (Fig. S4.1). Briefly, crude lysates in phosphate buffer (pH 6.1) from $(NH_4)_2SO_4$ precipitation were added to a Q-sepharose column (2:1 v/v) equilibrated in phosphate buffer (50 mM K_2HPO_4, pH 6.1; hereafter referred to as "phosphate buffer"). The Q-column was washed with 3 column volumes (CVs) of phosphate buffer and the un-adsorbed portion containing GAFP-1 (G3 line) or the corresponding control fraction (NC line) was collected. Alternatively, crude lysates (pH 2.8) from ascorbic acid isolation were added to an SP-sepharose column (15:1 v/v) equilibrated with 20 mM acetic acid. The SP-column was washed with 3 CVs of 20 mM acetic acid and the fraction containing GAFP-1 or the corresponding NC fraction was eluted with 3 CVs of 100 mM sodium acetate, pH 5.0 + 0.25 M NaCl. Eluates from either anionic or cationic exchange chromatography steps were adjusted to 2 M with solid $(NH_4)_2SO_4$ and loaded onto a D-mannose agarose (Sigma) (6:1 v/v) column equilibrated in phosphate buffer + 2 M $(NH_4)_2SO_4$. The column was washed with five

CVs of phosphate buffer + 1.15 M $(NH_4)_2SO_4$. The GAFP-1 containing fraction or the corresponding NC fraction was eluted in 3 CVs of phosphate buffer. The eluate was concentrated in an Amicon Ultracel® (3000 Da MWCO; Millipore, Billerica, MA, USA) and phosphate buffer exchanged before loading onto a Sephadex G-50 column (1% of total bed volume; Sigma) equilibrated in phosphate buffer + 100 mM NaCl. The column was washed with 1 CV of phosphate buffer + 100 mM NaCl, and GAFP-1 containing fractions or corresponding NC fractions were collected and pooled. Pooled eluates partially purified from $(NH_4)_2SO_4$ precipitated lysates were further concentrated and buffer exchanged with 20 mM acetate for cation exchange chromatography on an SP-column. Alternatively, pooled eluates partially purified from ascorbic acid isolated lysates were further concentrated and phosphate buffer exchanged for anion exchange chromatography on a Q-column. Buffer exchanged samples were loaded onto SP- or Q-sepharose (3:1 v/v) matrices and GAFP-1 containing fractions or corresponding NC fractions were eluted from the column(s) as described above. In all chromatographic methods GAFP-1 elution was monitored by Coomassie staining of SDS-PAGE separated fractions. The same overall chromatographic strategy was employed for GAFP-1 purification regardless of the isolation procedure. The sequence of chromatographic steps and additional elution parameters are summarized in Table S4.1.

GAFP-1 containing fractions or corresponding NC fractions from the final ion exchange chromotography step were phosphate buffer exchanged and concentrated to 70 µL. Protein concentration in NC and G3 purification products was estimated by measuring UV absorption at 280 nm with a Jasco V-550 UV-VIS spectrophotometer (Jasco Analytical Instruments, Easton, MD), using bovine serum albumin as a standard. Absorbance values for G3 purification products were normalized against the background absorbance of corresponding NC purification products

to determine the final GAFP-1 concentration. GAFP-1 concentration was further confirmed in Coomassie stained gels against known concentrations of lysozyme (expected size 14 kDa).

Pathogenicity tests

In vitro-grown cultures of *T. viride, P. cinnamomi* and *P. nicotianae* were challenged with GAFP-1. PDA or V8-Amp plates (5 mL medium in 8.5 cm diameter) were inoculated with plugs (6 mm) taken from the advancing margin of actively growing *T. viride* or *Phytophthora sp.* cultures. *T. viride* and *Phytophthora sp.* plates were incubated in the dark (22 ºC) for 24 and 72 h, respectively. NC or G3 purification products in 5 (*T. viride*) or 8 (*Phytophthora sp.*) µL total volume phosphate buffer were then spotted at the advancing margin of fungal or stramenopile cultures. Growth inhibition was assessed visually in *T. viride, P. cinnamomi,* and *P. nicotianae* after 6, 24 and 72 h, respectively. Inhibition of *P. cinnamomi* was further investigated in coated slide assays. Briefly, sterile microscope slides were dipped three times in molten V8-Amp medium and inoculated with plugs (6 mm) after the medium had solidified and cooled. Slides were incubated for 48 h in the dark (22 ºC) before NC and G3 solutions in 8 µL total volume phosphate buffer were spotted at the advancing margins of the mycelium. Effects were assessed visually after 48 h. All plate and coated slide assays were performed three times.

Nematodes were extracted from detached tomato root systems by shaking with 10% Clorox® (The Clorox Company, Oakland, CA, USA) NaOCl solution for 3 min. Roots were rinsed extensively with tap water over a nested 140:500-mesh sieve. Eggs and nematodes were collected from the 500-mesh sieve, diluted to 40 mL with water and centrifuged at 400 x g for 5 min (22 ºC). Approximately 75% of the supernatant was removed and replaced with sugar solution (1:1 w/v sucrose:water). Nematodes were centrifuged at 400 x g for 2 min (22 ºC) and

the supernatant containing the eggs was carefully removed and rinsed for 1 min on a 500-mesh sieve. Eggs were subsequently incubated on a 400-mesh sieve submerged in water for 72 h (22 ºC). Nematode eggs were collected from the sieve, re-suspended in phosphate buffer, and concentrated at 400 x g (22 ºC). Eggs (100 count) were added to NC and G3 purification products in phosphate buffer (50 µL total volume) in a 96-microwell plate (Fisher). Mobile juveniles (J2 stage) were counted under 4 x magnification on an Olympus BX41 microscope every 24 h for 96 h. NC and G3 treatments were performed in triplicate within an experimental replication to obtain an average J2 count. The average number of mobile J2 present at the start of the assay (0 h) was subtracted from average J2 counts at all other time points. The number of J2 emerging per day was determined by subtracting the previous day's count from the average count at a given time point, or #J2/day = $T_{(n+24)}$ - T_n where the time in hours is given by *n*. The rate of emergence was then averaged across the 96 h period. Nematode experiments were performed three times.

Cellular fractionation

T. viride and *P. cinnamomi* were grown in liquid culture for cellular fractionation. Potato dextrose broth (PDB) (Acumedia Manufacturer's, Inc., Lansing, MI, USA) or V8-Amp liquid medium (50 mL) were added to 125 mL Erlenmeyer flasks and inoculated with *T. viride* or *P. cinnamomi*, respectively. Flasks were shaken at 90 rpm for 72 h (22 ºC). Sterile liquid cultures were stored for a maximum of 30 d (4 ºC).

Prior to cellular fractionation, *T. viride* (10 mg) and *P. cinnamomi* mycelium (30 mg) were washed three times in phosphate buffer and treated with corresponding amounts of NC or G3 purification products (volume equal to 5 µg GAFP-1) in 50 µL total volume phosphate buffer (22 ºC). After lectin treatment, tissues were placed on ice and washed five times with ice-cold

phosphate buffer. Tissues were sonicated in PBS [7 mM Na_2HPO_4, 3 mM NaH_2PO_4, 130 mM NaCl, pH 6.8 + 5% general protease inhibitor (Sigma)] (80 µL total volume) and unbroken material was removed by centrifuging at 1000 x g for 30 s (4 ºC). Complete cell lysis was confirmed within the resulting supernatant at 10 x magnification and an aliquot (crude fraction) was saved for immunoblot and silver stain analysis. Tissue lysates were then separated at 3000 x g for 10 min (4 ºC). The supernatant was removed and again centrifuged at 7500 x g for 30 min (4 ºC). The resulting supernatant (soluble fraction) was saved for immunoblot and silver stain analysis. Isolation of fungal cell walls and extraction of cell wall surface-associated proteins was performed according to the methods of Pitarch *et al*. (2002). Briefly, the 3000 x g pellet was washed three times each with the following ice-cold solutions: dIH_2O, 0.85 M NaCl, and 0.15 M NaCl. Cell wall surface-associated proteins were extracted by boiling the pellet with SDS extraction buffer (50 mM Tris-HCl, pH 8.0, 100 mM EDTA, 2% SDS, 10 mM DTT) for 10 min. SDS-resistant cell wall components were pelleted at 3000 x g for 5 min (22 ºC), and the resulting supernatant containing SDS-extracted peptides (insoluble fraction) was removed and saved for immunoblot and silver stain analysis. Peptides from crude, soluble, and insoluble fractions were separated by SDS-PAGE on a 15% Tris-glycine gel. GAFP-1 was detected in 10 µL fraction aliquots by immunoblot analysis with affinity purified polyclonal GAFP-1 antibodies. Total protein profiles were analyzed in 0.5, 1, and 1 µL aliquots of crude, soluble, insoluble fractions, respectively, by silver stain analysis (ProteoSilver™ Plus Silver Stain Kit; Sigma) according to manufacturer's instructions.

To investigate the cell wall binding ability of GAFP-1, G3 (5 µg GAFP-1) purification products in phosphate buffer were pre-incubated for 30 min with slurries prepared from insoluble cell wall fractions of *T. viride* and *P. cinnamomi* mycelium (0 - 100 mg). After pre-incubation insoluble material was pelleted at 3000 x g for 10 min (4 ºC) and the resulting supernatant was

used for the challenge of *T. viride* (10 mg) and *P. cinnamomi* (30 mg) hyphae (60 min). Soluble fractions were prepared from tissues treated with pre-incubated G3 samples and analyzed by immunoblot and silver staining as described above.

Nocodazole treatment and densitometry

The effect of nocodazole on GAFP-1 localization was investigated in *T. viride* and *P. cinnamomi*. The mycelium of *T. viride* and *P. cinnamomi* (10 and 30 mg, respectively) was treated with the endocytic inhibitor nocodazole (30 µM) or DMSO (0.2%) for 3 and 24 h in PDB or V8-Amp liquid medium (50 µL total volume), respectively, prior to challenging tissues with G3 purification products (5 µg GAFP-1) in 50 µL total volume phosphate buffer for 0-60 min. Before G3 solutions were added to mycelium, tissues were equilibrated in phosphate buffer for 60 min in the presence of 0.2% DMSO or 30 µM nocodazole. The mycelium of *T. viride* and *P. cinnamomi* incubated in non-amended liquid medium (3 and 24 h, respectively) and phosphate buffer (60 min) prior to GAFP-1 challenge served as additional negative controls (medium pre-treated controls) for potential changes in GAFP-1 localization. Crude, soluble, and insoluble fractions were prepared from tissues and analyzed by immunoblot as described above.

Non-specific binding between the GAFP-1 antibody and high(er) molecular weight (HMW) epitopes (30 to 75 kDa) was consistently observed on immunoblots of all fractions from both species (Fig. S4.2), and has been reported previously for this antibody (Nagel *et al*., 2010). These HMW signals were used as internal standards when quantifying GAFP-1 signal intensity by densitometry. GAFP-1 and HMW signals within all fractions from *T. viride* and *P. cinnamomi* were quantified on immunoblots using ImageJ Software (NIH, Bethesda, MD). HMW intensity values within a fraction type were normalized against an average HMW intensity value taken

across the four time points. To control for variation in intensity between independent replications, an average crude HMW intensity value was determined for each blot (0-60 min) and normalized against the average crude HMW value taken across the three media control replications. GAFP-1 intensity values were adjusted according to normalized HMW fraction values as well as to normalized crude HMW value for the blot. Values and standard deviations were determined across three experimental replications.

Fluorescence microscopy and imaging

T. viride and *P. cinnamomi* were cultured on coverslips for fluorescence microscopy. Sterile coverslips were placed on PDA or V8-Amp plates (2 mL medium in 4.5 cm diameter) and molten PDA or V8-Amp medium (1 mL), respectively, was layered over the top of the coverslips and allowed to cool. Plugs (3 mm) from the advancing margin of active *T. viride* or *P. cinnamomi* cultures were placed at the edge of the coated coverslips and plates were incubated for 24 h in the dark (22 ºC). Coverslips containing the *T. viride* or *P. cinnamomi* mycelium were removed from plates and placed in PDB or V8-Amp liquid medium, respectively, containing 0.2% DMSO or 30 µM nocodazole. *T. viride* and *P. cinnamomi* coverslips were incubated for 3 and 24 h, respectively, and washed with ice-cold PDB or V8-Amp liquid medium lacking the inhibitor before dye loading. Coverslips were placed on ice and treated with FM4-64 lipophilic dye (64 µM; Invitrogen Corporation, Carlsbad, CA, USA) in ice-cold PDB or V8-Amp liquid medium for 10 min and then washed with cold media lacking dye. Coverslips were removed from ice and dye uptake was monitored in tissues on a Nikon E600 microscope under 40 x magnification using a standard TRITC filter set. Images (RGB) were acquired with Q-capture (QImaging, Surrey, British Columbia, Canada) imaging software. Binary images for the red channel were generated

from RGB stacks using Image J (NIH). Brightfield photographs of mycelium pre-treated with 0.2% DMSO or 30 µM nocodazole were imaged at 4 x magnification using an Olympus DP11 digital camera mounted on an Olympus BX41 microscope.

RESULTS

Crude protein lysates were isolated from leaves of NC and G3 tobacco lines and purified by ion exchange, affinity, and size exclusion chromatography (Fig. 4.1 A). The 12 kDa band present in final purification products from G3 lines was confirmed to be GAFP-1 by immunoblot analysis. G3 purification products in phosphate buffer (50 mM K_2HPO_4, pH 6.1) were able to inhibit growth of *T. viride* hyphae in a concentration dependent manner after 4 to 6 h (Fig. 4.1 B). Filaments were able to take over the area of inhibition (AOI) resulting from G3 solutions in less than 24 h, consistent with results from previous studies (Xu *et al.*, 1998), however the cleared GAFP-1 AOI advanced with the actively growing margin of the fungal culture. Final purification products from NC lines did not contain a signal at the 12 kDa position (Fig. 4.1 A). NC solutions from intermediate purification steps (Fig. S4.1) were inhibitory on the *T. viride* mycelium, but after the purification scheme was complete inhibition of fungal hyphae by corresponding NC solutions was absent (Fig. 4.1 B).

NC or G3 purification products in phosphate buffer were spotted at the periphery of actively growing *P. cinnamomi* and *P. nicotianae* cultures to determine whether these species are susceptible to GAFP-1. When cultured on plates (Fig. 4.2 A, left) or slides coated with V8-Amp medium (Fig. 4.2 A, right), *P. cinnamomi* mycelium were inhibited by G3 solutions in a concentration dependent manner after 24 and 48 h, respectively. Hyphae of *P. cinnamomi* from V8-Amp plate cultures appeared to be only partially inhibited by G3 solutions, whereas on coated

slides hyphae were completely inhibited. G3 solutions were able to inhibit hyphae of *P. nicotianae* on V8-Amp plates in a concentration dependent manner after 72 h (Fig. 4.2 B). Polymorphic growth among independent *P. nicotianae* cultures was observed, and both sparsely- (Fig. 4.2 B left) and densely- (Fig. 4.2 B right) growing forms were inhibited by G3 solutions. Corresponding NC solutions were not inhibitory on hyphae of *P. cinnamomi* or *P. nicotianae* after the respective incubation times on plates or coated slides (Figs. 4.2 A and B). In contrast to *T. viride*, the AOI resulting from G3 solutions persisted for over 96 h in *Phytophthora sp*. (data not shown).

Eggs of *M. incognita* were treated with NC or G3 purification products in phosphate buffer to investigate inhibitory effects of GAFP-1 on juvenile (J2 stage) nematodes. G3 solutions had little to no effect on J2 mobility or egg hatch under the experimental conditions employed (Table 4.1). The increase in the average number of mobile J2 over 96 h, as well as the positive values for rate of emergence, demonstrated that egg hatch was occurring in all treatments. After 96 h average mobile J2 counts became highly variable between independent replications (data not shown), likely reflecting inherent variability in population growth dynamics among individual egg pools. On average, G3-treated wells supported a lower number of mobile J2 compared to NC-treated wells at all time points, however mobile J2 counts in G3-treated wells were not at any time appreciably reduced compared to counts in buffer-treated wells. Increasing GAFP-1 concentration to 15 µg in 50 µL phosphate buffer did not amplify effects on J2 mobility. Values for rate of emergence, which represent the average number of mobile J2 appearing per day, were not considerably reduced in G3-treated wells compared to NC- and buffer-treated wells. These results suggest that GAFP-1 does not influence egg hatch or J2 mobility through contact effects in the short-term.

Localization of GAFP-1 in tissues of *T. viride* and *P. cinnamomi* was explored through cellular fractionation. Immunoblotting was performed on crude, soluble, and insoluble fractions prepared from mycelium tissues incubated with NC or G3 purification products in phosphate buffer for 60 min. In both species, the soluble fractions prepared from G3-treated hyphae contained the majority of the GAFP-1 signal (expected size 12 kDa) (Fig. 4.3 A). In *T. viride*, the intensity of the GAFP-1 signal in the soluble fraction was consistently on par with that in the crude fraction, while the insoluble fraction contained little to no GAFP-1 signal. In *P. cinnamomi*, GAFP-1 signal intensity was always highest in the crude fraction and lowest in the insoluble fraction. However, the degree of difference in signal intensity between crude/soluble and soluble/insoluble fractions varied between independent replications in *P. cinnamomi*. Fractions prepared from *T. viride* or *P. cinnamomi* mycelium treated with NC solutions contained no signal at the 12 kDa position. Silver stained fraction profiles revealed more qualitative differences between fraction types in *T. viride* then *P. cinnamomi*. The distribution of the GAFP-1 signal in cellular fractions was not affected by the protein isolation procedure employed (Fig. 4.3 B). Also, the mycelium were washed five times with phosphate buffer following G3-treatment and a scant GAFP-1 signal present in immunoblots of the last post-treatment wash confirmed that the soluble fraction GAFP-1 signal was not due to cross-contamination from lectin exposure (Fig. 4.3 C). Lastly, washing tissues with 130 mM NaCl in phosphate buffer after G3-treatment did not affect the final distribution of the GAFP-1 signal in either species (data not shown), suggesting that a specific association exists between GAFP-1 and tissues of *T. viride* and *P. cinnamomi*.

In preliminary time-course assays the intensity of the GAFP-1 signal increased over 60 min in immunoblots of crude and soluble fractions prepared from G3-treated mycelium of *T. viride* and *P. cinnamomi* (Fig. S4.3). The endocytic inhibitor nocodazole was employed to find out if cellular uptake was responsible for the presence of GAFP-1 within the soluble fractions of

T. viride and *P. cinnamomi*. When cultured on nocodazole-amended media, the diameter of *T. viride* and *P. cinnamomi* cultures was reduced by 77% and 57%, respectively, compared to DMSO controls (Fig. 4.4 A). Growth morphology was also altered in both species. After 3 and 24 h pre-incubation in nocodazole-amended media, both hyphae of *T. viride* and *P. cinnamomi* showed signs of increased lateral branching and stunted growth (Fig. 4.4 B). These results are consistent with the anti-mitotic mechanism of nocodazole, which acts to decrease the stability of microtubules through the depolymerization of β-tubulin (Sigma).

Effects of nocodazole on vesicle trafficking were assessed in both species by monitoring uptake of the fluorescent, lipophilic dye, FM4-64, in mycelium tissues. A diffuse fluorescent signal could be observed inside cells of DMSO pre-treated *T. viride* hyphae at all time points (Fig. 4.4 C). The cloudy internal signal likely represents dye intercalation into vesicle and organelle membranes. The fact that the outer membranes of DMSO pre-treated *T. viride* hyphae lacked a fluorescent signal when cells were first imaged (0 min) suggests that internalization of the dye is very rapid in *T. viride*. Conversely, the outer membranes of nocodazole pre-treated *T. viride* cells remained fluorescently stained up to 5 min after slides were removed from ice, and clearly defined, dye-containing vesicles could be seen budding from the outer membranes at earlier time-points (Fig. 4.4 C, white arrows). Dye uptake was slower in hyphae of *P. cinnamomi* compared to *T. viride*. Outer membranes of DMSO pre-treated *P. cinnamomi* hyphae contained a continuous fluorescent signal at 0 min, but by 10 min the signal became patchy likely due to dye internalization. By 20 min the interior fluorescence was almost indistinguishable from that of the outer membrane. The outer membranes of *P. cinnamomi* hyphae pre-treated with nocodazole, by contrast, retained a continuous fluorescent signal up to 10 min. Breaks in membrane fluorescence began to be apparent by 20 min. However, the difference between outer membrane and interior fluorescence could still be clearly perceived. Unlike *T. viride*, dye-containing vesicles were not

apparent in hyphae of *P. cinnamomi*. Neither species demonstrated inherent fluorescence in the red spectrum when treated with medium lacking FM4-64 dye (data not shown). The delay in FM4-64 internalization in nocodazole pre-treated hyphae versus that in DMSO pre-treated tissues suggests that this compound can inhibit endocytosis in both *T. viride* and *P. cinnamomi*.

Densitometric analysis performed on immunoblotted fractions from *T. viride* and *P. cinnamomi* demonstrated that nocodazole pre-treatment did not decrease the relative soluble fraction GAFP-1 signal intensity compared to DMSO pre-treated controls (Fig. 4.4 D). It therefore seems unlikely that microtubule-mediated endocytosis is contributing to GAFP-1 localization within the soluble fractions of either species. GAFP-1 signal intensity appeared to have a greater dependence on time in crude and soluble fractions from *T. viride* compared to *P. cinnamomi* (Fig. 4.4 D). Pre-incubation of *T. viride* tissues in medium alone did not change GAFP-1 signal distribution after 60 min compared to initial fractionation results (Fig. 4.3 versus Fig. 4.4 D, medium pre-treated control). Alternatively, when compared to initial fractionation results, medium pre-incubation of the *P. cinnamomi* mycelium did decrease soluble fraction GAFP-1 signal intensity relative to that of the insoluble fraction. This phenomenon may be the result of culture storage effects on GAFP-1 signal distribution in Fig. 4.3. GAFP-1 intensities in insoluble fractions of *T. viride* pre-treatments were low enough at all time-points to be considered negligible

To investigate whether GAFP-1 is able to bind cell wall components of *T. viride* and *P. cinnamomi*, G3 solutions were pre-incubated with cell wall pellets prepared from the mycelium of both species. When hyphae were treated with pre-incubated G3 solutions, GAFP-1 signal intensity decreased within the soluble fractions of *T. viride* and *P. cinnamomi* (Fig. 4.5 A). Moreover, the degree of GAFP-1 signal depletion correlated to the weight of the mycelium used for the generation of the insoluble material in the pre-incubation step. In neither species did non-

specific degradation appear to be responsible for the decrease in GAFP-1 concentration during the pre-incubation step, since Coomassie staining demonstrated there was no observable decrease in GAFP-1 band density in pre-incubation slurries after 30 min (Fig. 4.5 B). Following incubation with G3 solutions, the cell wall material was re-pelleted, washed with phosphate buffer, and associated peptides were removed by boiling with SDS extraction buffer. A strong GAFP-1 signal was found in immunoblotted SDS extracts from cell wall pellets of *T. viride* and *P. cinnamomi*, and the strength of the signal appeared to be directly related to the size of the pellet (Fig. 4.5 C). No more than a slight GAFP-1 signal in the last pellet wash confirmed that the intensity of the GAFP-1 signal in SDS extracts was not due to a large degree of cross-contamination. SDS-extracts from untreated pellets did not contain a corresponding 12 kDa band (Fig. 4.5 C).

DISCUSSION

Here we show for the first time that purified GAFP-1 is directly active against two *Phytophthora* species. Stramenopile species in this study were both used for disease challenge of transgenic tobacco and plum lines in previous studies (Cox *et al*., 2006; Nagel *et al*., 2008). We also provide evidence that GAFP-1 is able to associate with cell wall components from the stramenopile *P. cinnamomi* in addition to the fungus *T. viride*. Further work will be necessary to establish the direct action and localization of the lectin in the RKN *M. incognita*.

Some differences were noted between fungus and stramenopile species with respect to GAFP-1 inhibition. In contrast to *T. viride*, the mycelium of *P. cinnamomi* was only partially inhibited when V8-Amp plate cultures were spot-treated with the lectin. The *P. cinnamoi* mycelium was completely inhibited by GAFP-1, however, when cultured on coated microscope slides. The slides were coated with a very thin layer of V8-Amp medium to restrict the plane of

hyphal growth, and it would therefore appear that some filaments were able to avoid the lectin solution in the plate format by growing underneath the surface of the medium. Subterranean growth was not observed to a great extent in plates containing *P. nicotianae* cultures, the mycelium from which was also inhibited by GAFP-1. The mycelium of *T. viride* was able to overtake the lectin-generated AOI in less than 24 h, which has been reported in a previous study (Xu *et al*., 1998), however the AOI resulting from GAFP-1 treatment persisted up to 96 h both species of *Phytophthora*. When cultured on V8-Amp medium, the mycelium of *T. viride* was still able to overtake the GAFP-1 AOI (Fig. S4.4 A), suggesting that media effects were not responsible for observable differences in inhibition between the fungus and the stramenopiles. The fact that the cleared AOI advanced with the actively growing margin of the fungal culture on both types of media may indicate that the fungal hyphae can resume growth after temporary inhibition. The basidiomycete *Armillaria mellea*, the native target of GAFP, likely requires large amounts of the lectin to be completely inhibited judging from the high quantities of GAFP expressed within certain areas of the *G. elata* root system (Hu and Huang, 1994; Hu *et al*., 1988; Yang and Hu, 1990). The limited amount of GAFP-1 utilized to inhibit *T. viride* in these assays was probably insufficient to compensate for continued fungal growth. In general, a larger amount of GAFP-1 was necessary to elicit a minimal inhibitory effect on the mycelium of the stramenopile species compared to *T. viride*. However, consistent with similar experiments on *Valsa ambiens* (Wang *et al*., 2001), GAFP-1 activity varied between independent isolations from tobacco. This makes it difficult to predict an absolute threshold for inhibition on fungal and stramenopile species. The activity of GAFP-1 on *T. viride* in our study was comparable to that obtained by Wang *et al*. (2001) when *Valsa ambiens* hyphae were challenged with the NF isoform of GAFP isolated from tobacco.

Direct inhibition of *M. incognita* by GAFP-1 was not demonstrated in this study. Lectin treatment did not affect egg hatch or juvenile nematode mobility. Conversely, expression of GAFP-1 decreased symptoms of infection by the endo-parasitic RKN in two independently transformed plant systems (Cox *et al*., 2006, Nagel *et al*., 2008). Additionally, another MMBL, the insecticidal *Galanthus nivalis* agglutinin (GNA) from snowdrop, has been shown to inhibit galling by *M. incognita* when heterologously expressed in *Arabidopsis thaliana* (Ripoll *et al*., 2003). In a previous study it was determined that the production of GAFP-1 in roots of transgenic plum had no effect on the population growth of the ring nematode, *Mesocriconema xenoplax* (Nyczepir *et al*., 2009). Because the ecto-parasitic *M. xenoplax* would only be vulnerable to the nematode through feeding, we surmised that GAFP-1 might be active on the RKN through contact effects. Other research efforts have demonstrated that treatment of *M. javanica* with antibodies directed against surface antigens can limit penetration of the RKN into *Arabidopsis* (Sharon *et al*., 2002), and contact exposure to the lectin concanavalin A (ConA), which can bind glycoproteins in surface coat extracts of *Meloidogyne* (Spiegel and McClure, 1991; Davis *et al*., 1992), decreased *M. incognita* galling severity in roots of tomato (Marban-Mendoza *et al*., 1987). It is of course possible that *M. incognita* are inhibited by GAFP-1 through feeding, and that the different responses of *M. incognita* and *M. xenoplax* populations to GAFP-1 expressing root tissues simply reflect species specific reactions to lectin exposure. Alternatively, since cuticle molecular composition is known to vary between developmental stages in nematodes (Spiegel and McClure, 1991; Zuckerman and Kahane, 1983), it may be that only late-stage RKN are affected by contact with GAFP-1. Also, if *M. incognita* are ultimately susceptible to contact with the lectin, the RKN may require longer exposure to GAFP-1 (> 96 h) before impacts on activity can be observed. Marban-Mendoza *et al*. (1987), for instance, observed that consecutive applications of infected roots over 4 weeks with dilute ConA solutions were more effective at

reducing RKN galling than a single concentrated lectin application. In our study, however, we observed that nematodes in buffer-treated wells typically began to immobilize after 120-144 h, likely due to the lack of plant-derived chemoattractants which would direct them towards root tissues (Marban-Mendoza *et al.*, 1987). A better assessment of RKN responses to GAFP-1 over the complete RKN life-cycle awaits further investigation.

Our results suggest that GAFP-1 is not being internalized by the hyphae through microtubule-mediated endocytosis. Xu and Liu (2003) demonstrated that fluorescently tagged GAFP was concentrated within the developing cell wall septa and apices in hyphae of *T. viride* which had been exposed the lectin for 10 min. In this study, soluble fractions prepared from the G3-treated mycelium of *T. viride* and *P. cinnamomi* contained a relatively large portion of the GAFP-1 signal after an hour of lectin exposure. When pre-treated with nocodazole, however, the relative intensity of the GAFP-1 signal was not noticeably within soluble fractions of either species compared to their respective DMSO pre-treated controls. Nocodazole has been used in other studies to explore vesicle trafficking mechanisms in fungi (Peñalver *et al*., 1997), and the endocytic agent was able to impair uptake mechanisms in both *T. viride* and *P. cinnamomi* as demonstrated by time-course analysis of FM4-64 internalization. The lipophilic FM4-64 dye, which has been used as a reporter of endocytosis in fungi and plants (Fischer-Parton *et al.*, 2000; Leborgne-Castel *et al.*, 2008; Vida and Emr, 1995), is believed to be internalized in living cells by regulated cellular uptake mechanisms and not by unfacilitated diffusion (Betz *et al.*, 1996; Illinger and Kuhry, 1994). If endocytosis was contributing to the accumulation of the GAFP-1 signal in the soluble fraction of either species, then the soluble fraction signal intensity of nocodazole pre-treated hyphae would be expected to be depressed compared to that in the DMSO pre-treated control, particularly at earlier time-points. While it is true that the soluble fraction signal intensities were slightly lower than the DMSO-controls in nocodazole pre-treated cells of

T. viride and *P. cinnamomi* at 60 min, the relatively strong GAFP-1 signal in the soluble fractions of both species after only a few minutes of exposure cannot likely be attributed to cellular uptake of the lectin by endocytosis. It is possible that the lectin is able to move into the cell by some other means. Microtubule-independent endocytosis of membrane-localized receptors has been demonstrated in yeast (Penalver *et al*., 1997), and some chitin-binding plant lectins are thought to directly traverse the outer membrane and move intracellularly (Koo *et al.,* 1998). The latter pathway, where anti-microbial peptides were observed to be internalized as little as 15 min after treatment, resulted in severe morphological changes to the hyphae of both fungus and stramenopile species. Inhibition of the fungal mycelium by GAFP, however, has not been shown to have effects on hyphal morphology (Xu *et al.*, 1998).

The supposedly cell wall-targeted GAFP-1 lectin could be easily liberated from the carbohydrate matrix of *T. viride,* and to a lesser extent in *P. cinnamomi*, upon lysis, thus accounting for its presence within the soluble fractions of both species. Supporting the ability of the lectin to bind the cell wall components of *T. viride* and *P. cinnamomi* was the fact that GAFP-1 associated with cell wall pellets prepared from the basidiomycete, consistent with previous experiments in *T. viride* (Xu and Liu, 2003), as well as the stramenopile. Nocodazole pre-treatment provided evidence that GAFP-1 is not moving into the cell by vesicle trafficking. Weak binding interactions have previously been predicted between some lectins and their suspected ligands (Barboni *et al*., 1999; Brewer, 2004; Neumann *et al*., 2002; Van Damme *et al.,* 2000), and the presence of some secreted, cell-wall associated proteins in yeast culture supernatants may be attributed to potentially weak associations with cell wall moieties (Chaffin *et al.*, 1998). The lack of extended binding sites or additional protomer contacts to stabilize ligand binding in the monomeric lectin could certainly contribute to weak carbohydrate binding ability in GAFP-1 (Liu *et al.*, 2005; Hester and Wright, 1996).

The question of what the lectin is binding and why it may be freed from the cell wall matrix, particularly in *T. viride*, is surely tied to its inhibitory mechanism which is currently unknown. If GAFP is able to bind directly to the cell wall matrix, as it has been postulated to do by some (Liu *et al*., 2005; Xu and Liu, 2003), intercalation of the lectin into the carbohydrate strands could theoretically disrupt the turgor pressure necessary for cell wall expansion (Bartnicki-Garcia *et al*., 2000; Wessels, 1994). The localization of the lectin to dynamic apical and septa regions of the cell wall (Xu *et al*., 2003) would support this hypothesis since it is in these areas that synthesis of oligosaccharides would be high and effects on cell wall growth the most acute. Also, perhaps any observed dependence of GAFP-1 signal intensity on time in crude and soluble fractions from *T. viride* or *P. cinnamomi* is due to increased expression or presentation of the putative GAFP-1 ligand as a result of normal growth or as a specific response to the lectin. The fact that GAFP-1 was able to strongly associate with isolated cell wall pellets undermines the possibility that the lectin may be binding a ligand that is weakly associated with the carbohydrate matrix or the cellular exterior, such as a secreted glycoprotein (Chaffin *et al*., 1998; Pitarch *et al*., 2002) or membrane peripheral, since these weakly associated molecules would theoretically have been freed from the matrix after both cell lysis and the high salt wash. We found no evidence of GAFP-1 localization to the membrane fraction in either species, suggesting that GAFP-1 is not binding residual membrane components present in the insoluble pellet (data not shown). However extraction of membranes in detergent may have interrupted GAFP-1 binding to its putative target, which could have generated a false negative for the potential of the soluble GAFP-1 to bind a membrane peripheral.

The specific ligand preferred by GAFP has yet to be determined. As their name would suggest, lectins of the MMBL family are diagnostic for their ability to bind mannoside derivatives, however individual members vary in the finer points of molecule recognition (Hester

and Wright, 1996; Kaku *et al*., 1990; Liu *et al*., 2005; Shibuya *et al*., 1988; Van Damme *et al*., 2000). GAFP-1's three carbohydrate recognition domains contain the conserved binding motif common to all MMBLs (Barre *et al*., 2001; Liu *et al*. 2005; Wang *et al*. 2001), and it is likely, similar to other MMBLs, that that GAFP-1 can accommodate a 1,3 or 1,6-linked mannoside ligand(s) within at least one or more of its binding sites (Liu *et al.*, 2005). Xu *et al*. (1998) hypothesized that GAFP may also have chitin binding ability, since, in addition to mannose, the lectin was able to associate with N-acetylglucosamine and chitin on an affinity column. Although chitin-binding ability could contribute to GAFP-1's mechanism for binding within fungal cell walls, GAFP-1 was also active against the stramenopiles *P. cinnamomi* and *P. nicotianae* (this study) whose cell walls contain no chitin (Koo *et al*., 1998). Similar to GAFP-1, anti-microbial, chitin-binding Pn-AMP lectins from morning glory (*Pharbitis nil*.) are able to the inhibit growth of multiple species of plant pathogenic fungi and stramenopile species *in vitro* (Koo *et al*., 1998). Also, when heterologously expressed, Pn-AMPs conferred resistance to infection by *Fusarium oxysporum, Phytophthora capsici* (Lee *et al*., 2003), and *Phytophthora parasitica* (Koo *et al*., 2002). Further investigation demonstrated that the Pn-AMPs localized within the cell wall apices and septa in both fungal (*Botrytis cinerea*) and stramenopile (*Phytophthora parasitica*) pathogens (Koo *et al*., 1998) before eventually moving into the cytosol. If chitin-binding was playing a role in the inhibitory mechanism of Pn-AMPs, or GAFP for that matter, it might not necessarily be for the purpose of binding the extracellular carbohydrate matrix. It should be noted that we did not observe any association between GAFP-1 and chitinous egg shells (Clarke *et al*., 1967) of *M. incognita* in phosphate buffer (Fig. S4.4 B), and affinity column binding experiments conducted by Xu *et al*. (1998) were performed under high salt conditions that are not representative of a physiological environment for molecule association. The ability of GAFP-1 to bind chitin may

therefore be questionable. The saccharide binding specificity of GAFP-1 remains to be determined, and once known will likely aid elucidation of this lectin's inhibitory mechanism.

The GAFP lectin is known to be active against many species of plant pathogenic fungi, and recent evidence would suggest that it can target selected non-fungal pathogens as well (Cox *et al*. 2006; Nagel *et al*., 2008, this study). To our knowledge ours is the first example of an MMBL targeting an oomycete pathogen. Interestingly, it has recently been found that MMBL homologues (β-lectins or α-D-mannose specific plant lectins) are up-regulated in soybean upon infection by *Phytophthora sojae* (Jiang *et al*., 2010), perhaps providing a distant link between related dicotyledonous plant lectins and defense against stramenopile pathogens. Further work with *M. incognita* will require the co-cultivation of nematodes and GAFP-1 expressing roots so that effects of lectin exposure on the metazoan pathogen can be observed over a longer period of time. Evidence from this study suggests that GAFP-1 is targeted to the cell walls of *Phytophthora* just as it is in *Trichoderma* (Xu and Liu, 2003). Further work with cellular imaging will be necessary to determine the ultimate fate of GAFP-1 within the cells of fungi, stramenopiles, and nematodes.

FIGURES AND TABLES

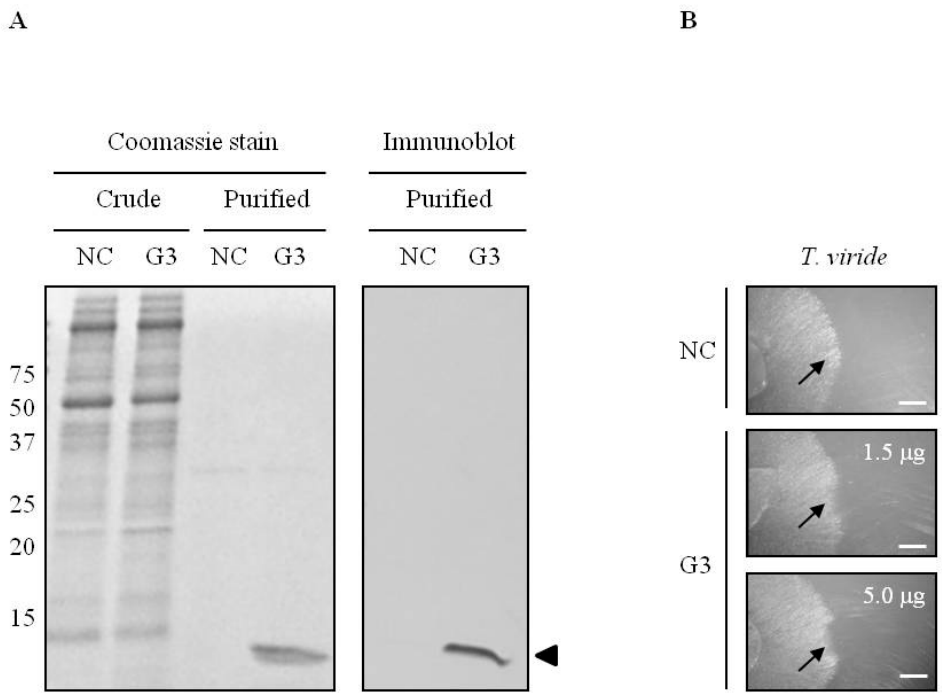
A
B
Coomassie stain
Immunoblot
Crude
Purified
Purified
NC
G3
NC
G3
NC
G3
75
50
37
25
20
15
T. viride
NC
G3
1.5 µg
5.0 µg

Figure 4.1. (A) Protein purified (purified) from crude lysates (crude) of NC or G3 tobacco lines was stained with Coomassie reagent or immunoblotted with polyclonal GAFP-1 antibodies. Coomassie-stained NC and G3 lanes were loaded with 34 µg crude protein or a volume of purified protein equal to 2.5 µg GAFP-1. Immunoblotted NC and G3 lanes were loaded with a volume of purified protein equal to 0.05 µg GAFP-1. The black arrow indicates the position of the GAFP-1 band (expected size 12 kDa). (B) Effects of NC and G3 purification products on *T. viride* mycelium growth after 6 h. NC or G3 solutions were spotted at the advancing margin (black arrows) of *T. viride* cultures. The amount of GAFP-1 used for challenge is indicated in the top right corner. NC solutions contained a volume of the control purification product equal to 5.0 µg GAFP-1. Scale bars = 3 mm.

A

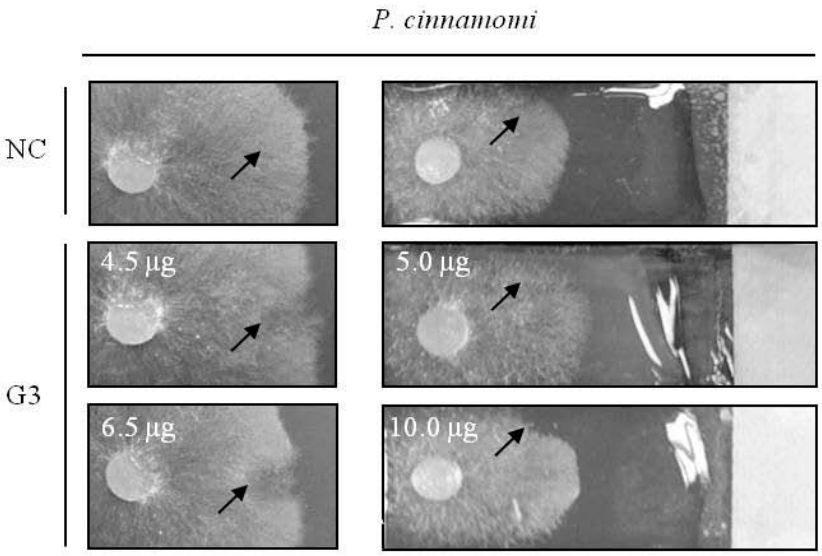
P. cinnamomi
NC
G3
4.5 µg
5.0 µg
6.5 µg
10.0 µg

B

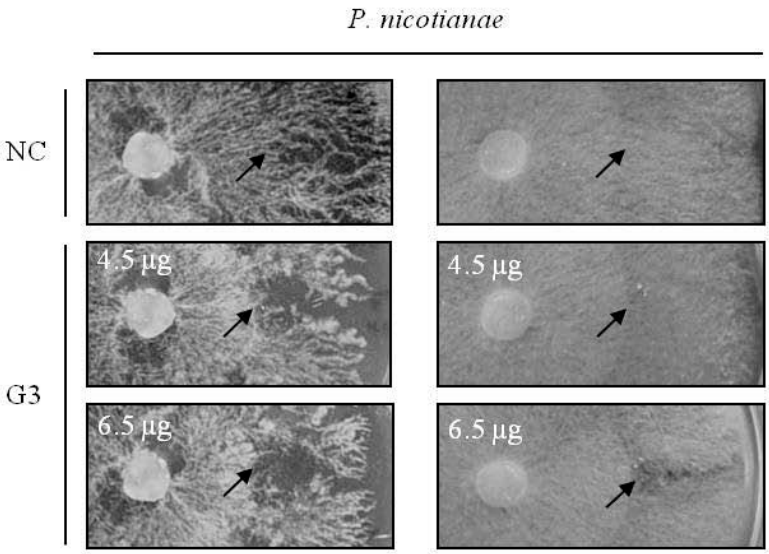
P. nicotianae
NC
G3
4.5 µg
4.5 µg
6.5 µg
6.5 µg

Figure 4.2. Effects of NC and G3 purification products on the growth of (A) *P. cinnamomi* and (B) *P. nicotianae* mycelium. NC or G3 solutions were spotted at the advancing margin (black arrows) of *Phytophthora* cultures. Effects on plate (left) and coated slide (right) cultures of *P. cinnamomi* were assessed after 24 and 48 h, respectively. Effects on plate cultures of *P. nicotianae* were assessed after 72 h. NC solutions contained a volume of the control purification product equal to 6.5 (plate) or 10 µg (coated slide) GAFP-1. Scale bars = 2 mm.

Table 4.1. *M. incognita* J2 mobility and egg hatch following GAFP-1 exposure.

Treatment[y]	GAFP-1	Number of mobile J2[z]				
		24 h	48 h	72 h	96 h	Rate[x]
50 mM K_2HPO_4	0	2.8 ± 3.0	6.8 ± 4.6	5.3 ± 4.3	9.8 ± 4.5	2.4 ± 1.1
NC	0	4.4 ± 2.6	7.1 ± 1.7	7.5 ± 3.8	11.5 ± 5.9	2.9 ± 1.5
G3	5	2.4 ± 1.0	4.6 ± 0.8	6.0 ± 1.8	7.8 ± 2.5	1.9 ± 0.6
G3	15	3.1 ± 2.1	4.0 ± 3.0	6.3 ± 1.7	8.8 ± 4.5	2.2 ± 1.1

[z]Average starting J2 counts (0 h) were subtracted from average daily J2 counts within a treatment. All values are means and standard deviations (±) taken across three experimental replications.

[y]NC solutions contained a volume of the control purification product equal to 15.0 µg GAFP-1.

[x]Average rate of emergence (rate) was determined over the 96 h period for a given treatment.

A

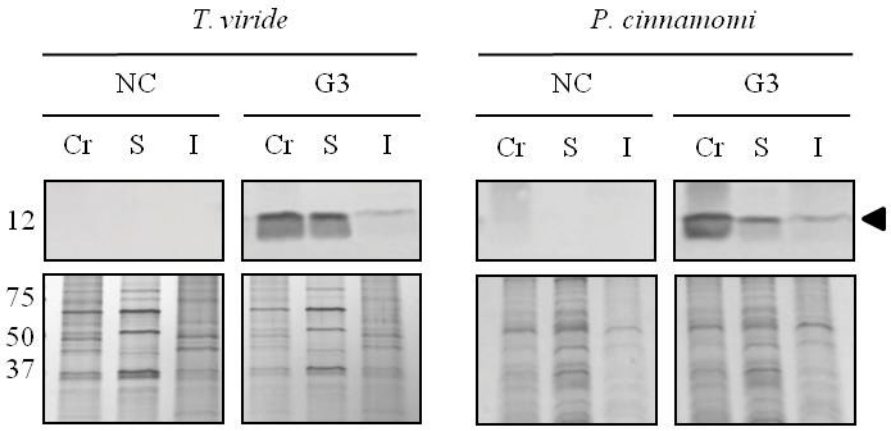
T. viride
P. cinnamomi
NC
G3
NC
G3
Cr S I Cr S I
Cr S I Cr S I
12
75
50
37

B

C

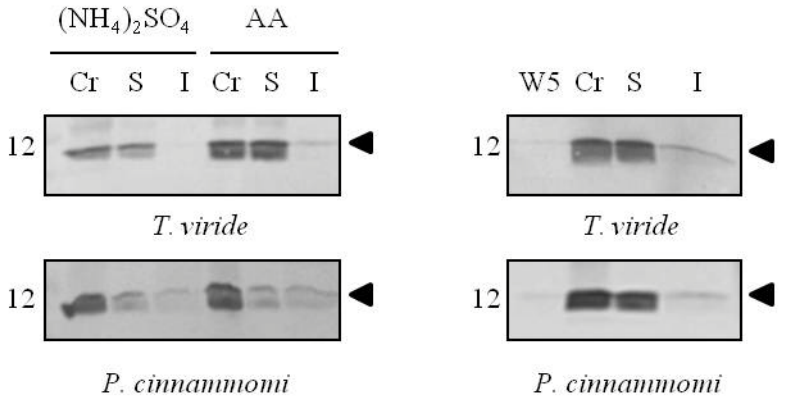
(NH4)2SO4
AA
Cr S I Cr S I
12
T. viride
12
P. cinnammomi
W5 Cr S I
12
T. viride
12
P. cinnammomi

Figure 4.3. GAFP-1 localization in immunoblotted crude (Cr), soluble (S), and insoluble (I) fractions prepared from the mycelium of *T. viride* and *P. cinnamomi*. (A) Mycelium fractions were analyzed by immunoblot (top) and silver stain (bottom) after 60 min of exposure to G3 solutions. The mycelium tissues of both species were also challenged with NC solutions containing a volume of the control purification product equal to 5 µg GAFP-1. (B) GAFP-1 signal distribution in the mycelium which had been challenged with GAFP-1 purified from ammonium sulfate [$(NH_4)_2SO_4$] or ascorbic acid crude lysates. (C) GAFP-1 signal distribution in immunoblotted Cr, S, and I fractions as well as in an equal volume (10 µL) of the last post-treatment wash (W5). The black arrows indicate the position of the GAFP-1 band (expected size 12 kDa).

A

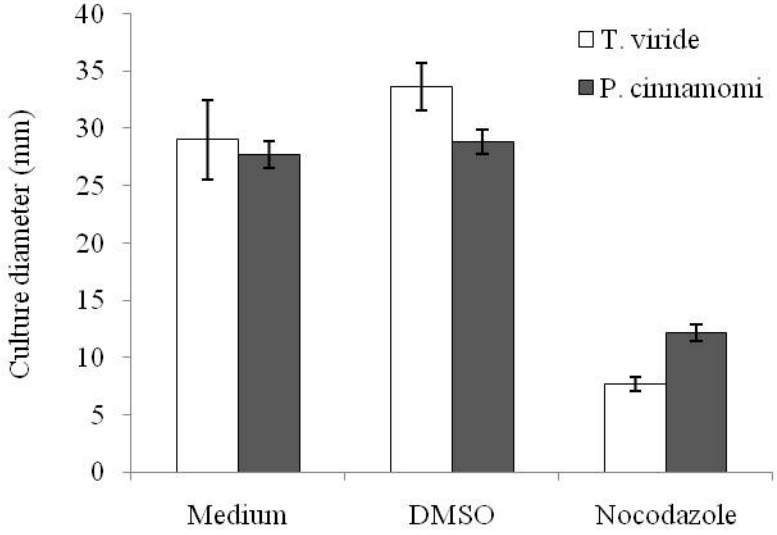
40
35
30
25
20
15
10
5
0
Culture diameter (mm)
T. viride
P. cinnamomi
Medium
DMSO
Nocodazole

B

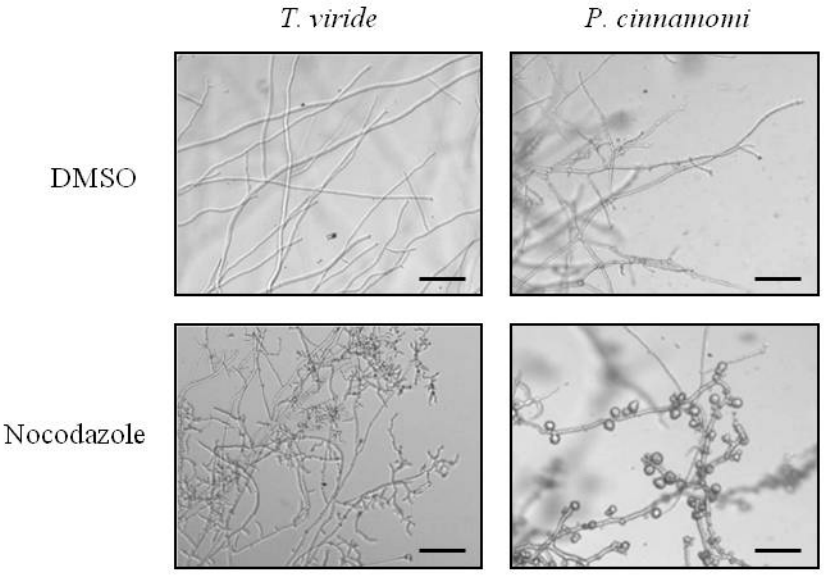
T. viride
P. cinnamomi
DMSO
Nocodazole

C

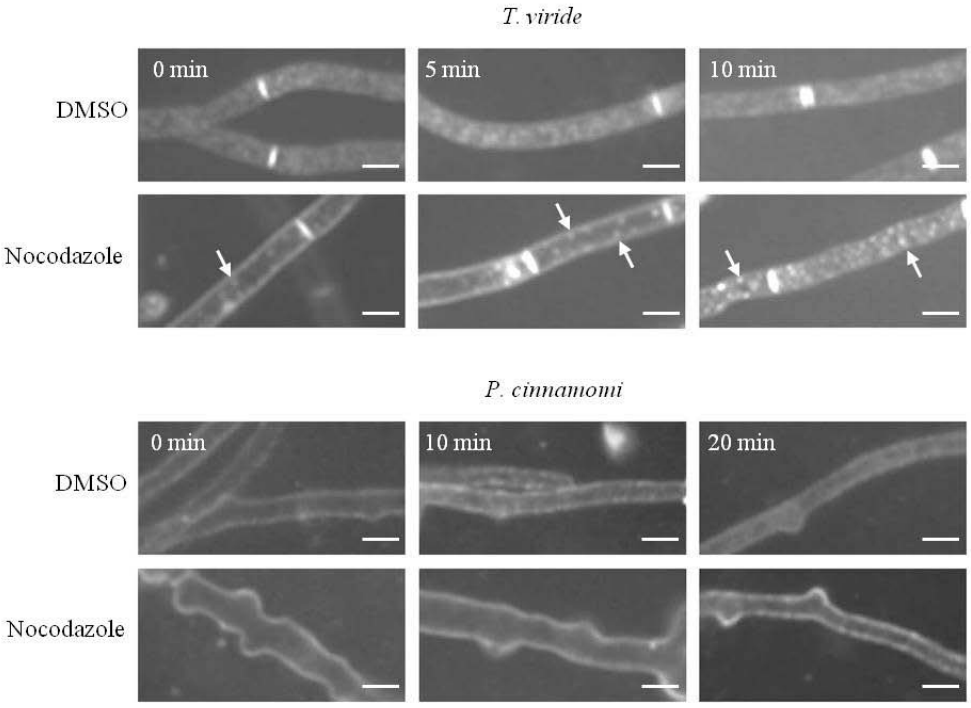
T. viride
0 min
5 min
10 min
DMSO
Nocodazole
P. cinnamomi
0 min
10 min
20 min
DMSO
Nocodazole

D

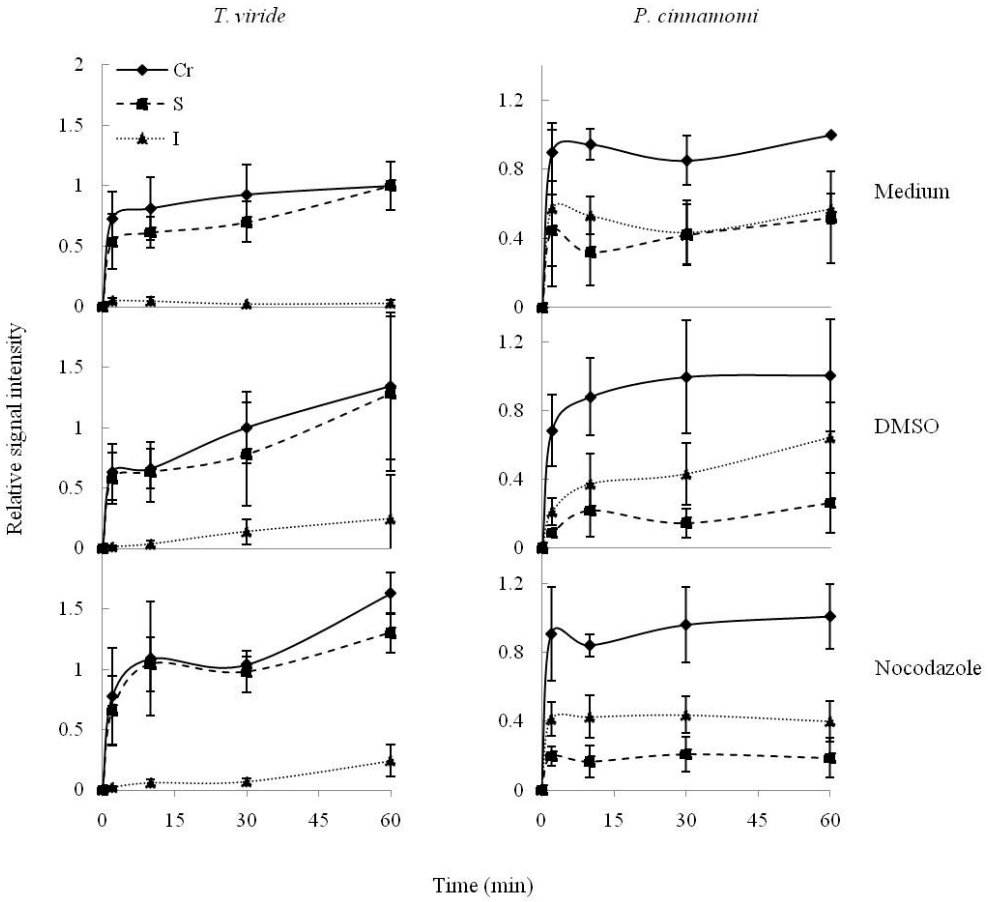
T. viride
P. cinnamomi
Cr
S
I
Medium
DMSO
Nocodazole
Relative signal intensity
Time (min)

Figure 4.4. Effects of nocodazole (30 µM) pre-treatment on growth, morphology, vesicle trafficking, and GAFP-1 localization in the mycelium of *T. viride* and *P. cinnamomi*. Non-amended medium (medium) or DMSO (0.2%) pre-treatments served as negative controls for inhibitor effects. (A) Culture growth on amended media was assessed after 48 h by measuring colony diameter. (B) Growth morphology of *T. viride* and *P. cinnamomi* hyphae was observed under 10 x magnification after 3 and 24 h pre-incubation with the inhibitor, respectively. Scale bars = 200 µM. (C) FM4-64 internalization was monitored in hyphae of *T. viride* and *P. cinnamomi* pre-treated with DMSO or nocodazole under 40 x magnification. Dye containing vesicles are indicated by white arrows. Scale bars = 20 and 10 µm for *T. viride* and *P. cinnamomi*, respectively. (D) The mycelium was pre-treated with DMSO, nocodazole, or non-amended medium prior to GAFP-1 challenge and subsequent cellular fractionation. Immunoblotted crude (Cr), soluble (S), and insoluble (I) fractions were analyzed by densitometry. All intensity values were normalized against that of the crude fraction at 60 min from the medium pre-treated control and are given as "relative intensity" values. For A and D, values represent averages and standard deviations taken across three experimental replications.

A

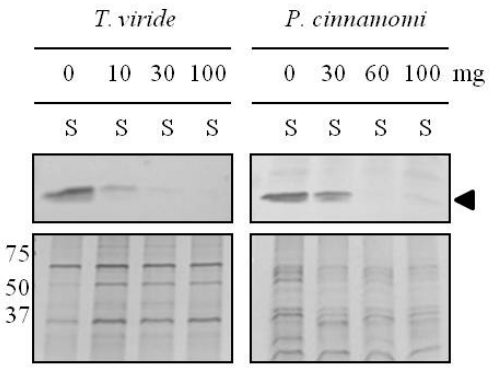
T. viride
P. cinnamomi
0 10 30 100
0 30 60 100 mg
S S S S
S S S S
75
50
37

B

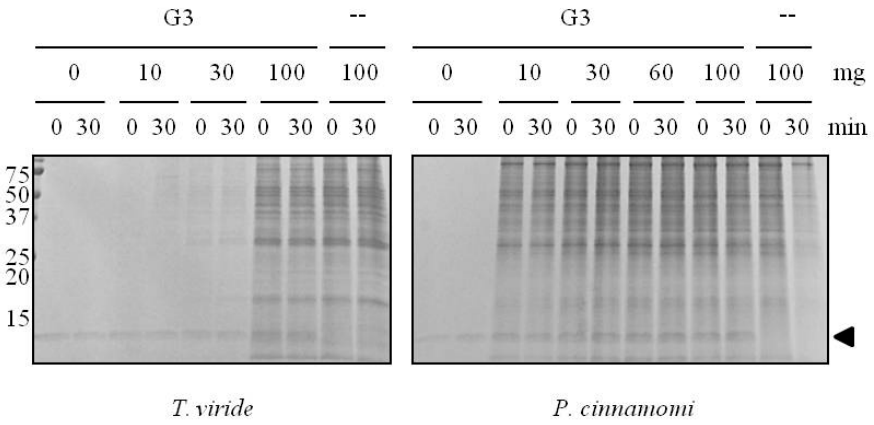
G3
--
G3
--
0 10 30 100 100
0 10 30 60 100 100 mg
0 30 0 30 0 30 0 30 0 30
0 30 0 30 0 30 0 30 0 30 0 30 min
75
50
37
25
20
15
T. viride
P. cinnamomi

C

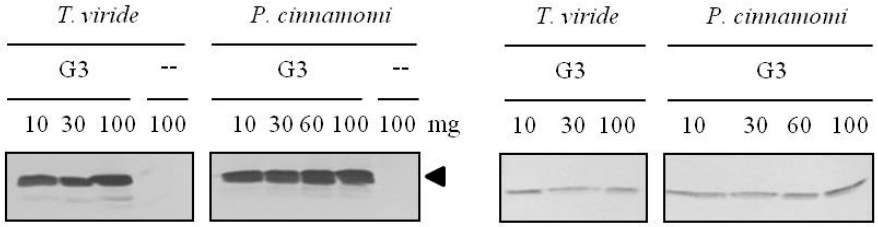
T. viride
P. cinnamomi
T. viride
P. cinnamomi
G3 --
G3 --
G3
G3
10 30 100 100
10 30 60 100 100 mg
10 30 100
10 30 60 100

Figure 4.5. GAFP-1 association with insoluble cell wall pellets prepared from the mycelium of *T. viride* and *P. cinnamomi*. (A) Insoluble fractions were prepared from 10-100 mg mycelium tissue and incubated with G3 solutions. Soluble (S) fractions prepared from the mycelium tissues treated with pre-incubated G3 solutions were analyzed by immunoblot (10 µL; top) and silver stain (1 µL; bottom). (B) Aliquots (5 µL) from the pre-incubation slurry were analyzed by staining with Coomassie reagent at 0 and 30 min. (C) GAFP-1 was extracted from the pre-incubation pellet by boiling with SDS extraction buffer (left) and analyzed by immunoblot. An equal volume (10 µL) of the last pellet wash was included in the immunoblot for comparison (right). For (B-C), insoluble pellets pre-incubated with phosphate buffer (--) served as negative controls. Black arrows indicate the position of the GAFP-1 band (expected size 12 kDa).

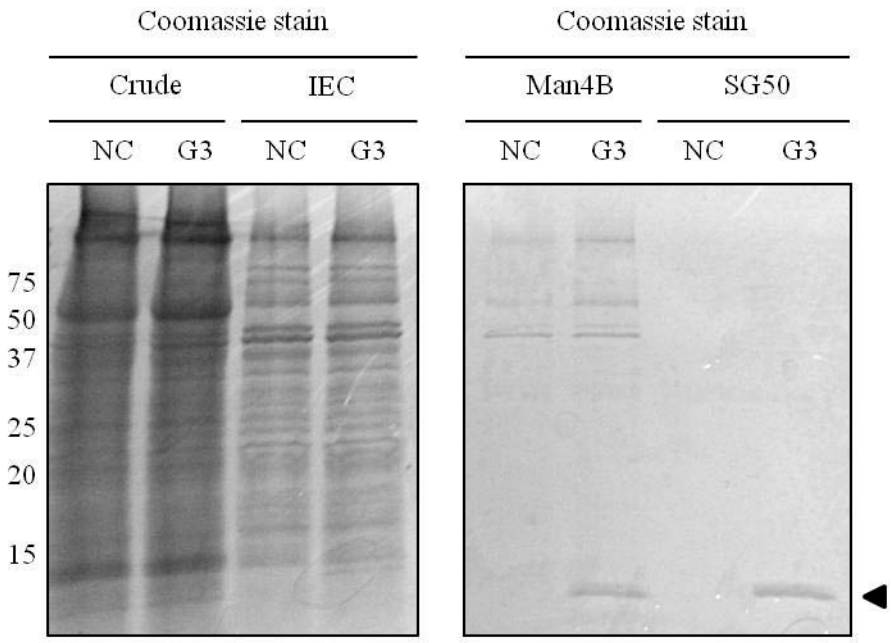
Coomassie stain
Coomassie stain
Crude
IEC
Man4B
SG50
NC
G3
NC
G3
NC
G3
NC
G3
75
50
37
25
20
15

Supplemental Figure 4.1. Purification of crude lysates (crude) from NC or G3 lines by ion exchange (IEC), affinity (Man4B), and size exclusion (SG50) chromatography. Molecular weight markers (kDa) are indicated at the left hand side of the figure. The black arrow indicates the position of the GAFP-1 band (expected size 12 kDa).

Supplemental Table 4.1. Sequence of chromatographic methods employed for purification of NC and G3 crude lysates.

Chromatography		Isolation method[z]							
		$(NH_4)_2SO_4$				Ascorbic Acid			
Step	Type	Matrix	pH	S:M	EV	Matrix	pH	S:M	EV
1	IEC	Q	6.1	40:20	60	SP	2.8	300:20	60
2	Affinity	Man4B	6.1	60:10	30	Man4B	2.8	60:10	30
3	SEC	SG50	6.1	1:10	3.2	SG50	6.1	1:10	3.2
4	IEC	SP	2.8	1.5:0.5	1.5	Q	6.1	1.5:0.5	1.5

[z]Crude lysates resulting from $(NH_4)_2SO_4$ or ascorbic acid isolation were separated by ion exchange chromatography (IEC) on Q- or SP-matrix (Q or SP), affinity chromatography (affinity) on mannose-linked agarose (Man4B), and size exclusion chromatography (SEC) on Sephadex G50 (SG50). The chromatographic matrices (matrix), working pH (pH), the supernatant to matrix ratio in mL (S:M), and the elution volume in mL (EV) are represente. Elution conditions are given in the Materials and Methods.

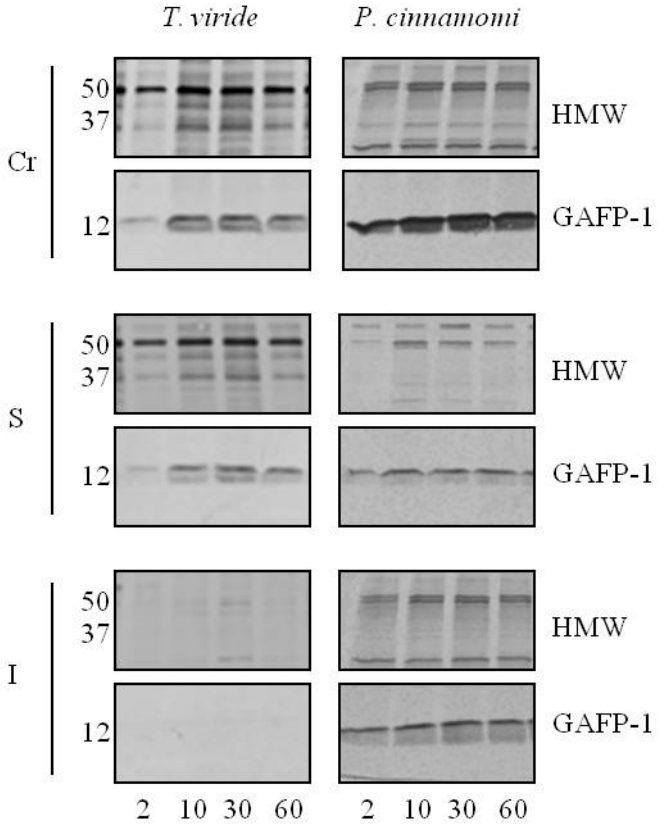
T. viride
P. cinnamomi
Cr
S
I
50
37
12
HMW
GAFP-1
2 10 30 60
2 10 30 60

Supplemental Figure 4.2. Cross-reaction of the GAFP-1 antibody with high(er) molecular weight (HMW) (30-75 kDa) peptides in immunoblotted fractions prepared from the mycelium of *T. viride* and *P. cinnamomi*. HMW signals in crude (Cr; top), soluble (S; middle), and insoluble (I; bottom) fractions at 2, 10, 30, and 60 min were used as internal controls for the quantification of GAFP-1 signal intensity in immunoblotted fractions by densitometry.

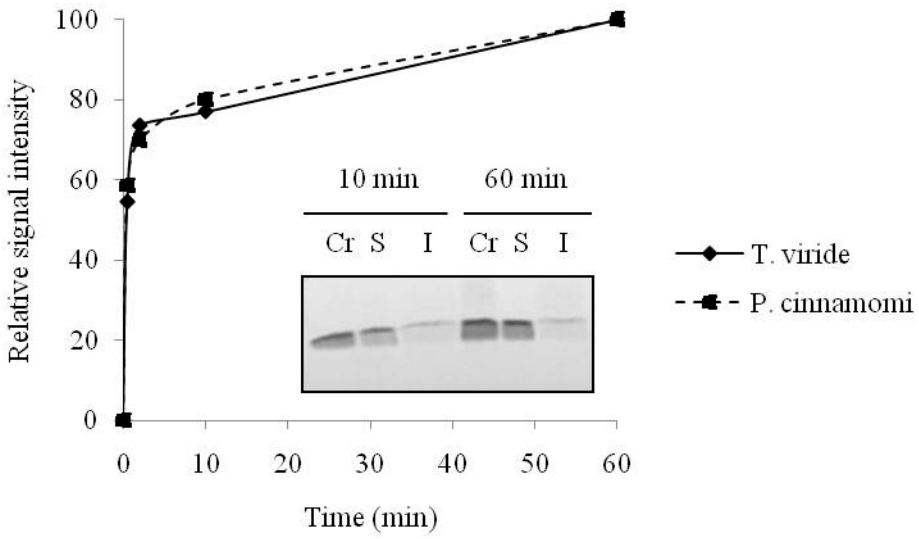
100
80
60
40
20
0
Relative signal intensity
0
10
20
30
40
50
60
Time (min)
10 min
60 min
Cr S I Cr S I
T. viride
P. cinnamomi

Supplemental Figure 4.3. Preliminary densitometric analysis of GAFP-1 signal intensity in soluble fractions prepared from the mycelium of *T. viride* and *P. cinnamomi*. The inset represents GAFP-1 signal distribution in crude (Cr), soluble (S), and insoluble (I) fractions prepared from the *T. viride* mycelium treated with GAFP-1 (5 µg) for 10 and 60 min.

A

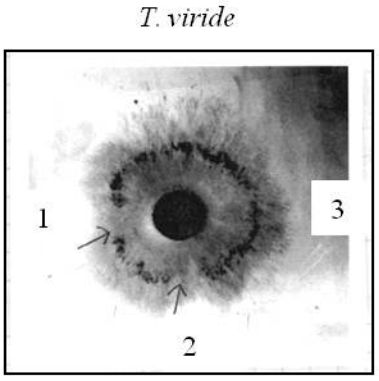
T. viride
1
2
3

B

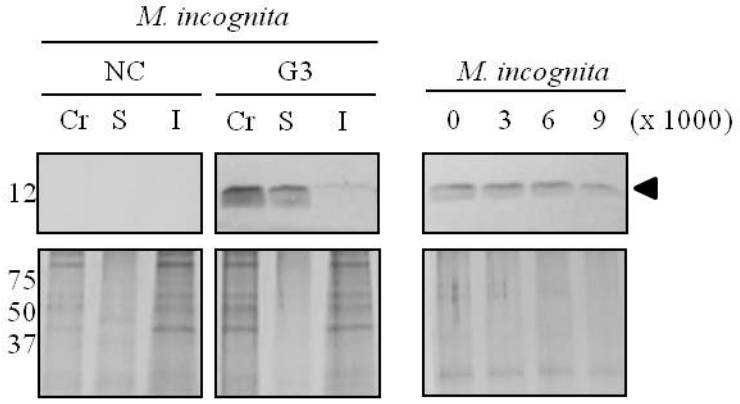
M. incognita
NC
G3
Cr S I
Cr S I
M. incognita
0 3 6 9 (x 1000)
12
75
50
37

Supplemental Figure 4.4. (A) Growth of V8-Amp-cultured *T. viride* mycelium 24 h after spotting with G3 (1, 5.0 µg; 2, 7.5 µg GAFP-1) or NC (3, volume equal to 7.5 µg GAFP-1) solutions. Black arrows indicate the initial leading edge of the mycelium. (B; left) Crude (Cr), soluble (S), and insoluble (I) fractions prepared from eggs of *M. incognita* (3000 count) exposed to G3 solutions (5 µg GAFP-1) for 60 min were analyzed by immunoblot (top) and silver stain (bottom). (B; right) Insoluble fractions were prepared from 3000-9000 eggs and incubated with G3 solutions. Soluble (S) fractions prepared from eggs treated with pre-incubated G3 solutions were analyzed by immunoblot (10 µL; top) and silver stain (1 µL; bottom). The black arrow indicates the position of the GAFP-1 band (expected size 12 kDa).

LITERATURE CITED

Barboni, E.M., S. Bawumia, and R.C. Hughes. 1999. Kinetic measurements of binding of galectin 3 to a laminin substratum. Glycoconjugate J. 16:365-373.

Bartnicki-Garcia, S., C.E. Bracker, G. Gierz, R. Lopez-Franco, and H. Lu. 2000. Mapping the growth of fungal hyphae: orthogonal cell wall expansion during tip growth and the role of turgor. Biophysical J. 79:2382-2390.

Barre, A., Y. Bourneb, E.J.M. Van Damme, W.J. Peumans, and P. Rougé. 2001. Mannose-binding plant lectins: different structural scaffolds for a common sugar-recognition process. Biochimie. 83:645 −651.

Betz, W.J., F. Mao, C.B. Smith. 1996. Imaging exocytosis and endocytosis. Curr. Opin. Neurobiol. 6:365-371.

Brewer, F.C. 2004. Thermodynamic binding studies of galectin-1, -3, and -7. Glycoconjugate J. 19:459-465.

Chaffin, W.L., J.L. Lopez-Ribot, M. Casanova, D. Gozalbo, and J.P. Martinez. 1998. Cell wall and secreted proteins of *Candida albicans*: identification, function, and expression. Microbiol. Mol. Biol. Rev. 62:130-180.

Clarke, A.J., P.M. Cox, and A.M. Shepherd. 1967. The chemical composition of the egg shells of the potato cyst-nematode, *Heterodera rostochiensis* Woll. Biochem. J. 104:1056-1060.

Cox, K., D. Layne, R. Scorza, and G. Schnabel. 2006. Gastrodia anti-fungal protein from the orchid *Gastrodia elata* confers disease resistance to root pathogens in transgenic tobacco. Planta 224:1373-1383.

Davis, E.L. and D.T. Kaplan. 1992. Lectin binding to aqueous-soluble and body wall proteins from infective juveniles of *Meloidogyne* species. Fundamental Appl. Nematol. 15:243-250.

Fischer-Parton, S., R.M. Parton, P.C. Hickey, J. Dijksterhuis, H.A. Atkinson, and N.D. Read. 2000. Confocal microscopy of FM4-64 as a tool for analysing endocytosis and vesicle trafficking in living fungal hyphae. J. Microscopy. 198:246-259.

Hester, G. and C.S. Wright. 1996. The mannose specific bulb lectin from *Galanthus nivalis* (snowdrop) binds mono- and dimannosides at distinct sites. Structure analysis of refined complexes at 2.3 Å and 3.0 Å resolution. J. Mol. Biol. 262:516–531.

Hu, Z. and Q. Z. Huang. 1994. Induction and accumulation of the antifungal protein in *Gastrodia elata*. Acta Botannica Yunnanica 16:169-177.

Hu, Z., Z. Yang, and J. Wang. 1988. Isolation and partial characterization of an antifungal protein from *Gastrodia elata* corm. Acta Botanica Yunnanica 10:373-380.

Illinger, D. and J.G. Kuhry. 1994. The kinetic aspects of intracellular fluorescence labeling with TMA-DPH support the maturation model for endocytosis in L929 cells. J. Cell Biol. 125:783-794.

Jiang, S.-Y., M. Zhigang, S. Ramachandran. 2010. Evolutionary history and stress regulation of the lectin superfamily in higher plants. BioMed Central Evolutionary Biol. 10:1-24

Kaku, H, E.J.M. Van Damme, W.J. Peumans, and I.J. Goldstein. 1990. Carbohydrate-binding specificity of the daffodil (*Narcissus pseudonarcissus*) and amaryllis (*Hippeastrum hybr.*) bulb lectins. Arch. Biochem. Biophys. 279(2):298 (abstr.).

Koo, J.C., S.Y. Lee, H.J. Chun, Y.H. Cheong, J.S. Choi, S. Kawabata, M. Miyagi, S. Tsunasawa, K.S. Ha, D.W. Bae, C.D. Han, B.L. Lee, and M.J. Cho. 1998. Two hevein homologs isolated from the seed of *Pharbitis nil* L. exhibit potent antifungal activity. Biochim. Biophys. Acta 1382:80–90.

Koo, J.C., H.J. Chun, H.C. Park, M.C. Kim, Y.D. Koo, S.C. Koo, H.M. Ok, S.J. Park, S.H. Lee, D.J. Yun, C.O. Lim, J.D. Bahk, S.Y. Lee, and M.J. Cho. 2002. Over-expression of a seed specific hevein-like antimicrobial peptide from *Pharbitis nil* enhances resistance to a fungal pathogen in transgenic tobacco plants. Plant Mol. Biol. 50:441–452.

Leborgne-Castel, N., J. Lherminier, C. Der, J. Fromentin, V. Houot, and F. Simon-Plas. 2008. The plant defense elicitor cryptogein stimulates clathrin-mediated endocytosis correlated with

reactive oxygen species production in bright yellow-2 tobacco cells. Plant Physiol. 146:1255-1266.

Lee, O.K., B. Lee, N. Park, J.C. Koo, Y.H. Kim, T.P. Da, C. Karigar, H.J. Chun, B.R. Jeonga, D.H. Kim, J. Nam, J.G. Yun, S.S. Kwak, M.J. Cho, D.J. Yun. 2003. Pn-AMPs, the hevein-like proteins from *Pharbitis nil* confers disease resistance against phytopathogenic fungi in tomato, *Lycopersicum esculentum.* Phytochemistry. 62:1073-1079.

Liu, W., N. Yang, D. Jingjin, R.H. Huang, Z. Hu, and D.C. Wang. 2005. Structural mechanism governing the quaternary organization of monocot-mannose binding lectin revealed by the novel monomeric structure of an orchid lectin. J. Biol. Chem. 280:14865-14876.

Marban-Mendoza N., A. Jeyaprakash, H.B. Jansson, R.A.J. Damon, and B.M. Zuckerman. 1987. Control of root-knot nematodes on tomato by lectins. J. Nematol. 19:331-335.

Nagel, A.K., R. Scorza, C. Petri, and G. Schnabel. 2008. Generation and characterization of transgenic plum lines expressing the *Gastrodia*-Anti Fungal Protein. HortSci. 43:1514–1521.

Nagel, A.K., H. Kalariya, and G. Schnabel. 2010. The *Gastrodia* anti-fungal protein (GAFP-1) and its transcript are absent from scions of chimeric-grafted plum. HortSci. 44:188-192.

Neumann, D., O. Kohlbacher, H.-P. Lenhor, and C.-M. Lehr. 2002. Lectin-sugar interaction: calculated versus experimental binding energies. Eur. J. Biochem. 269:1518-1524.

Nyczepir, A.P., A.K. Nagel, and G. Schnabel. 2009. Host status of three transgenic plum lines to *Mesocriconema xenoplax*. HortSci. 44:1932-1935.

Penalver, E., L. Ojeda, E. Moreno, and R. Lagunas. 1997. Role of the cytoskeleton in endocytosis of the yeast maltose transporter. Yeast. 13:541-549.

Pitarch, A., M. Sanchez, C. Nombela, and C. Gil. 2002. Gel analysis unravels the complexity of the dimorphic fungus *Candida albicans* cell wall proteome. Mol. Cell Proteomics. 1:967-982.

Ripoll, C., B. Favery, P. Lecomte, E. Van Damme, W. Peumans, P. Abad, L. Jouanin. 2003. Evaluation of the ability of lectin from snowdrop (*Galanthus nivalis*) to protect plants against root-knot nematodes. Plant Sci. 164:517-523.

Sharon, E., Y. Spiegel, R. Salomon, and R.H. Curtis. 2002. Characterization of *Meloidogyne javanica* surface coat with antibodies and their effect on nematode behaviour, Parasitology 125:177-185.

Shibuya, N., I. J. Goldstein, E. J. M. Van Damme, and W. J. Peumans. 1988. Binding properties of a mannose-specific lectin from the snowdrop (Galanthus nivalis) bulb. J. Biol. Chem. 263(2): 728 (abstr.).

Spiegel, Y. and M.A. McClure. 1991. Stage-specific differences in lectin binding to the surface of *Anguina tritici* and *Meloidogyne incognita*. J. Nematol. 23:259-263.

Vida, T.A. and S.D. Emr. 1995. A new vital stain for visualizing vacuolar membrane dynamics and endocytosis in yeast. J. Cell Biol. 128:779-792.

Wang, X., G. Bauw, E.J.M. Van Damme, W.J. Peumans, Z.-L. Chen, M. Van Montagu, G. Angenon, and W. Dillen. 2001. Gastrodianin-like mannose-binding proteins: a novel class of plant proteins with antifungal properties. Plant J. 25:651:661.

Wang, Y., D. Chen, D. Wang, Q. Huang, Z. Yao, F. Liu, X. Wei, R. Li, Z. Zhang, and Y. Sun. 2004. Over-expression of *Gastrodia* anti-fungal protein enhances *Verticillium* wilt resistance in coloured cotton. Plant Breeding 123:454-459.

Van Damme, E. J. M., C. H. Astoul, A. Barre, P. Rouge, and W. J. Peumans. 2000. Cloning and characterization of a monocot mannose-binding lectin from *Crocus vernus* (family Iridaceae) Eur. J. Biochem. 267:5067-5077.

Wessels, J.G.H. Developmental regulation of fungal cell wall formation. Ann. Rev. Phytopathol. 32:413-37.

Xu, Q., Y. Liu, X. Wang, H. Gu, and Z. Chen. 1998. Purification and characterization of a novel anti-fungal protein from *Gastrodia elata*. Plant Physiol. Biochem. 36:899-905.

Xu, R. H. and X. Z. Liu. 2003. Action site of Gastrodia anti-fungal protein on *Trichoderma* hyphae. Acta Botannica Yunnanica. 25.573-578.

Yang, S. L. and Z. Hu. 1990. A preliminary study on the chitinase and β-1,3-Glucanase in corms of *Gastrodia elata.* Acta Botannica Yunnanica 12:421-426.

Zuckerman, B. M. and I. Kahane. 1983. *Caenorhabditis elegans*: Stage specific differences in cuticle surface carbohydrates. J. Nematol. 15:535-538.

CHAPTER FIVE

MMGBSA ANALYSIS OF THE INTERACTION BETWEEN GASTRODIANIN AND α-D-MANNOSE

ABSTRACT

Asparagine to arginine substitutions made within the three carbohydrate recognition domains (CRDs) of the *Gastrodia* anti-fungal protein (GAFP or Gastrodianin) were previously shown to decrease anti-fungal activity of the lectin on *Trichoderma viride* (Wang *et al.*, 2003). In this study the same amino acid substitutions were made on peptides *in silico*, and the change in the interaction between the substituted peptides and α-D-mannose (α-D-Man) was investigated by molecular dynamics. Alpha-D-Man was modeled into CRDs 1 (residues 28-34), 2 (residues 57-65), and 3 (residues 88-96) of wild-type GAFP-1 (referred to as Gastrodianin in this study) by superimposition of the anti-fungal lectin and the complexed *Allium sativum* agglutinin (ASA). Three control (N30N, N61N, and N92N; collectively "NN") and three substituted (N30R, N61R, and N92R; collectively "NR") Gastrodianin peptides were generated from the wild-type lectin sequence using a PERL application. Alpha-D-Man molecules were subsequently transcribed into the appropriate CRDs of control or substituted peptides. Molecular dynamics (MD) simulations were conducted on NN and NR peptides complexed to α-D-Man. The energetic components of unbound peptide and α-D-Man molecules were extracted from the trajectories of the corresponding bound model, and single-state MMGBSA calculations were used to determine the free energy of binding (ΔG_{Bind}). ΔG_{Bind} values for the interaction of α-D-Man with the CRDs of substituted Gastrodianin peptides were not weakened by the arginine substitution as had been

previously hypothesized. The characteristics of our peptide models, as well as the implications of our results, are discussed.

INTRODUCTION

Many plant defense lectins have been shown to protect their hosts against foreign invaders such as bacteria, fungi, and herbivores (Van Damme *et al.*, 1998). The ability of the lectin to recognize a specific saccharide ligand likely contributes to the efficacy of the protein's mechanism against plant pathogens (Barre *et al*., 2001; Peumans and Van Damme, 1995). Conformational characteristics that control saccharide binding specificity occur at different levels of the peptide. The availability of the residues required for ligand binding is determined by conserved secondary and tertiary structural elements, while neighboring protomer subunits can contribute additional contacts (quaternary interactions) that stabilize saccharide association (Hester and Wright, 1996). Although related proteins may share common structural features, it is the differences that mediate the more subtle points of molecule recognition. Proteins from the monocot mannose-binding lectin (MMBL) family, for example, are diagnostic for their ability to accommodate mannoside derivatives. Individual lectin species, however, differ in their fine specificity (Van Damme *et al*., 1998). For instance, the *Galanthus nivalis* agglutinin (GNA) from garlic and *Crocus vernus* agglutinin (CVA) from iris prefer terminal α-1,3-dimannoside residues (Shibuya *et al*., 1988; Van Damme *et al*., 2000), but the agglutinins from the daffodil *Narcissus pseudonarcissus* (NPA) have the highest affinity for α-1.6-trimannosides. Amaryllis MMBLs (*Hippeastrum hybr.*) can bind both α-1,3 and α-1,6 linked oligomannosides of multiple residue lengths (Kaku *et al*., 1990). An MMBL has even been discovered in the non-vascular bryophyte *Marchantia polymorpha* which can accommodate α-methylated glucose in addition to α-

methylated and nitryl-fluorinated mannose (Peumans *et al*., 2002). This is the first lectin from the MMBL family to demonstrate binding of a glucose-derivative, and is a good example of how ligand specificity can be plastic among related peptides despite shared attributes.

The *Gastrodia* anti-fungal protein (GAFP or Gastrodianin) has three carbohydrate recognition domains (CRDs) which are characteristic to all MMBLs (Barre *et al*., 2001; Liu *et al*., 2005; Van Damme *et al*., 1998). The conserved binding motif QXDXNXVXY within MMBL CRDs is capable of hydrogen bonding with specific hydroxyl oxygens of α-D-mannosides (Barre *et al*., 2001; Hester and Wright, 1996; Ramachandraiah *et al*., 2002). The preferred mannoside of GAFP is unknown, however it has been surmised that mannose binding plays a role in the inhibitory mechanism of the lectin (Wang *et al*. 2003). These same authors demonstrated that substituting an arginine for a conserved asparagine within CRDs 1, 2, and 3 of GAFP decreased the anti-fungal activity of the lectin on *Trichoderma viride* by approximately 22, 37, and 29%, respectively. In this study the effect of those same arginine substitutions on the interaction of α-D-mannose (α-D-Man) with CRDs 1, 2, and 3 of GAFP-1 (referred to in this study as Gastrodianin; see Materials and Methods) was investigated *in silico*. Molecular dynamics (MD) simulations were conducted on three control (N30N, N61N, and N92N) and three substituted (N30R, N61R, and N92R) Gastrodianin peptides complexed to α-D-Man. The relative changes in the free energy of binding between the peptide and α-D-Man (ΔG_{Bind}) were determined using single-state MMGBSA calculations.

MATERIALS AND METHODS

Homology modeling

The atomic coordinates for GAFP-1 (PDB ID: 1XD5) (Liu *et al*., 2005) and the coordinates for the dimeric mannose-specific agglutinin from *Allium sativum* (ASA) in association with α-D-mannose (α-D-Man) (PDB ID: 1KJ1) (Ramachandraiah *et al.*, 2002) were obtained from the RCSB Protein Data Bank (http://www.rcsb.org/). It should be noted that the coordinates for GAFP-1 were obtained from the crystal structure elucidated by Liu *et al.* (2005). The "GAFP-1" designation does not refer specifically to the NF isoform of GAFP, which has also been designated as "GAFP-1" in other studies (Cox *et al*., 2006; Nagel *et al*., 2008; Nagel *et al*. 2010; Nyczepir *et al*., 2009) In the interests of clarity, we will hereafter refer to the GAFP-1 peptide sequence determined by Liu *et al*. (2005) as "Gastrodianin."

Excess protein, saccharide, and solvent coordinates were removed from the original ASA model, leaving the coordinates of a single ASA protomer in association with three α-D-Man molecules. Gastrodianin coordinates were superimposed over those of the α-D-Man-complexed ASA peptide using Discovery Accelrys ™ software. ASA protein coordinates were then manually deleted from the model, leaving only Gastrodianin and α-D-Man coordinates. Preliminary MD simulations were conducted on each α-D-Man molecule individually (see parameters in the *Molecular Dynamics* section of Materials and Methods) in the absence of the Gastrodianin peptide. To avoid introducing an extra source of variation into the system, the saccharide molecule coordinates with the lowest average ΔG_{System} (see equations below) were replicated twice to generate three new α-D-Man molecules, and the two original, higher energy α-D-Man molecules were deleted. Each new α-D-Man molecule was manually centered over CRDs 1 (residues 88-96), 2 (residues 57-65), and 3 (residues 26-34) of wild-type Gastrodianin and then translated approximately 10 Å from each binding site to create the template model (Fig. 5.1).

Generation of substituted peptides

A PERL application was used to generate arginine-substituted N92R, N61R, and N26R peptides (referred to collectively as NR peptides) from the wild-type Gastrodianin sequence. N92N, N61N, and N92N Gastrodianin peptides (referred to collectively as NN peptides) were also created by mutating the corresponding asparagine to a glycine and then back to an asparagine. NN peptides served as negative controls for script effects on wild-type peptide energetics. Alpha-D-Man coordinates were transcribed into the appropriate CRDs of NN and NR peptides from the template model.

Molecular Dynamics

MD simulations were performed on NN or NR peptides in association with α-D-Man (bound) within the CHARMM® force-field (Brooks *et al.*, 1983) in implicit solvent. Distance restraints were created between oxygen atoms of α-D-Man and functional groups of polar amino acids Q, D, N, and Y of bound NN and NR peptides based upon the binding mode which is documented to occur in MMBLs (Barre *et al.* 2001) (Table 5.1, Fig. 5.2). The restraint between the substituted arginine and α-D-Man O2 was omitted in NR models, but otherwise all restraint parameters were identical to those created in NN peptides. Distance restraint parameters were defined differently at different stages of the simulation (Table 5.2). Briefly, bound peptide models underwent two rounds of minimization prior to MD in order to quickly optimize molecule contacts along a potential energy function. Distance cutoffs were set at 4.5 Å for each atom pair during the first round of minimization in order to 'pull' ligand molecules into the binding region from their starting position 10 Å away from the CRD. In the second round of minimization, and in subsequent MD simulations, distance restraints were 'relaxed' to 5.5 Å to allow the ligand

greater range of motion within the binding pocket. When any defined atom violated the distance cutoff, a restraint force was applied to the molecules so that all atoms satisfied the distance cutoff parameters. It should be noted that all distance cutoffs were greater than the defined length of a hydrogen bond (3Å) (Jiang *et al.*, 2002).

MMGBSA

The binding affinity (ΔG_{bind}) between a protein and its ligand can be defined by the MMGBSA (Molecular Mechanics – Generalized-Born Surface Area) equation to be

$$\Delta G_{bind} = \Delta G_{complex} - (\Delta G_{protein} + \Delta G_{ligand})$$

(Zou *et al*., 1999). The change in the total free energy of the system(s), which in this case are the Gastrodianin peptide alone, α-D-Man alone, or Gastrodianin in complex with α-D-Man, between an arbitrarily defined timestep (*n*) is represented by ΔG (given in the following as ΔG_{System}), so that

$$\Delta G_{System} = G_{n'} - G_{n.}$$

The change in the ΔG_{System} is also defined by changes in the energetic contributions from the solute (the molecule) and the solvent, or

$$\Delta G_{System} = \Delta G_{solute} + \Delta G_{solvent}$$

so that

$$\Delta G_{solute} = E_{MM} + T\Delta S$$

$$\Delta G_{solvent} = \Delta G_{GB} + \Delta G_{SA.}$$

For the solute, the electromechanical energy, temperature (Kelvin), and change in system entropy are given by E_{MM}, T, and ΔS terms, respectively. Solvent contributions are made up of electrostatic (ΔG_{GB}) and non-electrostatic components (ΔG_{SA}) defined by the Generalized-Born continuum solvent model (GBSW), which approximates calculated solvation free energies of the Poisson-Boltzmann algorithm (Bashford and Case, 2000; Jayaram *et al.*, 1998). The vibrational and configurational entropic contributions for the solute are ignored within the CHARMM® force-field unless explicitly defined. Therefore, in an implicit system, ΔG_{System} is comprised of the non-bonded terms, given by $\Delta G_{solvent}$, and the terms of the E_{MM} equation, where

$$E_{MM} = E_{Trans} + E_{Rot} + E_{Elec} + E_{Vdw} + E_{Bond.}$$

E_{MM} energy components represent the intermolecular interaction energy (electrostatic and van der Waals terms given by E_{Elec} and E_{VDW}, respectively) as well as the intramolecular interaction energy (translational, rotational, and bonded terms given by E_{Trans}, E_{Rot}, and E_{Bond}, respectively) of the system. In this study E_{Bond} represents the sum of the three terms for intramolecular interaction energy and is calculated by subtracting the non-bonded solute and solvent energy components E_{Elec}, E_{VDW}, E_{GB}, E_{SA} (where $E_{GB} = G_{GB}$ and $E_{SA} = G_{SA}$) from the ΔG_{System} values computed within the CHARMM® force-field.

Single-State MMGBSA Calculations

Total free energy (ΔG_{System}) values and energy components of the solute (E_{Elec}, E_{VDW}, E_{Bond}) and solvent (E_{GB}, E_{SA}) were collected every 1000 steps from the last nanosecond of production time (timestep = 0.001 ps) in MD simulations on bound NN and NR peptides. The system was considered minimized if the curve for ΔG_{System} remained at a plateau for at least 1 ns of production time. Total free energy and energy component values for unbound α-D-Man and peptide molecules were extracted from the corresponding trajectories of bound NN and NR peptides. Energy terms for which a restraint force was applied to the α-D-Man molecule could be identified in the system output post-simulation. These energy values, along with those from the next 5000 timesteps, were arbitrarily defined as a 're-equilibration period' and were removed from the data sets of corresponding unbound α-D-Man, unbound peptide, and bound peptide/α-D-Man models. MD was performed on each bound model five times under different random seeds. Energy component averages and standard deviations were taken across the five independent replications.

RESULTS

Coordinates of Gastrodianin and α-D-Man-complexed ASA were superimposed to generate coordinates for α-D-Man within the CRDs of wild-type Gastrodianin (Fig. 5.1). The appropriate α-D-Man molecule was transcribed into the CRDs of NN and NR Gastrodianin peptides from the resulting template model. Sequence alignment between ASA and Gastrodianin resulted in 51.6% sequence identity (data not shown).

MD simulations were conducted on NN and NR Gastrodianin peptides complexed to α-D-Man. ΔG_{Bind}, and changes to bonded and non-bonded energy terms that contribute to ΔG_{Bind}, were calculated for NN and NR Gastrodianin peptides upon binding of α-D-Man using the MMGBSA equation (Table 5.3). Energy component values of unbound and bound NN and NR Gastrodianin models, as well as those for unbound α-D-mannose, are given in Table 5.4. Association of α-D-Man with CRDs 1, 2, and 3 resulted in very favorable ΔG_{Bind} values for all models. Substitution of the conserved asparagines for a basic arginine decreased ΔG_{Bind} values in CRDs 1 and 2 by 12.8% and 9.0% respectively, however ΔG_{Bind} in CRD 3 was increased by 2.1%. While the arginine substitution increased the favorability of the interaction between α-D-Man and CRD 1 relative to the corresponding N92N peptide, the margins of error for ΔG_{Bind} in N61R and N30R peptides would suggest that the α-D-Man binding affinity with these peptides was not significantly affected by the amino acid substitution (Fig. 5.3). Favorable changes in Coulomb (ΔE_{Elec}) and van der Waals (ΔE_{VDW}) interactions were observed in all models upon binding of α-D-Man (Table 5.3). However the unfavorable changes to the ΔE_{SA} term in N92N, N92R, and N61N models did not favor ligand association with the CRDs of these models. Additionally, the negative change in the E_{GB} term was of a high magnitude in the N61N model, but was balanced by the high magnitude of the positive change in the hydrophobic component (ΔE_{SA}). Both of these terms were accompanied by noticeably large standard deviations. Likewise, the unbound N61N model displayed less and more favorable E_{GB} and E_{SA} energy components, respectively, and both values again had unusually high standard deviations compared to other unbound control models (Table 5.4). Binding of α-D-Man did seem to bring the overall solvation energy components of the N61N system in line with that of other bound NN peptides though. The more realistic magnitudes of corresponding energy components in bound and unbound N61R models might explain the more favorable ΔG_{Bind} value for the interaction of α-D-Man with CRD

2 compared to the control peptide. Although the arginine substitution in CRD 2 improved the favorability of the solvation component in unbound and bound models, the E_{GB} term of the N61R system was slightly elevated over that of bound and unbound N92R and N30R peptides.

DISCUSSION

The binding affinity between α-D-Man and Gastrodianin was analyzed in this study after substituting a basic arginine for a conserved asparagine within the binding motif of CRDs 1, 2, and 3. In contrast to the hypothesis of Wang *et al.* (2003), the arginine substitution appeared to stabilize α-D-Man binding with CRD 1. The interaction of α-D-Man with CRDs 2 and 3 did not appear to be affected greatly by the arginine substitution, however. As would be expected, favorable changes in electrostatic Coulomb and van der Waals interactions were observed upon binding in all models. Also, except for the N61R system, all other models exhibited good convergence as indicated by the fairly small changes to bonded energy terms (E_{Bond}). Distance cutoffs between functional groups of α-D-Man and the conserved amino acids Q, D, N, and Y (Fig. 5.2) were optimized during preliminary runs so that the α-D-Man ligand was correctly positioned within the CRDs of Gastrodianin without necessarily forcing a given conformation. Moreover, a re-equilibration period in which α-D-Man was theoretically allowed to re-discover an optimal association with the peptide CRD after the application of restraint force was taken into account. Because energy terms for which a restraint force was actively being applied, as well as those of the re-equilibration period, were excluded from data analysis, resulting energy component values included only conformational states of the peptide where the ligand remained within binding range of NN and NR peptide CRDs.

Analysis of energy component values and energetic changes to the Gastrodianin peptides upon binding of α-D-Man did yield some unexpected results, however. The changes in the electrostatic and hydrophobic solvation terms (ΔE_{GB} and ΔE_{SA}, respectively) of the N61N model upon binding α-D-Man, while favorable, were of a very high magnitude. Although the terms balanced each other, their values fluctuated considerably among independent models as indicated by their large values of standard deviation. The reflection of that phenomenon in the unbound N61N model suggests an inherent issue with this particular peptide resulting from script effects, since properties of the control peptide should not vary appreciably from that of the other unbound control peptides. Also, there should not have been unfavorable changes in hydrophobic solvation energy (ΔE_{SA}) in N92N, N92R, and N61N models upon association with α-D-Man, since water molecules that become displaced from the solute 'shells' upon binding should result in more favorable energy of cavitation. Again, however, these terms were balanced by favorable electrostatic solvation contributions (ΔE_{GB}) in these same models. It should be noted that the standard deviations of ΔE_{GB} and ΔE_{SA} terms in many NN and NR models indicate that average values for these terms spanned both positive and negative values among independent replications (Table 5.3). This might suggest that despite the high ΔG_{Bind} in these models, which would be driven by the polar ΔE_{Elec} component, binding of the free mannoside by NN and NR peptides is very unstable from the standpoint of solvation. The lack of extended molecule contacts in the solvent exposed CRDs of other MMBLs has been postulated to decrease ligand occupancy (Hester and Wright, 1996; Liu *et al.*, 2005), and such a phenomenon could certainly be playing a role in weak ligand binding in the monomeric Gastrodianin. Because of the idiosyncrasies in our model data, it is unclear if our findings reflect changes in Gastrodianin binding behavior that would actually occur upon arginine substitution, or if they are the result of flaws inherent within our parameters.

It is likely that GAFP binds an oligomannoside of a specific linkage state (Barre *et al*., 2001; Van Damme *et al*., 1998), and our procedural investigation of Gastrodianin binding to mannose *in silico* would be substantially improved by any information on binding specificity in this lectin. Because there is currently no information on the specific mannoside preferred by Gastrodianin, we modeled free α-D-Man into the binding sites of the peptide. Despite the fact that ASA was able to be crystallized in association with the α-D-Man monosaccharide, the experimentally determined binding affinity between free α-D-Man and an MMBL is thought to be very weak (K_i = 200 mM) (Van Damme *et al*., 1998; Kaku *et al*., 1990). Even if we were aware of the specific saccharide accommodated by Gastrodianin, interactions between lectins and their saccharide ligands generally fall on the weaker side (≥ -5 kcal/mol) of the range of experimentally determined binding affinities between proteins and their partners (-18 to -1 kcal/mol) (Barboni *et al*., 1999; Brewer, 2004; Jiang *et al*., 2002; Neumann *et al*., 2002; Van Damme *et al*., 2000). This presents extra challenges when modeling molecule interactions computationally. Inherently weak binding between Gastrodianin and α-D-Man may explain why ligand molecules easily moved outside of the CRDs in preliminary MD, particularly in sites 1 and 2. It was this behavior of the bound system that necessitated the implementation of distance restraint cutoffs between interacting functional groups on the ligand and conserved residues within the CRDs of the peptide. The approximation of the solvent electrostatic contribution given by the GBSW algorithm is probably not sufficient to define ordered water molecules which may mediate H-bond contacts between functional groups of weakly interacting α-D-Man and Gastrodianin molecules. Additionally, the large source of error originating from the GBSW solvent approximation and the lack of explicitly defined entropic contributions in our model could also have contributed to the unrealistically favorable ΔG_{bind} values resulting for complex formation between α-D-Man and Gastrodianin *in silico*. Prediction of ΔG_{Bind} between α-D-Man

and Gastrodianin will likely be improved by employing MD on an explicitly solvated complex within the CHARMM force-field.

FIGURES AND TABLES

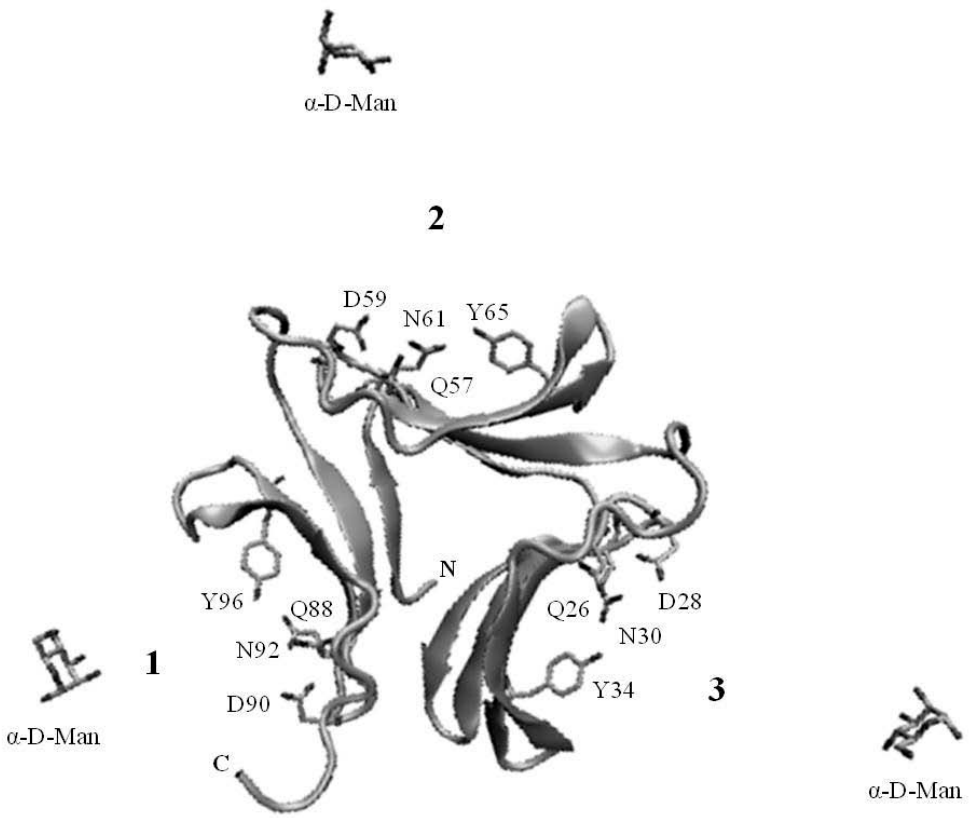
α-D-Man
2
D59
N61
Y65
Q57
N
Y96
Q88
N92
D90
C
Q26
D28
N30
Y34
1
α-D-Man
3
α-D-Man

Figure 5.1. Template model of α-D-Man within the carbohydrate recognition domains (CRDs) 1 (residues 88-96), 2 (residues (57-61), and 3 (residues 26-34) of Gastrodianin. Alpha-D-Man molecules were positioned approximately 10 Å away from each CRD.

Table 5.1. Distance restraints between atoms of α-D-Man and conserved polar residues Q, D, N, and Y of Gastrodianin.

α-D-mannose	Gastrodianin		
Atom	Atom	Residue Number (NN)	Residue Number (NR)
O2[z]	OD1	D28, D59, D90	D28, D59, D90
	ND2	N30, N61, N92	--
O3	OE1	Q26, Q57 Q88	Q26, Q57 Q88
O4	OH	Y34, Y65, Y96	Y34, Y65, Y96

[z]The distance restraint between α-D-Man O2 and R30, R61, and R92 was omitted.

Table 5.2. Parameters employed during minimization [rounds (1) and (2)] and molecular dynamics (MD) simulations on unbound α-D-Man, unbound Gastrodianin, or the bound α-D-Man/Gastrodianin complex.

Simulation	Phase		Parameters[z]
Minimization			
		Method	Adapted-basis Newton-Raphson
		Solvent	GBSW, 0.15 M NaCl
		Distance restraints (1)	Distance cutoff = 4.5 Å
			Force = 1000 kcal/mol
		Distance restraints (2)	Distance cutoff = 5.5 Å
			Force = 500 kcal/mol
		Steps	20, 000
MD			
		Solvent	GBSW, 0.15 M NaCl
		Distance restraints	Distance cutoff = 5.5 Å
			Force = 500 kcal/mol
	Heating		
		Start Temperature	50 K
		End Temperature	300 K
		Heat Time	0.08 ns
		Heat Frequency	500 steps
		Heat Increment	1.56 K
		Time step	1.0×10^{-6} ns

Dynamics		
	Equilibration Frequency	1000 steps
	Equilibration Time	$1 < t < 2$ ns
	Production Time	1 ns
	Time step	1.0×10^{-6} ns

A

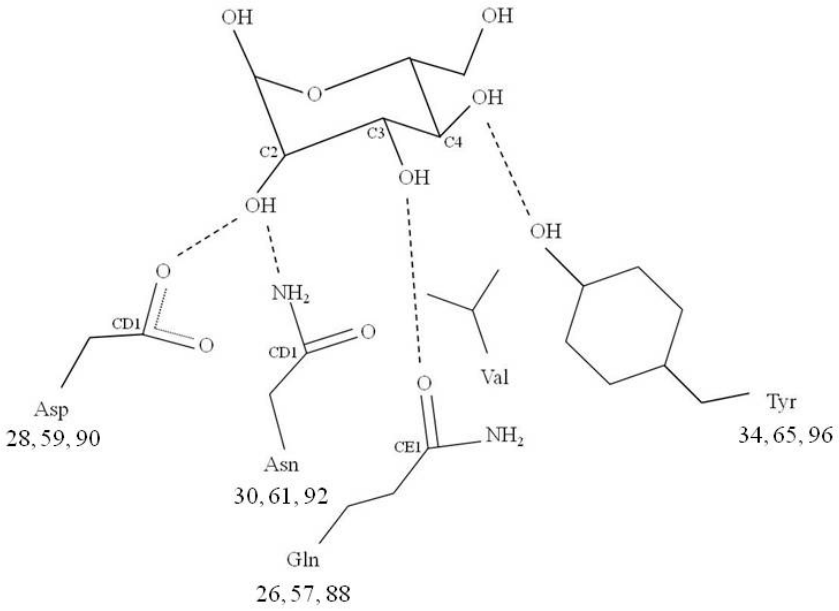
OH
OH
O
OH
C3
C4
C2
OH
OH
OH
O
NH2
CD1
O
CD1
O
Val
Asp
28, 59, 90
O
Tyr
34, 65, 96
CE1
NH2
Asn
30, 61, 92
Gln
26, 57, 88

B

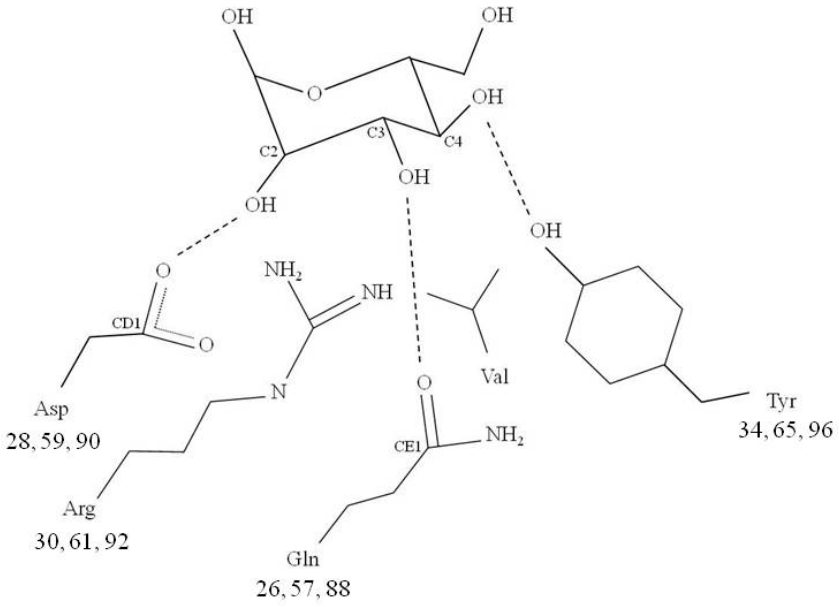
OH
OH
O
OH
C3
C4
C2
OH
OH
OH
O
NH2
NH
CD1
O
Val
Asp
28, 59, 90
N
O
Tyr
34, 65, 96
CE1
NH2
Arg
30, 61, 92
Gln
26, 57, 88

Figure 5.2. Distance cutoffs created between conserved, polar residues Q, D, N, and Y (Barre *et al.*, 2001) and α-D-Man in carbohydrate recognition domains (CRDs) 1 (residues 26-34), 2 (residues 57-65), and 3 (residues 88-96) of un-substituted (A) and substituted (B) Gastrodianin peptides. Parameters are given in Table 5.2.

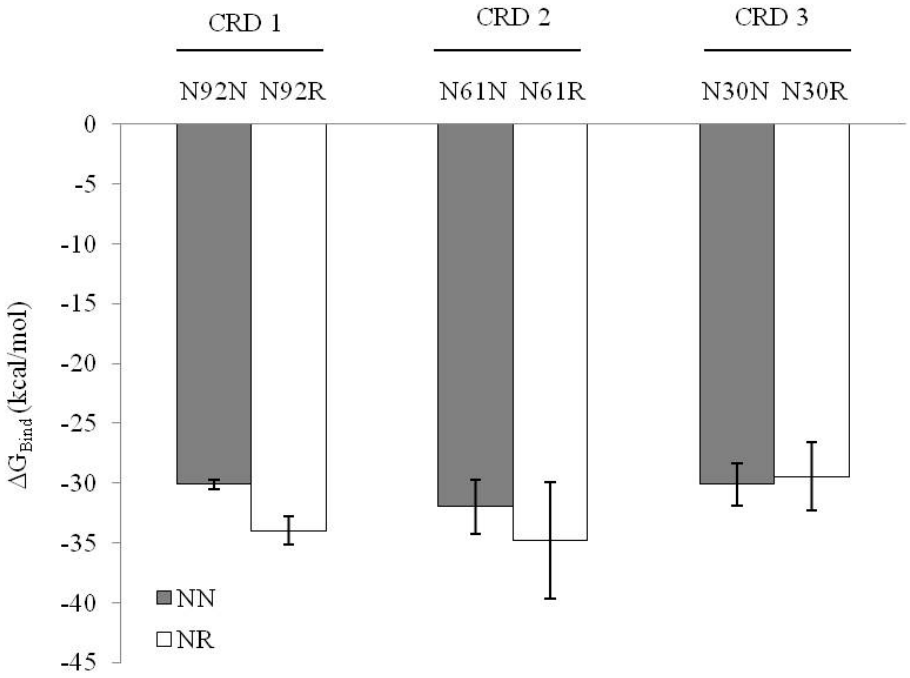
CRD 1
CRD 2
CRD 3
N92N N92R
N61N N61R
N30N N30R
0
-5
-10
-15
-20
-25
-30
-35
-40
-45
ΔG_Bind (kcal/mol)
NN
NR

Figure 5.3. Free energy of binding (ΔG_{bind}) between α-D-Man and carbohydrate recognition domains (CRDs) 1 (residues 26-34), 2 (residues 57-65), and 3 (residues 88-96) of un-substituted (NN) and substituted (NR) Gastrodianin peptides.

Table 5.3. Energetic contributions to the free energy of binding (ΔG_{bind}) between α-D-Man and carbohydrate recognition domains (CRDs) 1 (residues 26-34), 2 (residues 57-65), and 3 (residues 88-96) of un-substituted (NN) and substituted (NR) Gastrodianin peptides.

CRD	Model		$\Delta G_{bind}{}^{z,y}$	ΔE_{Elec}	ΔE_{VDW}	ΔE_{GB}	ΔE_{SA}	ΔE_{Bond}
1	N92N	AV	-30.1	-14.5	-8.8	-7.0	0.2	0.0
		SD	0.4	3.2	0.8	3.2	0.6	0.0
	N92R	AV	-34.0	-21.3	-9.8	-3.4	0.4	0.0
		SD	1.2	5.5	0.5	7.6	1.2	0.0
2	N61N	AV	-32.0	-22.5	-8.8	-157.0	156.4	-0.1
		SD	2.3	8.1	1.2	358.9	350.7	0.2
	N61R	AV	-34.8	-24.0	-9.0	-11.1	-0.8	10.0
		SD	4.9	4.7	0.9	21.4	0.8	21.9
3	N30N	AV	-30.1	-24.6	-8.7	4.4	-1.5	0.2
		SD	1.7	9.5	2.0	11.7	0.4	1.0
	N30R	AV	-29.5	-37.2	-7.2	15.8	-0.8	0.0
		SD	2.9	8.1	1.5	5.7	0.6	0.0

[z]Averages (AV) and standard deviations (SD) were taken across five MD simulations run under different random seeds.

Table 5.4. Energetic contributions to the change in total free energy of the system (ΔG_{System}) for unbound α-D-Man and unbound un-substituted (NN) and substituted (NR) Gastrodianin peptides.

Model		ΔG_{System}	E_{Elec}	E_{VDW}	E_{GB}	E_{SA}	E_{Bond}
MAN	AV	75.2	83.8	6.0	-2.31	3.51	-15.8
	SD	1.3	0.7	1.2	4.4	0.9	3.6
				Unbound			
N92N	AV	-2607.4	-3139.3	-482.5	-1122.5	195.4	1941.5
	SD	9.9	34.7	3.2	37.9	1.2	3.3
N61N	AV	-2596.4	-3155.6	-479.4	-944.1	38.5	1944.1
	SD	12.8	59.3	5.7	403.5	351.0	6.0
N30N	AV	-2597.9	-3105.6	-475.9	-1159.7	197.4	1945.8
	SD	2.9	55.4	1.7	56.8	1.4	1.5
				Bound			
N92N	AV	-2561.6	-3069.7	-486.1	-1132.3	198.0	1928.5
	SD	10.0	34.8	3.3	38.0	1.3	3.1
N61N	AV	-2554.3	-3094.7	-480.5	-1106.2	199.5	1927.6
	SD	11.1	59.4	5.6	58.9	1.1	6.0
N30N	AV	-2551.9	-3046.1	-479.5	-1159.4	199.8	1933.3
	SD	2.5	51.1	1.1	50.6	0.6	2.6

Model		ΔG_{System}	E_{Elec}	E_{VDW}	E_{GB}	E_{SA}	E_{Bond}
			Unbound				
N92R	AV	-2779.9	-3292.5	-483.2	-1160.91	197.5	1959.3
	SD	7.4	34.7	3.3	33.5	1.0	2.9
N61R	AV	-2770.6	-3162.5	-478.82	-1291.8	198.8	1963.7
	SD	2.6	44.7	3.1	48.8	0.8	2.2
N30R	AV	-2781.41	-3248.9	-481.3	-1206.3	197.2	1957.7
	SD	2.8	58.6	3.3	59.4	0.7	4.6
			Bound				
N92R	AV	-2738.9	-3230.9	-487.7	-1166.7	200.3	1946.1
	SD	7.5	30.5	3.1	28.3	1.18	2.7
N61R	AV	-2728.8	-3103.1	-482.7	-1296.5	201.8	1951.6
	SD	3.1	43.4	2.6	48.04	0.65	2.45
N30R	AV	-2737.5	-3201.3	-481.1	-1196.1	200.32	1940.6
	SD	5.0	64.8	3.4	63.6	0.9	4.9

[z]Averages (AV) and standard deviations (SD) for bound and unbound peptides were taken across five MD simulations run under different random seeds. Average energy component values for unbound α-D-Man were determined for each model across five independent MD simulations and then further averaged across the six peptide models.

LITERATURE CITED

Barboni, E.M., S. Bawumia, and R.C. Hughes. 1999. Kinetic measurements of binding of galectin 3 to a laminin substratum. Glycoconjugate J. 16:365-373.

Brewer, F.C. 2004. Thermodynamic binding studies of galectin-1, -3, and -7. Glycoconjugate J. 19:459-465.

Bashford, D. and D.A. Case. 2000. Generalized born models of macromolecular solvation effects. Annu. Rev. Phys. Chem. 51:129-152.

Barre, A., Y. Bourneb, E. J. M. Van Damme, W. J. Peumans, and P. Rougé. 2001. Mannose-binding plant lectins: Different structural scaffolds for a common sugar-recognition process. Biochimie 83:645−651.

Brooks, B.R., R.E. Bruccoleri, B.D. Olafson, D.J. States, S. Swaminathan, and M. Karplus. 1983. CHARMM: A Program for Macromolecular Energy, Minimization, and Dynamics Calculations. J. Comp. Chem. 4:187-217.

Cox, K., D. Layne, R. Scorza, and G. Schnabel. 2006. Gastrodia anti-fungal protein from the orchid *Gastrodia elata* confers disease resistance to root pathogens in transgenic tobacco. Planta 224:1373-1383.

Hester, G. and C.S. Wright. 1996. The mannose-specific bulb lectin from *Galanthus nivalis* (Snowdrop) binds mono- and dimannosides at distinct sites. Structure analysis of refined complexes at 2.3 and 3.0 resolution. J. Mol. Biol. 262:516-531.

Jayaram, B., D. Sprous, and D.L. Beveridge. 1998. Solvation free energy of biomacromolecules: parameters for a modified generalized born model consistent with the AMBER force field. J. Phys. Chem. B. 102:9571-9576.

Jiang, L., Y. Gao, F. Mao, Z. Liu, and L. Lai. 2002. Potential of mean force for protein-protein interaction studies. Prot. Stucture, Function, and Gen. 46:190-196.

Kaku, H., E. J. M. Van Damme, W. J. Peumans, and I. J. Goldstein. 1990. Carbohydrate-binding specificity of the daffodil (*Narcissus pseudonarcissus*) and amaryllis (*Hippeastrum hybr.*) bulb lectins. Arch. Biochem. Biophys. 279:298–304.

Liu W., N. Yang, D. Jingjin, R. H. Huang, Z. Hu, and D. C. Wang. 2005. Structural mechanism governing the quaternary organization of monocot-mannose binding lectin revealed by the novel monomeric structure of an orchid lectin. J. Biol. Chem. 280:14865-14876.

Nagel, A.K., R. Scorza, C. Petri, and G. Schnabel. 2008. Generation and characterization of transgenic plum lines expressing the *Gastrodia*-Anti Fungal Protein. HortSci. 43:1514–1521.

Nagel, A.K., H. Kalariya, and G. Schnabel. 2010. The *Gastrodia* anti-fungal protein (GAFP-1) and its transcript are absent from scions of chimeric-grafted plum. HortSci. 44:188-192.

Neumann, D., O. Kohlbacher, H.-P. Lenhor, and C.-M. Lehr. 2002. Lectin-sugar interaction: calculated versus experimental binding energies. Eur. J. Biochem. 269:1518-1524.

Nyczepir, A.P., A.K. Nagel, and G. Schnabel. 2009. Host status of three transgenic plum lines to *Mesocriconema xenoplax*. HortSci. 44:1932-1935.

Peumans, W.J. and E.J.M. Van Damme. 1995. Lectins as plant defense proteins. Plant Physiol. 109:347–352.

Peumans, W. J., A. Barre, J. Bras, P. Rouge, P. Proost, E. J. M. Van Damme. 2002. The liverwort contains a lectin that is structurally and evolutionary related to the monocot mannose-binding lectins. Plant Phys. 129:1054-1065.

Ramachandraiah, G., N.R. Chandra, A. Surolia, and M. Vijayan. 2002. Re-refinement using reprocessed data to improve the quality of the structure: a case study involving garlic lectin. Acta Crystallographica Section D Biol. Crystallography. 58:414-420.

Shibuya, N., I. J. Goldstein, E. J. M. Van Damme, and W. J. Peumans. 1988. Binding properties of a mannose-specific lectin from the snowdrop (Galanthus nivalis) bulb. J. Biol. Chem. 263(2):728 (abstr.).

Wang, P., Y. Wang, Q. Sa, W. Li, and Y. Sun. 2003. The site-directed mutagenesis of Gastrodia anti-fungal protein mannose-binding sites and its expression in *Escherichia coli*. 10:599-606.

Van Damme, E. J. M., W.J. Peumans, A. Barre, and P. Rouge. 1998. Plant Lectins: a composite of several distinct families of structurally and evolutionary related proteins with diverse biological roles. Critical Rev. Plant Sci. 17:575–692.

Van Damme, E. J. M., C. H. Astoul, A. Barre, P. Rouge, and W. J. Peumans. 2000. Cloning and characterization of a monocot mannose-binding lectin from *Crocus vernus* (family Iridaceae) Eur. J. Biochem. 267:5067-5077.

Zou, X., Y. Sun, and I.D. Kuntz. 1999. Inclusion of solvation in ligand binding free energy calculations using the generalized-born model. J. Amer. Chem. Soc. 121:8033-8043.

CHAPTER SIX

CONCLUSION

The *Gastrodia* anti-fungal protein (GAFP-1) is a promising candidate for enhancing field resistance in *Prunus* to a wide range of soil-borne pathogens. In addition to the multiple species of plant pathogenic fungi shown to be targeted by the lectin (Cox *et al.*, 2006; Hu and Huang, 1994; Xu *et al*., 1998; Wang *et al.*, 2004), my work has demonstrated that GAFP-1 is directly active against the stramenopiles *Phytophthora nicotianae* and *P. cinnamomi*, and that expression of the lectin in tobacco and plum confers protection to Phytophthora root rot and the root-knot nematode *Meloidogyne incognita* (Cox *et al*., 2006; Nagel *et al*. 2008). Field and *in vitro* tests on single-insertion, 4J plum lines are underway to investigate whether GAFP-1 expression can slow infection by *Armillaria tabescens*, a relative of the lectin's target pathogen *A. mellea* (Hu *et al*., 1988), and one of the causal agents of an economically important disease known as Armillaria root rot (ARR) in the Southeast (Beckman, 1998). It would be interesting to eventually compare disease resistance in our transgenic plum lines, in which constitutive expression of GAFP-1 is controlled by the CaMV-35S promoter, to lines which express GAFP-1 under the direction of one of its native promoters. The GAFP-2 promoter characterized by Sa *et al*. (2003) drove the high expression of β-glucuronidase in response to plant defense hormones jasmonic and salicylic acid in a tissue specific manner, and a disease-resistant *Prunus* rootstock would likely be improved by a greater degree of inducible and tissue-specific expression.

The mechanism of GAFP's action against fungal, stramenopile, and nematode pathogens requires further investigation. My work suggests that the lectin can bind cell wall components of the basidiomycete *Trichoderma viride* and the stramenopile *P. cinnamomi*, which is consistent

with previous findings in fungus (Xu and Liu, 2003). Cell walls of fungi and stramenopiles are functionally similar, but they differ in their molecular composition. Fungal cell walls are comprised of chitin, 1,3 and 1,6-linked β-glucans, and an outer layer rich in embedded mannoproteins (Lipke and Ovalle, 1998; Pitarch *et al.*, 2002). Cell walls of heterokonts such as *Phytophthora sp*. are comprised of cellulose (4-20%) and hydroxyproline, however they do contain 1,3 and 1,6-linked β-glucans similar to their fungal counterparts (Alexopoulos *et al*., 1996). Chitin-binding ability in GAFP has been proposed to contribute to the lectin's mode-of-action in fungal cell walls (Liu *et al*., 2005; Xu and Liu, 2003; Xu *et al.*, 1998), but this has yet to be proven experimentally and is not supported by our data. The question of whether GAFP-1 is binding directly to the carbohydrate matrix or another type of ligand remains to be answered. The lectin has been shown to inhibit growth of fungal hyphae and spores *in vitro*, but GAFP appears to possess only fungistatic activity, since hyphae can eventually overtake the zone of inhibition, and hyphal morphogenesis is not altered (Xu *et al*., 1998; Wang *et al*., 2001; these studies).

The ideal system in *Prunus* would be one in which the GAFP-1 lectin was retained within an engineered, disease-resistant rootstock grafted to non-transgenic scion tissues on which the fruit would be produced. Analysis of greenhouse-grafted plum lines suggests that the lectin is not moving into the wild-type tissues of chimeric-grafted trees (Nagel *et al*., 2010). Anecdotal evidence, however, does indicate that GAFP would not be harmful if ingested (Dharmananda, 1998). Indeed, the potential medicinal properties of GAFP-1 are fascinating. GAFP-expressing *G. elata* corms have been a holistic remedy in China for centuries, being used to treat headaches and vertigo (Dharmananda, 1998). New studies even suggest that *G. elata* can improve brain-function (Xu and Liu, 2003). Other MMBLs from the *Orchidaceae* family, such as EHMBP and LOMBP from *Epipactus helleborine* and *Listera ovata*, respectively, have recently been shown to be inhibitory against human and animal retroviruses such as HIV (Balzarini *et al*., 1991; Balzarini *et*

al., 1992). A scenario might even be imagined where GAFP's inhibitory properties were directed against human fungal pathogens like the basidiomycete yeasts *Candida albicans* and *Cryptococcus neoformans*. Such possibilities only enhance the interest of a lectin which already has great potential for agricultural application.

LITERATURE CITED

Alexopoulos, C.J., C.W. Mims, and M. Blackwell. 1996. *Introductory Mycology*. John Wiley and Sons, New York, NY. p. 687-688.

Balzarini, J., D. Schols, J. Neyts, E. Van Damme, W. Peumans, E. and De Clercq. 1991. α-(1–3)- and α-(1–6)-D-mannose-specific plant lectins are markedly inhibitory to human immunodeficiency virus and cytomegalovirus infections in vitro. Antimicrobial Agents Chemotherapy. 35:410–416.

Balzarini, J., J. Neyts, D. Schols, M. Hosoya, E. Van Damme, W. Peumans, E. and De Clercq. 1992. The mannose-specific plant lectins from *Cymbidium* hybrid and *Epipactis helleborine* and the (*N*-Acetylglucosamine)n-specific plant lectin from *Urtica dioica* are potent and selective inhibitors of human immunodeficiency virus and cytomegalovirus replication in vitro. Antiviral Res. 18:191–207.

Beckman, T.G. 1998. Developing Armillaria resistant rootstocks for peach. Acta Hort. (ISHS) 465:219-224. <http://www.actahort.org/books/465/465_26.htm/>.

Cox, K., D. Layne, R. Scorza, and G. Schnabel. 2006. Gastrodia anti-fungal protein from the orchid *Gastrodia elata* confers disease resistance to root pathogens in transgenic tobacco. Planta 224:1373-1383.

Dharmananda, S. 1998. Gastrodia. 4 December 2001. <http://www.itmonline.org/arts/gastrod.htm/>.

Hu, Z., Z. Yang, and J. Wang. 1988. Isolation and partial characterization of an antifungal protein from *Gastrodia elata* corm. Acta Botanica Yunnanica 10:373-380.

Hu, Z. and Q.Z. Huang. 1994. Induction and accumulation of the antifungal protein in Gastrodia elata. Acta Botannica Yunnanica 16:169-177.

Lipke, P.N. and R. Ovalle. 1998. Cell wall architecture in yeast: new structure and new challenges. J. Bacteriol. 180:3735-3740.

Liu, W., N. Yang, D. Jingjin, R.H. Huang, Z. Hu, and D.C. Wang. 2005. Structural mechanism governing the quaternary organization of monocot-mannose binding lectin revealed by the novel monomeric structure of an orchid lectin. J. Biol. Chem. 280:14865-14876.

Nagel, A.K., R. Scorza, C. Petri, and G. Schnabel. 2008. Generation and characterization of transgenic plum lines expressing the *Gastrodia*-Anti Fungal Protein. HortSci. 43:1514–1521.

Nagel, A.K., H. Kalariya, and G. Schnabel. 2010. The *Gastrodia* anti-fungal protein (GAFP-1) and its transcript are absent from scions of chimeric-grafted plum. HortSci. 44:188-192.

Pitarch, A., M. Sanchez, C. Nombela, and C. Gil. 2002. Gel analysis unravels the complexity of the dimorphic fungus *Candida albicans* cell wall proteome. Mol. Cell Proteomics. 1:967-982.

Sa, Q., Y. Wang, W. Li, L. Zhang, Y. Sun. 2003. The promoter of an antifungal protein gene from *Gastrodia elata* confers tissue-specific and fungus-inducible expression patterns and responds to both salicylic acid and jasmonic acid. Plant Cell Rep. 22:79-84.

Xu, Q., Y. Liu, X. Wang, H. Gu, and Z. Chen. 1998. Purification and characterization of a novel anti-fungal protein from *Gastrodia elata*. Plant Physiol. Biochem. 36:899-905.

Xu, R. H. and X. Z. Liu. 2003. Action site of Gastrodia anti-fungal protein on *Trichoderma* hyphae. Acta Botannica Yunnanica. 25.573-578.

Wang, X., G. Bauw, E.J.M. Van Damme, W.J. Peumans, Z.-L. Chen, M. Van Montagu, G. Angenon, and W. Dillen. 2001. Gastrodianin-like mannose-binding proteins: a novel class of plant proteins with antifungal properties. Plant J. 25:651:661.

Wang, Y., D. Chen, D. Wang, Q. Huang, Z. Yao, F. Liu, X. Wei, R. Li, Z. Zhang, and Y. Sun. 2004. Over-expression of *Gastrodia* anti-fungal protein enhances *Verticillium* wilt resistance in coloured cotton. Plant Breeding 123:454-459.